CHAPTER 11 - ARCH DAMS

Federal Energy Regulatory Commission
Division of Dam Safety and Inspections
Washington, DC 20426

October, 1999

TABLE OF CONTENTS

CHAPTER 11 - ARCH DAM

11-1 INTRODUCTION

11-1.1 Purpose

This chapter of the Guidelines provides guidance on the criteria and procedures used by the FERC to evaluate the safety and structural integrity of existing arch dams under its jurisdiction. The intent of this guidance is to outline criteria and evaluation procedures including foundation considerations, material properties and testing, loading, methods of analyses, and predicted and observed performance that provide the basis for review and approval of the analysis and inspection studies submitted to the FERC.

The material presented in this chapter assumes that the reader has a general knowledge and understanding of the basic principles of arch dams, i.e., how they are designed, constructed, operated, and maintained. For detailed discussions on design and a better understanding of the arch dam behavior, consult the US Bureau of Reclamation "*Design of Arch Dams*," (USBR 1977) and the US Army Corps of Engineers EM 1110-2-2201 "*Arch Dam Design*," (COE 1994) ," (USBR 1977). This chapter presents much information. The intent of this chapter not to mandate new analyses and investigations regardless of whether or not they are needed. Rather, the variety of issues addressed and computation methods put forward are an attempt to anticipate the variety of problems that could be encountered. This chapter should not be interpreted as requiring every test, analysis, and investigation that it describes at every dam. It may well be that for a given dam, specific failure mechanisms suggested in this chapter are not pertinent. Analysis of arch dam safety should always start with simple analysis techniques and conservative assumptions. If simple analyses indicate problems, more complicated and rigorous analyses may be in order.

11-1.2 Applicability

This guidance is applicable to FERC engineers and licensees engaged in the safety evaluation of existing arch dams. The design of new arch dams should follow the guidance and criteria of the references (USBR, 1977 and COE, 1994) , but could also benefit from the evaluationphilosophy presented in this chapter.

11-1.3 Definition of Safety

Safety is defined as their adequacy against an uncontrolled release of reservoir water. The structural integrity is maintained and the dam is considered safe if overstressing, sliding, and other possible modes of failure will not occur. A safety evaluation, therefore, should identify all significant failure modes and conduct appropriate analyses to assure that the structural stability of the dam is maintained.

Overstressing of concrete arch dams may exhibit a tendency toward developing a partial failure, if large tensile stresses from the linear-elastic analysis indicate extensive joint opening and cracking . Considering that the ultimate load-resisting capacity of an arch dam is limited by the compressive strength of the concrete (unless foundation or other mode of failures occur first), severe and widespread joint opening and cracking might eventually exhaust the capacity of the concrete to carry compression due to subsequent load redistributions, or might form surfaces along which partial sliding could occur. Whether such partial failures could actually occur is unknown, because they have not been observed previously, and also because of the inherent redundancy in arch dams and the fact that arch action might restrain movements of the portions separated by joint opening and cracking.

With respect to sliding failures, two types of potential foundation sliding instability cases should be considered. The first type is potential sliding of rock wedges within the foundation and in contact with the dam, and the second is potential sliding along the contact between the dam and foundation rock. The sliding of rock wedges typically occurs along one potential failure plane (plane sliding) or along the line of intersection of two of these planes (wedge sliding). For a rock wedge to be kinematically capable of failure, the direction of sliding must intersect or "*daylight*" a free surface downstream from the dam. While an arch dam might be capable of bridging a small unstable foundation block at the bottom, large, unstable wedges of rock in the abutments could endanger the safety of the dam. In fact, the first failure of an arch dam at Malpasset Dam in 1959 resulted from displacements of a large wedge of rock in the left abutment.

Sliding stability along the dam-foundation contact of a concrete arch dam is less likely because of the wedging produced by arch action and embedment of the structure into the rock. However, arch dams with relatively flat abutment slopes, or arch dams with abutment thrust blocks supported by rock foundations with inadequate shear strength could be susceptible to sliding along the foundation contact and should be considered.

Other cases requiring special considerations include structural deformations and deterioration of concrete caused by alkali-aggregate reactions, and foundation or abutment erosion due to overtopping, which if severe, could lead to instability.

11-1.4 Evaluation Criteria

Existing concrete arch dams should be evaluated by conducting a review and analysis of all existing data, a field inspection, and any analyses necessary to determine the safety of the dam for continued normal operation and resistance against the unusual and extreme loading conditions.

11-1.4.1 Review of Existing Data and Site Inspection

A thorough knowledge must first be gained on a dam's original design and its performance history and records, to provide a basis for evaluation and any further studies that might be required. The existing data for review can be obtained from the owner's files or from the files maintained by the FERC. The review should reveal whether the original design criteria and assumptions, materials investigations, geological and seismological studies, and design analyses are satisfactory based on the current practice, and if not, whether they are acceptable. The same should also be applied to any modifications or alterations in design and on any subsequent analyses, investigations, or reviews. Of particular value are data on instrument readings that provide information on actual performance of the dam.

It is sometimes difficult to locate historic data from older projects. In addition to the owner’s and FERC’s files, other sources may include articles in periodicals and technical journals, state dam safety engineer’s files, consultant’s records, construction contractor’s records and personal files of individuals who worked on the project.

After completion of the review of existing data, a site inspection should be carried out to observe the present condition of the dam, and to resolve any discrepancy that may exist concerning available data such as drawings, instrument data, and other pertinent information. The inspection should also provide the opportunity to identify any cracks, deteriorated joints, and other distress conditions that need to be considered in the evaluation of dam safety.

In some cases, an adequate determination of dam safety might be possible from the review and analysis of existing data and field observations. If the review and observations indicate that additional analyses are required, then these analyses should be performed as follows:

11-1.4.2 Method of Analysis

Three dimensional finite-element analysis is preferred for the static and dynamic analysis of arch dams. Trial load method may be used for static stress analysis only, if the dam has a simple geometry and uniform material parameters can be assumed for the concrete and for the foundation rock. Other mathematical formulations and approaches can also be employed, but the accuracy of such methods should be verified by comparison with the finite-element analyses.

11-1.4.3 Evaluation for Static Loading

The performance of concrete arch dams under static loading conditions should be evaluated using deflections and stresses. Concrete and foundation rock material parameters used in the analyses should be determined on the basis of field and laboratory investigations (Sections 11-2.4 and 11-3). In situations where determination of certain material parameters is neither cost effective nor conclusive, their effects on the dam response should be evaluated by parameter sensitivity analyses (Section 11-5.5). All applicable static loads should be considered and combined according to their probabilities of occurrence in three categories of Usual, Unusual, and Special loading combinations (Section 11-4).

The basic results of analyses should include both deflections and stresses developed in the dam. Plots of computed deflections provide a visual means for checking the numerical results, and whenever possible they should be correlated with the observed deflections measured by instrumentation monitoring (Section 11-7), in order to verify and possibly calibrate the mathematical model. The initial position and temperature of the dam is not typically known. For this reason, when comparing computed deflections to observed deflections, it is the differential deflection rather than the absolute deflection that is meaningful.

Stress results are used to evaluate the dam performance in the response to each loading combination. The evaluation starts with comparison of the computed stresses with strength of the concrete reduced by a factor of safety (Table 11-1.1), but will also involve determination of location, magnitude, extent, and direction of high stresses should some crack-inducing stresses be expected. If all factors of safety are met the dam is considered to perform satisfactorily, even though some minor contraction joint opening may occur. Otherwise joint opening and cracking could be significant and should be evaluated in accordance with procedures outlined in Sections 11-1.4.3.1, 11-1.4.3.2, and 11-1.4.4.

Table 11-1.1 Factors of Safety for Existing Arch Dams

Loading Combination	Compressive Stresses	Tensile Stresses	Internal Shear Stresses	Sliding [1] Stability
Usual (normal operating)	2.0	1.0	2.0	1.5
Unusual (flood condition)	1.5	1.0	1.5	1.5
Extreme (seismic)	1.1	1.0	1.1	1.1

[1] Factors of safety valid for the assumption of no cohesion.

11-1.4.3.1 Performance for Usual and Unusual Loading Combinations

Arch dams resist applied static loads by developing primarily compressive stresses along the arch sections. The adequacy of the dam under a given load combination should be evaluated in accordance with the compressive stress and shear stress criteria listed in Table 11-1.1.

The stress results produced by the linear-elastic finite-element analysis usually indicate some areas of tensile stress in the dam. While tensile strength of the intact concrete can reach several hundred psi, the fact that a typical arch dam is made of concrete blocks divided by lift joints, vertical contraction joints, and pre-existing cracks should be considered in the evaluation of tensile stresses (Figure 11-1.1).

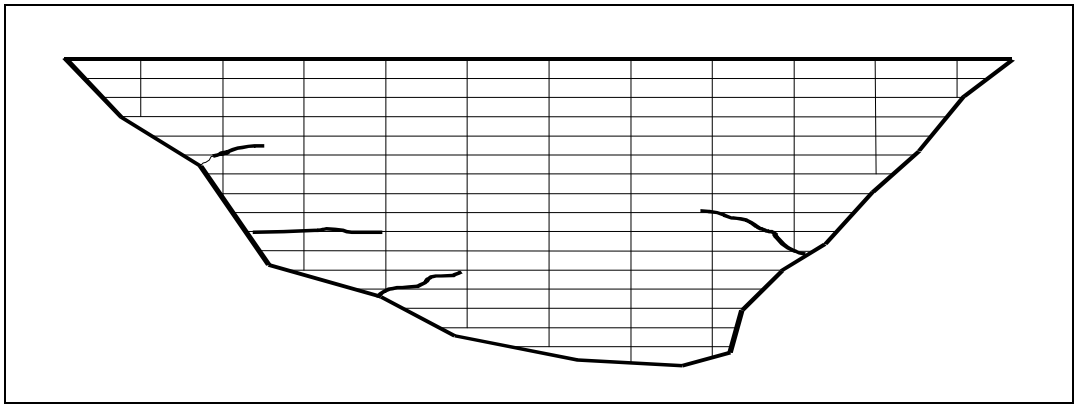

Fig. 11-1.1 Existing arch dam with vertical contraction joints, horizontal lift joints, and pre-exiting cracks

The tensile strength in the direction normal to the contraction joints and cracks is very small, and across the lift joints may be only a fraction of the tensile strength of the intact

concrete. In some cases, joints and cracks may have no tensile strength at all. For this reason, it is not appropriate to evaluate the indicated tensile stresses of a finite element model in terms of an allowable tensile stress for the intact concrete alone.

When a finite element model does indicate regions of tensile stress, the reviewer must realize that these stresses are probably not an indication of the actual stress state of the dam, but a consequence of the modeling assumptions of linear elasticity and structural continuity. Thus, large areas of indicated tensile stress may reveal a problem with the assumption of linear-elastic behavior and not necessarily a problem with the performance of the dam.

The effect of tensile stress relief by joints and cracks is to increase compressive and possibly shear stress in other areas of the dam. If a finite-element model indicates large areas of tensile stress, or tensile stresses that are high (see Section 11 -3.7.2), the finite element model should be modified to account for the loss of tensile resistance due to joint opening or cracking. The modified model should then be re-run and evaluated. This process will require some judgement on the part of the reviewer and the analyst as to when indicated tension is excessive thus requiring model modification. If the combination of linear finite element analysis and engineering judgement is not sufficient to determine whether or not a dam is safe, non-linear finite element analysis may be required.

11-1.4.4 Evaluation for Seismic Loading

The performance of concrete arch dams under earthquake loading should be evaluated by conducting a three-dimensional linear-elastic dynamic analysis using the finite-element method (Section 11-6). The FE model of the dam system should account for the dam-water and the dam-foundation rock interaction effects. Material parameters for the concrete and foundation rock should be established by giving due consideration to the effects of the rate of loading typical of earthquake response. The design earthquake for the safety evaluation of arch dams is the maximum credible earthquake (MCE). The MCE is an extremely rare event capable of producing the largest ground motion that could ever occur at the dam site. An MCE should be considered to be an extreme loading condition, for which significant damage would be acceptable, but the dam must not rupture and thus threaten life and property downstream. Seismic input ground motions for the MCE should be developed from a deterministic ground motion analysis, but may be supplemented by a probabilistic ground motion analysis should evaluation of the likelihood of the MCE ground motions become desirable. The earthquake response of the dam may be computed using the response-spectrum mode-superposition method, but if maximum

stresses exceed the allowable values a linear time-history analysis can be helful to assessing the severity of joint opening and tensile cracking .

For evaluation of the earthquake performance of arch dams using response-spectrum method, dynamic stresses are combined with static stresses due to the usual loading combination and compared with the allowable values. The evaluation criterion for time-history analysis, however, is more involved than simple stress checks. It considers not only the maximum stress values, but also the sequencing, spatial extent, and number of excursions beyond the allowable values. In addition, in cases where severe damage is predicted, sensitivity analyses should be performed to account for uncertainties associated with modeling assumptions, seismic input application, and material properties. Horizontal lift joints and vertical contraction joints should be assumed to crack when subjected to tensile stresses exceeding their tensile strengths. In situations where there is a net tensile force across a vertical contraction joint, it should be assumed that the contraction joint will open through the full thickness of the dam, possibly forming a free cantilever block. (See 11-6.3.3.5) The evaluation of dam safety using linear elastic assumptions requires a qualitative judgement of how stresses will be redistributed during joint opening and cracking. This evaluation is done in lieu of more sophisticated nonlinear analysis. This approach may not be sufficient for some situations and a more detailed analysis using non-linear techniques may be required. The dam may be considered safe for the MCE if, after the effects of crack and joint opening have been accounted for, it can be shown that the concrete is not over-compressed and free cantilevers do not topple.

11-1.4.4.1 Post-earthquake Safety Evaluation

A post-earthquake safety evaluation is required to assure the safety of the dam if, a damaging MCE should occur near the dam site, or the predicted performance of the dam due to a postulated MCE should indicate substantial damage. This evaluation should consider the effects of static loads as well as severe aftershock earthquakes that invariably occur after any major quake. Factors of safety for the post-earthquake conditions are the same as those given in Table 11-1.1 for the usual case.

11-1.4.5 Sliding Stability

To assure safety against sliding along identified kinematically admissible failure planes in the dam , at the dam foundation/interface, or in the foundation, the shear friction factor of safety assuming no cohesion shall be 1.5 for normal and unusual loading, and greater than 1 for extreme loading. These safety factors assume that stability has been evaluated with respect to conservative shear strength parameters.

For major dam structures subjected to severe seismic loading, response history analyses should be performed for abutment and foundation stability instead of the usual pseudo-static analyses. In response history analyses, factor of safety varies with time and may become less than 1.0 for one or more cycles provided that the resulting cumulative sliding displacement is very small and can be tolerable.

11-2 FOUNDATION CONSIDERATIONS

11-2.1 General

The abutment foundations of an arch dam are particularly critical to the stability of the dam because they are required to resist the majority of the reservoir forces that attempt to push the structure in a downstream direction. The modulus of deformation of the abutments and the foundation is also an important element in analyzing the performance of the dam since the flexibility of the foundation directly affects the *stresses in* the dam. Foundation information must provide sufficient geological detail to identify and locate any potential sliding wedges of rock that could cause instability. If such features are found to exist, a stability analysis must be performed to assure that there is an adequate factor of safety against abutment sliding. For some existing dams, sufficient data and analyses are already available to provide the necessary information. In other cases it will be necessary to perform field investigations and conduct stability analyses. In either event, the staff must require that sufficient abutment foundation information and analysis be provided to support a review that verifies the findings with regard to the stability of the foundation and abutments. The same requirement is true for the foundation modulus of deformation.

11-2.2 Field Investigations

Field investigations are well described in Chapter 5 of these Guidelines and in the U.S. Army Corps of Engineers EM 1110-2-2201 (1994). Additional details are contained in EM 1110-1-1804 (1984) and EM 1110-1-2908 (1994) (See References). The following narrative is intended as a summary and for the purpose of additional elaboration where required to specifically address the requirements of this Guideline.

It is imperative that the conditions of the foundation at the site be well defined. In particular, geologic investigations as outlined in Chapter 5 should provide an interpretation of the rock type and quality, identify the discontinuity (joint) pattern, locate any planes or wedges of rock which could fail under the structural loading, provide samples and data for determining the rock mass modulus of deformation, the bearing capacity and the shear strength available to resist failure.

11-2.2.1 Foundation Features That Create Stability Concerns and Warning Signs

Jointing - A feature of primary concern is a large wedge of rock in an abutment foundation created by a planar rock fracture or the intersection of two or more rock fractures whose intersection trend daylights in a downstream direction. Refer to EM 1110-2-2201, pages 10-28 and 29, for examples. Because of the high intact strength of most rock formations,

failure is improbable unless it can occur along preexisting fractures. For a failure to occur, movement of the rock wedge must be kinematically possible. In other words, the orientation of the trend of the intersection of the rock fractures or slide plane must normally daylight in a direction which would allow movement to take place under the applied loads without shearing a great deal of intact rock. A relatively small amount of intact rock may sometimes be sheared when the trend comes close to daylighting without it actually occurring.

In addition to joint orientation, joint connectivity must be considered. Joint connectivity determines whether kinematically possible wedges are small, and of little consequence, or large and capable of compromising the stability of the dam.

Hydrostatic Pressure - The stability of an abutment rock wedge is affected by the hydrostatic pressure in the joints that define the wedge as can be seen in the figure below. The drilling of joint drainage holes to relieve hydrostatic pressure is often very effective in increasing wedge stability.

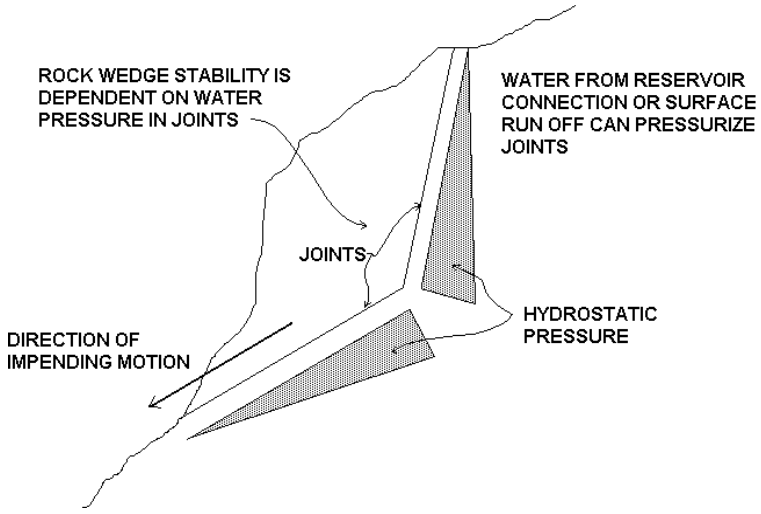

Fig. 11-2.1

Faults - Zones of faulted or sheared rock within the foundation must be carefully considered. A fault is a rock fracture distinguished from a joint by virtue of translational movement of one wall relative to the other wall at some time during the geologic record. If a fault is found to be present, the question as to whether it is active or inactive must be answered. If it is determined to be an active fault, its effect upon the structure during movement must be very carefully assessed and appropriately acted upon.

Next, the fault's effect upon the static stability of the foundation must be determined. Since

it is a presheared feature in the rock, it probably provides a plane of reduced strength to resist movement. In many cases slickensides and clay gouge are formed which greatly reduce the rock strength. Its orientation is significant in the effect it has on reducing stability against sliding in the foundation.

Another concern is the permeability of a through-going fault. If the sheared rock was very brittle and the shearing process formed a zone of primarily broken rock (breccia), it may form a highly permeable path for water passage beneath the dam. If the shearing movement forms a clay gouge within the breccia zone, the result may be a very impervious barrier in the foundation. Such a barrier to seepage can in some configurations result in the development of abnormally high uplift pressure in the foundation. These questions must be addressed, satisfactorily answered and incorporated into the stability analysis of the dam. Treatment may consist of curtain and consolidation grouting of a highly pervious shear zone or drains to relieve abnormal uplift created by a highly impervious shear zone. The possibility of erosion of gouge must also be considered.

The effect of a large faulted shear zone on the modulus of deformation of the foundation must be taken into consideration. A large change in modulus over a very short distance may result in the formation of concentrated stresses in the concrete of the dam if the shear zone was not properly treated during construction. Treatment usually consists of excavation of the sheared material to a depth from two to three times its width followed by backfill with dental concrete.

Coal Seams - Coal seams or beds in the foundation of an arch dam are a feature of concern. The clay layers associated with coal beds are an even greater concern. This combination in the foundation of an arch dam can form a plane with significantly lower shearing resistance than the surrounding rock. It should be evaluated both for planar failure and as a wedge in combination with the fracture pattern existing in the rock mass.

Planar Features - Planar features such as bedding, fisility, shale or clay seams, schistocity, foliation, cleavage, and stress relief features such as exfoliation and valley relief joints may all form sides of a rock wedge and therefore are features of some concern to be included in the abutment foundation stability analysis.

Sudden Changes in Stiffness - Adjacent rock beds with radically different moduli of deformation are of some concern. This difference must be taken into account during the stress analysis for the dam.

11-2.3 Material Parameter Selection

Experienced engineering and geologic judgement are very important in the selection of foundation material parameters for use in the analytical procedures. Since it is often not feasible to make prototype tests and measure directly the rock mass strength and deformation properties, it is necessary to use laboratory tests of small samples as the basis for estimating these properties. Laboratory testing may be required to identify rock types and to provide shear strength and rock mass modulus of deformation data. The testing program must be carefully developed by the Independent Consultant to provide sufficient tests to establish a statistically sound basis for estimating shear strengths of all critical features as well as the rock mass modulus of deformation. Refer to the Rock Testing Handbook (1990) and to Chapter 10 of EM 1110-2-2201 (1994) for more detail on laboratory testing than is provided in this Guideline.

Three parameters may be involved in providing shearing resistance to sliding at the interface, in the foundation and in the abutments. These include angle of friction, cohesion, and the angle of the rock asperities. Circumstances will dictate the applicability of using cohesion versus asperity angle. With smaller structures where the normal force applied by the dam and the weight of the overlying rock is insufficient to shear through the rock asperities during sliding, no cohesion parameter should be counted in the analysis. Instead, the angle of the asperities should be added to the angle of friction as a resisting parameter, since no movement can occur without overriding the asperities. This results in dilation or lifting, thereby requiring an increased driving force to slide the structure. Conversely, in large dams that impose high normal forces, shearing through asperities may occur rather than riding over them during sliding failure. In this circumstance it is proper to use cohesion as a resisting force rather than the angle of the asperities. Further explanation is contained in the following paragraphs.

11-2.3.1 Shear Strength of Foundation Interface

Factors to be considered in estimating the shear strength of the foundation interface include strength of the bond of the concrete to the rock foundation, roughness or asperity angle "i" of the interface, and embedment of the structure into the rock. Laboratory testing of intact core samples of the interface can provide data on which to estimate the bond strength. Sufficient core samples of the interface must be obtained to allow a statistically sound appraisal of the percentage of the interface that can be reliably assumed to be bonded.

The roughness or asperity angle may be very difficult to estimate and because of this may have to be ignored. In some cases it may be possible to estimate from photographs of the foundation taken just before concrete placement. Another possibility is to estimate the

irregularity from closely spaced core borings. Refer to Figure 11-2.2b for a diagrammatic representation of interface roughness.

Where information exists for determination of an asperity angle at the interface between the structure and the foundation, this angle may be added to the friction angle as a resisting force in the stability analysis if the least resistance to sliding includes overriding the irregularities. It is not applicable where the least resistance is developed by shearing through the rock of the irregularities. Refer to Figure 11-2.2b for an example to illustrate the effect that foundation roughness may have in resisting sliding at the interface.

Embedment may possibly be determined from as-built drawings, construction photographs, and borings. This factor can be very important for preventing sliding on the interface provided the concrete is placed against the embedded surface, which would mobilize the downstream rock strength before movement could occur.

The process of determining interface strength for arch dams is not as straight forward as is the case of gravity dams. This is because failure mechanisms must be considered in 3 dimensions. As can be seen in Figure 11-2.2a, the direction of shear force at the dam/foundation interface changes with respect to position along the valley. In one area, the shear force may be parallel to the strike of the asperities, in another area it may be perpendicular. Strength must be defined with respect to the direction of shearing force. As in the case of indicated tensile stresses, local exceedance of the shear strength of the interface may not be an indication of dam failure. Excessive shear stress may be able to be re-distributed.

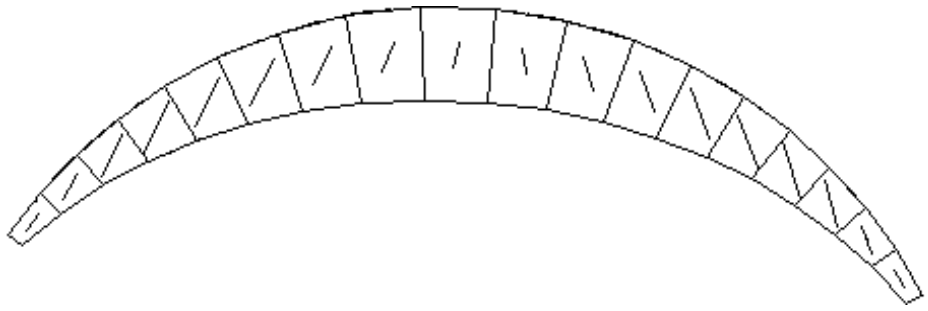

Fig. 11-2.2a Direction of shear stress at dam/foundation interface

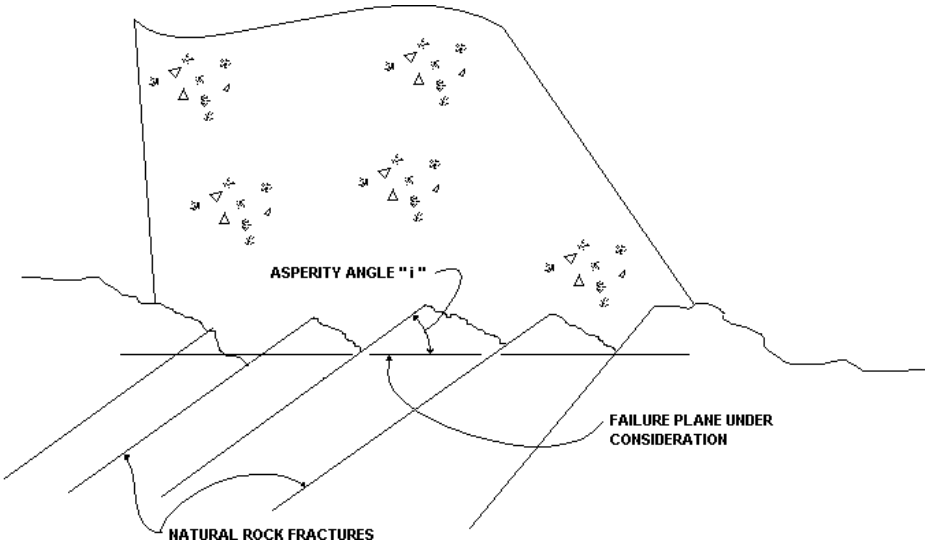

Fig. 11-2.2b Concrete to rock foundation interface showing asperities interrupting potential failure plane

The strength of the concrete to rock interface where the concrete is bonded is represented by the angle of friction plus cohesion. Data needed for determination of conservative values of the angle of friction and cohesion are obtained by laboratory direct shear tests. Normal stresses for these tests are determined by bracketing the stress level expected in the foundation. The tests should include a suite of core samples where the concrete is bonded to the foundation rock.

The strength of the concrete to rock interface where the concrete is not bonded to the rock is represented by the angle of friction and either the apparent cohesion or the asperity angle. To determine the angle of friction and the apparent cohesion, a suite of core samples should be tested in which the interface is either not bonded naturally or the bond has been previously broken. Judgement must be carefully exercised in determining whether apparent cohesion may be allowed along unbonded portions of the potential failure plane. Test results will frequently result in a cohesion intercept on the shear stress diagram even though the contact is unbonded. This is probably explained by shearing of the concrete during testing due to the roughness of the interface. If it is determined that apparent cohesion is to be used, it is prudent to ignore the asperity angle since they both reflect shearing resistance due to interface roughness. There may be some exceptions where it can be demonstrated that there are two or more orders of asperity angles existing at the interface, i.e. fine versus coarse irregularities. In this case, the tested samples would reflect shearing strength caused by the fine asperities, while the structure itself would mobilize the resistance provided by both fine and coarse asperities.

If it is decided that shear resistance is a combination of shear through asperities and asperity ride up, strain compatibility may become an issue. It is likely that the shear through asperities will occur at lower strains than asperity ride up. Therefore, frictional resistance from aspertity ride up may not be mobilized simultaneously, and can not be added to the ultimate shear strength.

The strength parameters resisting failure along a plane at the interface should be weighted according to the percentage of the plane where bonding of concrete to rock is expected, the percentage where unbonded contact is expected, and the percentage where shear through rock or dilation over the rock irregularities is expected. Where shear through rock is a factor, it must be determined whether the failure would likely follow a natural rock fracture or would be required to shear through intact rock. The latter determination can make a very large difference in the estimation of resisting forces because of the large difference in the strength of intact rock versus fractured rock.

Since there is likely to be a great deal of scatter in the results of the laboratory tests, it is

prudent to rationalize and select conservative strength parameters based on the test results.

11-2.3.2 Shear Strength of Potential Foundation Failure Planes and Wedges

The abutment foundations are particularly critical to the stability of an arch dam as previously discussed in Sections 11.2.1 and 11-2.2.1. Abutment instability can develop along either a planar discontinuity or a combination of planar discontinuities which intersect to form an unstable wedge. Procedures for determining the shear strength of potential foundation failure planes and wedges are discussed in detail in Chapter 5 of these guidelines.

11-2.3.3 Foundation Modulus of Deformation

The deformability of the foundation of an arch dam can affect the behavior of the structure because the dam and foundation function together as an integrated unit. The modulus of deformation provides a measure of this property. It is a representation of the deformational property of the rock mass as a whole, with all its discontinuities, as contrasted with the modulus of elasticity of an intact specimen of the rock.

There are different approaches to developing an estimation of the modulus of deformation. The most direct measurement can be made by performing static in situ jacking tests in abutment adits. There are also procedures available for measuring the dynamic elastic properties of a rock mass using seismic techniques. It is generally accepted that the lower modulus values provided by the jacking tests are more appropriate for use in arch dam foundation analysis because it appears that this technique better models the effect that discontinuities have on the foundation. However, the results obtained from a jacking test are very local in nature, and may not be appropriate for the foundation in another area.

In the case of existing structures it is unlikely that an adit will be available in which to perform either jacking or seismic tests. In some cases these tests may have been performed for the original design and the results may still be available. In this case a review of the existing data may be all that is required to develop an estimate of the foundation modulus of deformation.

Where no data is available, it is possible to develop an estimate of the foundation modulus by testing representative intact specimens of the rock obtained from core samples to determine modulus of elasticity of intact rock, then applying an appropriate reduction factor to

convert from the modulus of elasticity of the intact rock to the modulus of deformation of the rock mass. Refer to Hendron (1968) for a study which demonstrated that the fracture frequency in the rock mass is a primary factor in the reduction of the elastic modulus of a rock mass from the modulus of an intact specimen. He provides examples of how rock quality designation (*RQD*) and velocity ratio may be used to estimate the appropriate reduction factor.

TABLE 11-2.1 (From Bieniawski, 1990)
GEOMECHANICS CLASSIFICATION OF JOINTED ROCK MASSES

A. CLASSIFICATION PARAMETERS AND THEIR RATINGS

PARAMETER			RANGE OF VALUES						
1	Strength of intact rack material	Point-load strength index	>10MPa	2 - 4 Mpa	2 - 4 MPa	1 - 2 Mpa	For this low range, uniaxial compressive test is preferred		
		Uniaxial compressive strength	>250MPa	100-250MPa	50–100 MPa	25-50MPa	5-25 MPa	1 -5 MPa	<1 MPa
	Rating		15	12	7	4	2	1	0
2	Drill core quality RQD		90% - 100%	75% - 90%	50% - 75%	25%- 50%	<25%		
	Rating		20	17	13	8	3		
3	Spacing of discontinuities		> 2 m	0.6 -2 m	200-600 mm	60 - 200 mm	< 60 mm		
	Rating		20	15	10	8	5		
4	Condition of discontinuities		Very rough surface Not continuous No separation Unweathered wall rack	Slightly rough surface Separation < 1 mm slightly weathered walls	Slightly rough surface Separation < 1 mm Highly weathered walls	Sickensided surface OR Gauge < 5 mm thick OR Separation 15 mm continuous	Soft gauge > 5 mm thick OR Separation >5 mm Continuous		
	Rating		30	25	20	10	0		
5	Ground Water	inflow per 10 m tunnel length	None	< 10 liters/min	10-25 liters/min	25-125 iters/min	> 125 liters/min		
		Ratio: (joint water pressure)/(major principle stress)	0	0.0 - 0.1	0.1 - 0.2	0.2 - 0.5	> 0.5		
		General Conditions	Dry	Damp	Wet	Dripping	Flowing		
	Rating		15	10	7	4	0		

B. RATING ADJUSTMENT FOR JOINT ORIENTAITON

Strike and dip orientations for joints		Very favorable	Favorable	Fair	Unfavorable	Very unfavorable
Ratings	Tunnels	0	-2	-5	-10	-12
	Foundations	0	-2	-7	-15	-25
	Slopes	0	-5	-25	-50	-60

C. ROCK MASS CLASSES DETERMINED FROM TOTAL RATING

Rating	100←81	80←61	60←41	40←21	<20
Class No.	I	II	III	IV	V
Description	Very good rock	Good rock	Fair rock	Poor rock	Very poor rock

D. MEANING OF ROCK MASS CLASSES

Class No.	I	II	III	IV	V
Average Stand-up time	10 years for 15 m span	6 months for 8 m span	1 week for 5 m span	10 hours for 2.5m span	30 minute for 1 m span
Cohesion of the rock mass	> 400 kPa	300-400 kPa	200-300 kPa	100-200 kPa	<100 kPa
Friction angle of the rock mass	>45	35 - 45	25 – 35	15 - 25	<15

Serafim and Pereira (1983) developed a relationship between Bieniawski's (1979) Rock Mass Rating (RMR) system and the modulus of deformation of rock masses which has been shown to be valid on other projects. This relationship is as follows:

$$\text{For RMR's} < 58 \qquad E = 10^{\frac{(RMR-10)}{40}}$$

$$\text{For RMR's} > 58 \qquad E = 2 \cdot (RMR) - 100 \qquad (11\text{-}2.1)$$

E = Modulus of Deformation measured in gigapascals (GPa)
1 GPa = 145,037.7 psi.

Factors included in Bieniawski's *RMR* are unconfined compressive strength or point load strength index, *RQD*, spacing of discontinuities, condition of discontinuities, and ground water. Refer to Table 11-2.1 for his Geomechanics Classification of Jointed Rock Masses.

The above described systems may be used to develop a rational basis for estimating the modulus of deformation of the foundation of an existing dam. It must, however, be considered that different parts of a foundation may have very different moduli depending upon rock type variations, abutment and valley location, geologic structure, etc. Refer to EM 1110-2-

2201 (1994) for additional guidance.

Borehole dilatometers and pressure meters are also available for performing *in situ* deformation tests in boreholes. Data from these tests may also be useful in estimating the rock mass modulus of deformation

It must be realized that the modulus of deformation is often difficult to quantify. The techniques discussed above can be useful, however it may be more prudent to run several analyses with differing foundation modulii bracketing reasonable expected values rather than to spend effort in laboratory testing and field investigations attempting to more precisely quantify the modulus of deformation.

11-2.4 Foundation Rock Erodibility

The erosion of a plunge-pool downstream of a functioning arch dam spillway is a common occurrence unless measures have been taken to prevent it. It is a natural way for the energy of the falling water to be dissipated. Erosion of even very strong and massive rock can occur at the location of impingement of the water falling from a high dam spillway. Two examples of deep erosion of strong rock include the 79 ft. (24m) deep plunge-pool eroded in blocky andesite at Alder Dam in the USA and the 65 ft. (20m) deep plunge-pool eroded in excellent granite at Picote Dam in Portugal described by Mason (1984). Typically, the rate of plunge-pool erosion decreases with depth until a stable configuration is reached. Plunge-pools are sometimes planned for in the design of a spillway as a means of energy dissipation, but plunge-pool formation can cause a stability problem if it continues to grow laterally, eroding the dam foundation.

11-2.4.1 Field Investigations

Field investigations are conducted to determe the extent of previous erosion that may have occurred and to provide data for determining the threat to the structure posed by possible future erosion during flood events. The investigations should consider the erosion that has occurred around the spillway(s) and at or near the toe of the dam with the intent of assessing the long-term erodibility of the rock in these locations. Investigations may include hydrographic surveys to establish the depth and extent of an existing plunge-pool, and by repeating surveys after spillway flows it is possible to determine plunge-pool stabilization or continued growth. Engineering geology investigations are conducted to provide data on the foundation rock conditions including such things as rock type, fracture spacing and condition, bedding

frequency, zones of weaker rock such as softer beds and sheared rock zones, unconfined compressive strength, orientation of beds and fractures, etc. Borings may be required to provide data for the engineering geology investigations.

11-2.4.2 Assessing the Erodibility of Rock

The erodibility of rock has been the subject of numerous studies by both engineering geologists and hydraulic engineers. These studies have provided considerable insight into this very complex problem. The complexity of the interaction of the water forces with the endless variety of rock conditions encountered, however, makes each situation unique.

Rock erodibility is controlled by the following factors:

1. Intact rock strength (unconfined compressive strength).

2. Fracture frequency (size of individual rock blocks).

3. Orientation of fracture sets.

4. Shear strength and condition of fractures (continuity, roughness, aperture opening, in-filling material and alteration or weathering condition of wall rock).

5. Weak planes in the intact rock (bedding, foliation, schistocity, fissility, etc.)

6. Faults and shear zones.

An assessment of rock erodibility must take these factors into account. The integration of these factors is best accomplished by the use of one or more of the rock classification systems, such as the Geomechanics Classification developed by Bieniawski (1979 and 1990) and Barton's Q System (1974 and 1988).

Plunge-pool growth is a function of hydrologic factors as much as erodibility of the bed material. Mason (1984) presented an equation which related depth of scour to unit flow, head drop, acceleration of gravity, tail-water depth and particle size of bed material. This equation is lacking in that it looks at only one aspect of the bed's resistance to erosion, that being particle size. He did, however, calibrate the equation using both model tests and actual case histories and developed reasonable agreement with actual plunge-pools.

There have been studies made which related rock erodibility to an RMR System. Annandale (1995) presents an erodibility index related to a rippability index developed by Kirsten (1982 and 1988) using Barton's (1974 and 1988) Q System as a basis. Another study was performed by Cameron et al. (1986, 1988a, 1988b, and 1989) which relates rock erosion in emergency chute spillways to Bieniawski's Geomechanics Classification System (1979 and 1990). These may be useful in assisting the independent consultant in his evaluation of the likelihood of further development of a plunge-pool. This subject is still under investigation by government agencies and other institutions. More reports further defining rock erodibility may be expected in the literature in the future.

11-2.4.2.1 Quantitative Method of Assessing the Erodibility of Rock

There are two situations in which rock downstream from an arch dam can be subject to erosion. Some arch dams are designed with an overflow spillway which is an integral part of the dam. When the spillway operates, the rock in the area impacted by the jet can be eroded. A plunge-pool is usually provided in the area where the jet falling from the spillway impacts. The plunge-pool acts to dissipate the energy of the falling water and minimize potential for erosion of the rock. If the rock in the impact area is hard and free of fractures, an excavated but unlined plunge-pool may allow for satisfactory energy dissipation and adequately limit erosion. However, if the rock in the impact area is fractured, a substantial concrete lining of the plunge-pool may be required. For low arch dams with sound rock under and downstream from the dam, the falling jet may not have the potential to erode the rock.

An arch dam may be subject to overtopping during extreme floods if spillway capacity is not sufficient. When overtopping occurs, water falling from the dam crest will impact rock all along the downstream of the dam and the potential for erosion of the abutments becomes a concern. Erosion of abutments is a particular concern for arch dams for which rock in the abutments is not sound. Such overtopping can pluck out loose rock. Joints in the abutment rock will make the abutments particularly susceptible to erosion. Thus, it is important to consider the possible effects of erosion that would result from overtopping of the dam as that resulting from operation of the spillway.

Two questions need to be answered relative to the erodibility of a given rock resulting from overtopping of the dam or from spillway operation: 1.) Will the rock erode as a result of the impact of the falling water?, and 2.) If the rock will erode, will the extent of erosion cause a stability problem?. To answer the first question, information must be obtained on the

overall quality of the rock and the degree to which it is fractured; and a measure of the energy with which the water impacts the rock must also be developed. At present, the second question can only be answered in terms of past experience.

An article by Annandale (1995) provides a quantitative methodology by which an assessment can be made of whether or not a given rock will erode under the action of falling water. The method assumes that there is a relationship between the rate at which energy is dissipated in the receiving pool of water (the stream power P) and the erodibility of the rock. The following Erodibility Index, developed by Kirsten (1982), was used as a quantitative estimate of erodibility:

$$K_h = M_s K_b K_d J_s \qquad (11\text{-}2.2)$$

where K_h is the erodibility index, M_s is the mass strength number, K_b is the particle block size number, K_d is the discontinuity or inter-particle bond shear strength-number and J_s is the relative ground-structure number. Higher values of the Erodibility Index indicate greater resistance to erosion. In evaluating the Erodibility Index the following equations are required:

$$K_b = RQD/J_n \qquad (11\text{-}2.3)$$

where RQD is the Rock Quality Designation, a standard parameter in drill-core logging (Deere 1988), and J_n is the joint-set number, which is a function of the number of joint sets in a rock mass (Table 11-2.7). The particle block size number for cohesionless granular materials can be determined directly with the following equation:

$$K_b = 1000\ (D_{50})^3 \qquad (11\text{-}2.4)$$

where, for a cohesionless granular material, D_{50} is the mean particle size. K_d is evaluated in terms of the ratio J_r/J_a where J_r is the joint roughness number and J_a is joint alteration number. All of the independent parameters required to evaluate the Erodibility Index can be assessed with standard geotechnical field techniques and laboratory tests. Tables 11-2.2 through 11-2.10, developed by Kirsten (1982), provide the means for quantitatively evaluating these parameters from the results of field observations and standard geotechnical tests.

A collection of data obtained for unlined spillways by the U.S. Soil Conservation Service and the U.S. Bureau of Reclamation was used to develop a graphic relationship between the erodibility index and rate of dissipation in the plunge-pool. The data included values for materials ranging from 0.1 mm diameter through gravels, cohesive soils, vegetated soils, weathered rock, and jointed and fractured rock. The resulting relationship between the Erodibility Index and energy dissipation is plotted in Fig. 11-2.7, which indicates a division between cases where erosion has and has not occurred.

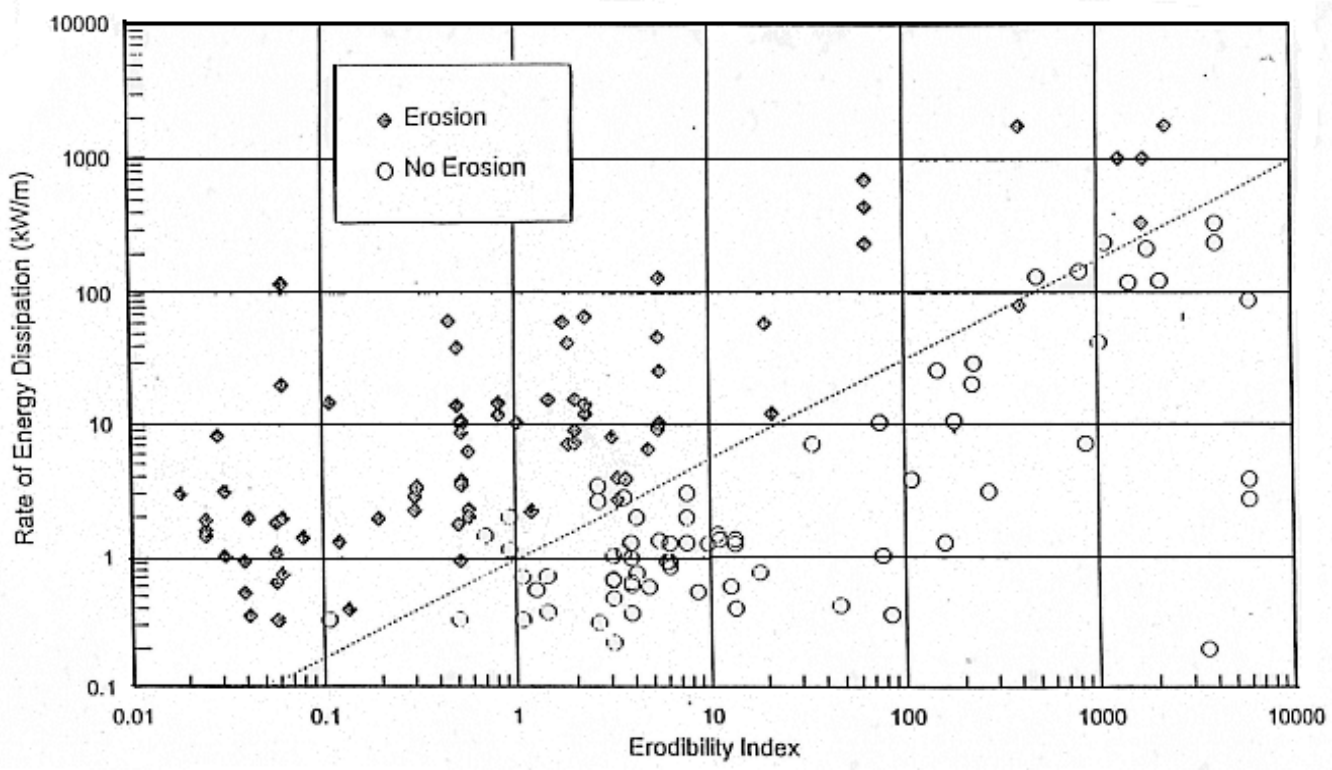

Fig 11-3 Erodibility of Rock and Earth Materials by Hydraulic Jets (Annandale, 1995)

To use the method proposed by Annandale, the Erodibility Index must be evaluated for the rock in which the plunge-pool will develop, which will require field observations and laboratory tests. In general, the equation for Stream Power is:

$$P = Q \gamma E \qquad (11\text{-}2.5)$$

Where P is the stream power, Q is the flow rate, γ is the unit weight of water (62.4 Lb/ft^3), and E is the reduction in velocity head that occurs in the impact area ($V^2/2g$). The rate at which energy dissipation will occur in the impact area must then be evaluated. Techniques and relationships for evaluation of the rate of energy dissipation can be found in The Handbook of Hydraulics by Davis and Sorensen (1969), Open Channel Flow by Henderson

(1966), Hydraulic Engineering by Roberson, Cassidy, and Chaudry (1988), and Open Channel Hydraulics by Chow (1959).

The method proposed by Annandale is at present (1997) the only available method by which a quantitative estimate of erodibility can be made in terms of the hydraulic parameters of a plunging spillway jet and characteristics of the rock in the impact area. It has had limited application at the present time, and the results should be used with caution. Nevertheless, Fig. 11-2.3 appears to indicate that the use of this method can give a reasonable conclusion as to whether the rock downstream from a given dam should be expected to erode.

Table 11-2.2. Mass Strength Number for Granular Soils (M)

Consistency	**Identification in Profile**	**SPT Blow Count**	**Mass Strength Number (M)**
Very loose	Crumbles very easily when scraped with geological pick	0-4	0.02
Loose	Small resistance to penetration by sharp end of geological pick	4-10	0.04
Medium dense	Considerable resistance to penetration by sharp end of geological pick	10-30	0.09
Dense	Very high resistance to penetration of sharp end of geological pick - requires many blows of pick for excavation	30-50	0.19
Very dense	High resistance to repeated blows of geological pick - requires power tools for excavation	50-80	0.41
Note: Granular materials in which the SPT blow count exceeds 80 to be taken as rock – see Table 11-2.4.			

Table 11-2.3 Mass Strength Number for Cohesive Soils (M)

Consistency	Identification	Vane Shear Strength (kPa)	Mass Strength Number (M)
Very soft	Pick head can easily be pushed in up to the shaft of handle. Easily moulded by fingers.	0 - 80	0.02
Soft	Easily penetrated by thumb; sharp end of pick can be pushed in 30 mm - 40 mm; moulded by fingers with some pressure.	80 - 140	0.04
Firm	Indented by thumb with effort; sharp end of pick can be pushed in up to 10 mm; very difficult to mould with fingers. Can just be penetrated with an ordinary hand spade.	140 - 210	0.09
Stiff	Penetrated by thumbnail; slight indentation produced by pushing pick point into soil; cannot be moulded by fingers. Requires hand pick for excavation.	210 - 350	0.19
Very stiff	Indented by thumbnail with difficulty; slight indentation produced by blow of pick point. Requires power tools for excavation.	350 - 750	0.41
Note: Cohesive materials of which the vane shear strength exceeds 750 kPa to be Taken as rock - see Table 11-2.4.			

Table 11-2.4 Mass Strength Number for Rock (M).

Hardness	Identification in Profile	Unconfined Compressive Strength (MPa)	Mass Strength Number (M)
Very soft rock	Material crumbles under firm (moderate) blows with sharp end of geological pick and can be peeled off with a knife; is too hard to cut triaxial sample by hand.	Less than 1.7 1.7 - 3.3	0.87 1.86
Soft rock	Can just be scraped and peeled with a knife; indentations 1 mm to 3 mm show in the specimen with firm (moderate) blows of the pick point.	3.3 - 6.6 6.6 - 13.2	3.95 8.39
Hard rock	Cannot be scraped or peeled with a knife; hand-held specimen can be broken with hammer end of geological pick with a single firm (moderate) blow.	13.2 - 26.4	17.70
Very hard rock	Hand-held specimen breaks with hammer end of pick under more than one blow.	26.4 - 53.0 53.0 - 106.0	35.0 70.0
Extremely hard rock	Specimen requires many blows with geological pick to break through intact material.	Larger than 212.0	280.0

Table 11-2.5 Mass Strength Number for Detritus (M).

Consistency	Identification in Profile	In Situ Deformation Modulus (MPa)	Mass Strength Number (M)
Very loose	Particles very loosely packed. High percentage voids and very easily dislodged by hand. Matrix crumbles very easily when scraped with geological pick. Raveling often occurs in excavated faces.	0 - 4	0.02
Loose	Particles loosely packed. Some resistance to being dislodged by hand. Large number of voids. Matrix shows small resistance to penetration by sharp end of geological pick.	4 - 10	0.05
Medium dense	Particles closely packed. Difficult to dislodge individual particles by hand. Voids less apparent. Matrix has considerable resistance to penetration by sharp end of geological pick.	10 - 30	0.10
Dense	Particles very closely packed and occasionally very weakly cemented. Cannot dislodge individual particles by hand. The mass has a very high resistance to penetration by sharp end of geological pick - requires many blows to dislodge particles.	30 - 80	0.21
Very dense	Particles very densely packed and usually cemented together. The mass has a high resistance to repeated blows of geological pick - requires power tools for excavation.	80 - 200	0.44
Note: Determined by plate bearing test of diameter 760 mm.			

Table 11-2.6 Joint Count Number (J_C).

Number of Joints Per Cubic Meter (J_C)	Ground Quality Designation (RQD)	Number of Joints Per Cubic Meter (J_C)	Ground Quality Designation (RQD)
33	5	18	55
32	10	17	60
30	15	15	65
29	20	14	70
27	25	12	75
26	30	11	80
24	35	9	85
23	40	8	90
21	45	6	95
20	50	5	100

Table 11-2.7 Joint Set Number (J_n).

Number of Joint Sets	**Joint Set Number (J_n)**
Intact, no or few joints/fissures	1.00
One joint/fissure set	1.22
One joint/fissure set plus random	1.50
Two joint/fissure sets	1.83
Two joint/fissure sets plus random	2.24
Three joint/fissure sets	2.73
Three joint/fissure sets plus random	3.34
Four joint/fissure sets	4.09
Multiple joint/fissure sets	5.00

Table 11-2.8 Relative Ground Structure Number (J_S).

Dip Direction of Closer Spaced Joint Set (degrees)	**Dip Angle of Closer Spaced Joint Set (degrees)**	**Ratio of Joint Spacing, r**			
		1:1	**1:2**	**1:4**	**1:8**
180/0	90	1.14	1.20	1.24	1.26
In direction of stream flow	89	0.78	0.71	0.65	0.61
	85	0.73	0.66	0.61	0.57
	80	0.67	0.60	0.55	0.52
	70	0.56	0.50	0.46	0.43
	60	0.50	0.46	0.42	0.40
	50	0.49	0.46	0.43	0.41
	40	0.53	0.49	0.46	0.45
	30	0.63	0.59	0.55	0.53
	20	0.84	0.77	0.71	0.67
	10	1.25	1.10	0.98	0.90
	5	1.39	1.23	1.09	1.01
	1	1.50	1.33	1.19	1.10
0/180	0	1.14	1.09	1.05	1.02
Against direction of stream flow	-1	0.78	0.85	0.90	0.94
	-5	0.73	0.79	0.84	0.88
	-10	0.67	0.72	0.78	0.81
	-20	0.56	0.62	0.66	0.69
	-30	0.50	0.55	0.58	0.60
	-40	0.49	0.52	0.55	0.57
	-50	0.53	0.56	0.59	0.61
	-60	0.63	0.68	0.71	0.73
	-70	0.84	0.91	0.97	1.01
	-80	1.26	1.41	1.53	1.61
	-85	1.39	1.55	1.69	1.77
	-89	1.50	1.68	1.82	1.91
180/0	-90	1.14	1.20	1.24	1.26

Notes: 1. For intact material take $K_S = 1.0$

2. For values of r greater than 8 take K_S as for r = 8

Table 11-2.9 Joint Roughness Number (J_r).

Joint Separation	Condition of Joint	Joint Roughness Number
Joints/fissures tight or closing during excavation	Discontinuous joints/fissures Rough or irregular, undulating Smooth undulating Slickensided undulating Rough or irregular, planar Smooth Planar Slickensided planar	4.0 3.0 2.0 1.5 1.5 1.0 0.5
Joints/fissures open and remain open during excavation	Joints/fissures either open or containing relatively soft gouge of sufficient thickness to prevent joint/fissure wall contact upon excavation. Shattered or micro-shattered clays	1.0 1.0

Table 11-2.10 Joint Alteration Number (J_a).

Description of Gouge	**Joint Alteration Number (J_a) for Joint Separation (mm)**		
	1.0[1]	**1.0 - 5.0[2]**	**5.0[3]**
Tightly healed, hard, non-softening im-permeable filling	0.75		
Unaltered joint walls, surface staining only	1.0		
Slightly altered, non-softening, non-cohesive rock mineral or crushed rock filling	2.0	2.0	4.0
Non-softening, slightly clayey non-cohesive filling	3.0	6.0*	10.0*
Non-softening, strongly over-consolidated clay mineral filling, with or without crushed rock	3.0*	6.0**	10.0
Softening or low friction clay mineral coatings and small quantities of swelling clays	4.0	8.0*	13.0*
Softening moderately over-consolidated clay mineral filling, with or without crushed rock	4.0*	8.0*	13.0
Shattered or micro-shattered (swelling) clay gouge, with or without crushed rock	5.0*	10.0*	18.0

Note:
1. Joint walls effectively in contact.
2. Joint walls come into contact after approximately 100 mm shear
3. Joint walls do not come into contact at all upon shear
4. * Values added to Barton et al's data
5. ** Also applies when crushed rock occurs in clay gouge without rock wall contact

11-2.4.3 Erosion Downstream from the Dam

Jets that impact the downstream area with a large velocity (100 ft/sec or larger) will usually produce erosion unless the rock is extremely hard and quite sound. Cases where erosion has not occurred are rarely described in the technical literature since they do not create problems. In actuality, erosion of rock has occurred in almost all cases where a high-velocity jet impacts on rock, particularly if the rock in the impact area is of poor quality or is highly weathered or fractured.

11-2.4.3.1 Historic Observations of the Depth and Extent of Erosion

Cases in which erosion downstream from spillways has occurred are abundant in the technical literature. However, information on erosion due to overtopping of a dam is scarce. Data from the reported cases of erosion downstream from spillways has been used by several engineers to provide an estimate of the depth of expected erosion due to impact of a falling jet of water. The depth of erosion is a function of the velocity at which the jet enters the plunge-pool, the angle at which the jet enters, the depth of water in the impact area, and the physical character of the rock. Field and laboratory observations have shown that erosion will continue with further operations, but at a decreasing rate. Bulletin Number 58 of the International Commission on Large Dams (1985) states that significant plunge-pool erosion has not been observed for many existing spillways. However, in many cases those spillways have operated only for short durations and at small discharges since they were constructed. Table 11-2.11 provides a summary of information on several cases where erosion downstream from a spillway has been observed and recorded.

Table 11-2.11 shows that in some cases deep erosion has been experienced even though the rock in the impact area was apparently hard. In general the depth of erosion depends upon the energy of the falling jet, the duration of the flow, and the character of the rock. The extent of erosion depends mostly on the character of the rock. If the upper layers of rock are more erodible than the deeper layers, the lateral extent of the erosion will spread to form a wider hole since the harder lower layers will deflect the high velocities toward the more erodible sides.

Table 11-2.11 Historic Scour Depths of Plunge-pools

	Material	**Country**	**q**[1]	**Head**[3]	**Depth**[3]
Alder	Andesite	USA	20,000[2]	300	79
Na-ciemento	SS,MS[4]	USA		250	
Picote	Granite	Portugal	1250	213	118
Kariba	Gneiss	Zimbabwe		415	160
Tarbela	Limestone	Pakistan	570 854	320 323	121 160
Karakaya		Turkey	1034 619	413 403	131 90
Keban		Turkey	351	360 335	75 44
Killckaya		Turkey	130	245	39
Elmali	Granite		32	89	49
Kondo-poga	Granite		149	39	21
Cabora Bassa		Mozam-bique	2957 283	300 315	223 75
Ukai	Basalt	India	854	154	95
Guri	Basalt	Venezuela	52,800[2]		118

[1] Discharge q is unit discharge in cfs/ft.
[2] Only the total discharge for the spillway was available.
[3] Head is given in feet.
[4] Abbreviations are: SS-Sandstone, MS-Mudstone.

11-2.4.3.2 Analytical Methods for Calculating Erosion Depth Downstream from Spillways

Maximum Depth of Scour. As pointed out in Section 11-2.5.2.1, erosion of concern can occur downstream from an arch dam due to spillway operation if the spillway is located on the dam.

Over the years, a large number of empirical equations have been developed for estimation of the depth of erosion which should be expected in the area impacted by the jet produced by operation of an overflow spillway. Mason (1985) has documented 25 different equations developed for this purpose, dating from 1937. Figure 11-2.4 shows a typical cross section

of an arch dam with an overflow spillway and the parameters that have been found to be important in the estimation of depth of erosion. Erosion of rock by an impacting jet occurs when the rock is fractured. Turbulent eddies unsteady pressures produced by the impacting jet attack, move, and eventually pluck out particles of rock. Tailwater depth has an important influence on the maximum depth of erosion since deeper water in the impact area results in greater energy dissipation within the pool. Deeper tailwater results in less erosion.

The parameters which have been found to be important in determining the depth of erosion D are shown on Fig. 11-2.4. They include the head H (the vertical distance between the reservoir surface and the tailwater surface), the tailwater depth h_2, the angle at which the jet enters the pool Θ, the discharge per unit width of the jet q, and the size of fractured rock particles d.

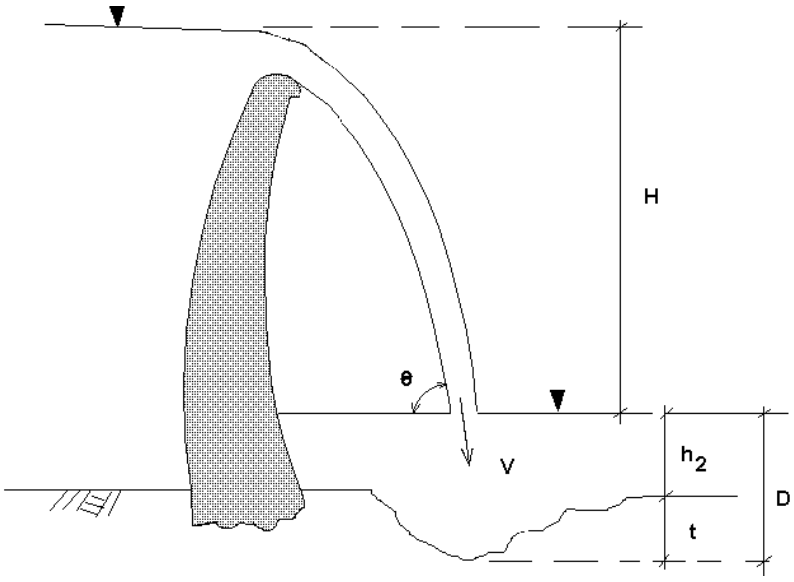

Fig 11-2.4 Typical arch dam with overflow spillway and plunge-pool

The best known of these equations, and the simplest, is that by Veronese (1937):

$$D = 1.32\ H^{0.225}\ q^{0.54} \qquad (11\text{-}2.6)$$

where D is the maximum scour depth (FT), H is the difference in elevation between the reservoir and the tailwater surfaces (FT), and q is the unit discharge (CFS). The Veronese Equation, as is true of all other forms of the equation, was derived by empirical analysis of recorded data on erosion downstream of flip-bucket and overflow spillways. In the Veronese Equation, the scour depth D is measured from the tailwater elevation. Thus, tailwater depth

is considered explicitly. This equation has been widely used by the design profession and is given in the U.S. Bureau of Reclamation Design of Small Dams (1987).

Yildiz (1994) reasoned that the Veronese Equation had been developed for cases where the spillway jet entered the tailwater at a nearly vertical angle as would occur for an overflow spillway on a high arch dam as shown in Fig. 11-2.3. Yildiz suggested that the depth of scour as given by Eq. 11-2.6 should be measured along a line tangent to the direction of the jet as it enters the plunge-pool. Fig. 11-2.4 shows such a configuration. Yildiz then modified the Veronese Equation as:

$$D = 1.32\, H^{0.225}\, q^{0.54}\, \text{Sin}\, \Theta \qquad (11\text{-}2.7)$$

where Θ is the angle of inclination of the jet at the water surface in the plunge-pool. The resulting scour-depth predictions using Eq. 11-2.7 give a better fit to the recorded erosion depths downstream from spillways than is achieved using Eq. 11-2.8.

Although the size of fractured rock (the size of the fractured particles of rock that would be plucked out by the action of the spillway jet) is considered to be important, neither Eq. 11-2.8 nor Eq. 11-2.9 considers rock size. Mason (1985), on the basis of data from model studies as well as prototype experience, derived the following equation for depth of erosion:

$$D = 3.72\, \frac{q^{0.60} H^{0.05} h_2^{.015}}{g^{0.30} d^{0.10}} \qquad (11\text{-}2.8)$$

In Eq. 11-2.8, g is the acceleration due to gravity, d is the mean rock size, and h_2 is the tailwater depth. Mason found that Eq. 11-2.8 gave scour depth predictions which agreed well with prototype experience and also yielded maximum scour depths which agreed well with the results obtained in model studies when H was considered to be the total energy in the jet as it leaves the spillway. For prototypes, he found that the effect of accounting for energy loss occurring on the spillway surface was negligible.

It appears that either the modified Veronese Equation 11-2.7 or Mason's Equation 11-2.8 is as good as is available for estimating depth of erosion downstream from a spillway. However, the user should always be aware of the fact that both equations are strictly empirical and could either overestimate or underestimate the potential scour depth for a particular rock condition or jet configuration.

Pattern of Erosion. The pattern of erosion downstream from a spillway is very much dependent upon the characteristics of the rock in the impact area. If the joint pattern and hardness of the rock is uniform throughout the area of impact and does not change with depth, the pattern will be generally symmetric about the centerline of the impacting jet. The length of the eroded hole will be from 3 to 5 times the depth of erosion and the width of the hole will be from 2.0 to 2.5 times the width of the spillway jet.

If discontinuities in the rock exist, the potential scour depth and pattern may be strongly affected. For example, if part of the rock is much harder and more durable than the average, erosion will be uneven and strong lateral currents can be created in the basin. If lower layers of the rock are more sound than the upper layers, both the lateral and longitudinal extent of erosion will be increased significantly as a result of the high velocity of the jet being deflected toward the edges of the hole.

11-2.4.3.3 Erosion Resulting from Overtopping of an Arch Dam

Erosion downstream from an arch dam due to overtopping is quite different than that which occurs as a result of operation of an overflow spillway. The depth of erosion in either case is very much dependent upon the duration of the flow. Deep erosion downstream from a spillway is to be expected and the overflow spillway is designed so that the jet from the spillway impacts as far from the toe of the dam as possible. However, during overtopping water would fall from the top of the dam and impact very near its toe. Depths of erosion would be very much dependent upon the depth of overtopping; large depths of overtopping would result in greater energy impacting the rock producing deeper erosion. By contrast, depths of overtopping of a foot or less should not produce significant erosion of rock at an arch dam site. If deep erosion were to occur near the toe of the dam the safety of the dam could be compromised. Erosion of the abutments can be a serious concern because material in the abutments is often less sound and more erodible than the rock at the toe of the highest portion of the dam.

Spills are a relatively common occurrence and, depending upon the magnitude of the passing flood, often occur with long durations. As a result, the depth and extent of erosion downstream from spillways have been documented for many cases as was shown in Section 11-2.4.3.1. By contrast, overtopping of a dam, which is an infrequent event of relatively short duration, has received less attention in the technical literature. A number of arch dams that have been overtopped are listed in the technical literature. Unfortunately, little has been published on any erosion resulting from the overtopping. Gibson Dam on the Sun River in

Montana is an exception; it was overtopped by depths of up to 6.5 feet for 20 hours in June 1964. Although some loose rocks were plucked out during the overtopping, the resulting erosion was minor and did not have any effect on the safety of the dam.

Equations 11-2.7 and 11-2.8 were developed from data on long term operation of spillways. They are not applicable for estimating the maximum depth of erosion which might occur as a result of a single overtopping, since overtopping is a rare event of relatively short duration. As the overtopping of Gibson Dam has shown, there is little reason to be concerned about erosion from overtopping if the rock which is impacted by the falling jet is sound even for relatively large depths of overtopping. However, if the rock is jointed, and analysis shows that the dam could be overtopped by significant depths during passage of a flood, there may be reasons to take precautions against damage by erosion, particularly on the abutments. Such precautions could include removal of the rock in question and replacing it with dental concrete, covering the rock in question with a layer of shotcrete, or placement of a reinforced concrete slab along the toe of the dam in the area of concern.

1-2.4.3.4 Examples of Calculations for Maximum Scour Depth

The following table presents data and the results of calculating maximum scour depth for several cases using both Equations 11-2.9 and 11-2.10. The cases were selected from Table 11-2.11 for those cases where all information needed for the calculation was available. For the use in his equation (11-2.10), Mason used a rock particle size of 0.8 feet, which predicted scour depths in close agreement with prototype experience for cases where the rock size was not available.

Comparing the field-measured scour depths in Table 11-2.11 with the predictions of values computed using the modified Veronese (Eq. 11-2.7) and Mason (Eq. 11-2.8) equations shows that the two equations predict some situations well but miss others significantly. The modified Veronese Equation appears to give relatively good agreement, while Mason's equation appears to over-predict the maximum scour depth. Part of this may be due to the assumed d = 0.8 ft for all of the cases where information on the fractured size of the rock was not available. If the actual rock size were greater than 0.8 ft, the predicted scour depth would be less. The results shown in Table 11-2.11 indicate that the modified Veronese Equation (Eq. 11-2.7) gives a reasonable estimate of scour depth and can be used for evaluation purposes.

Table 11-2.11 Example Calculations of Maximum Scour Depths

Name	q (cfs)	Θ	h_2 (ft)	H (ft)	Field (ft)	Eq. 11-2.7 (ft)	Eq. 11-2.8 (ft)
Elmali	337	40^o	13.1	88.6	49	54	81
Kondopoga	150	30^o	3.3	39.4	21	23	39
Tarbela	80	50^o	50.8	323.1	161	142	185
Picote	1252	39^o	68.9	213.2	118	131	239
Ukai	851	43^o	13.1	154.2	95	107	145

1-2.4.3.5 Developing Water-Surface Profiles

In order to check potential scour conditions downstream from an arch dam, it is necessary to calculate a point of impact of the spillway jet during passage of the flood. Computation of the nappe trajectory provides the necessary parameters for use of the equations for estimation of maximum scour depth, which are listed earlier in this section. This computation involves the computation of the trajectory of the nappe leaving the spillway lip. Procedures for estimating the nappe trajectory are given in the USBR's "Design of Arch Dams".

11-3 CONCRETE MATERIAL PARAMETERS

To perform a safety evaluation of a concrete arch dam as described in this chapter, the properties of the dam concrete must be known. In the case of an existing dam, information on the concrete properties may be available from the previous studies or construction documents. If such information is adequate, only a review and interpretation of the data may be necessary. Where little or no information, additional concrete investigations may be required. The scope of new investigations will depend on the amount and quality of the available data and also on the existing conditions of the dam concrete.

The purpose of concrete investigation is to establish the quality of concrete and to obtain its necessary properties for use in the structural analysis. It usually consists of the following field investigations and laboratory test activities:

11-3.1 Visual Inspection of the Concrete

A visual inspection of the dam is required to establish the extent of concrete deterioration, conditions of construction joints, location and size of cracks, areas of distressed concrete, and locations for core drilling. All accessible concrete of the dam should be visually inspected. Similarly, concrete cores taken for laboratory tests should be visually inspected for voids, debris, joints, deterioration, and other defects.

Careful visual inspection is the most important investigation that can be done. For example, it is usually the case that a crack in the concrete has far more effect on the behavior of the dam than does a variation in ultimate compressive strength or the modulus of elasticity. At times, elaborate and expensive coring and testing programs have been undertaken, which in the end, reveal far less than an astute visual observation of the site.

11-3.2 Ultrasonic Pulse Velocity Test

The purpose of in-situ ultrasonic pulse velocity or UPV testing is to evaluate the overall quality of concrete in existing concrete dams. Suitable equipment and standard procedure for pulse velocity tests are described in ASTM C-597. The method is based on the principle that the velocity of an ultrasonic pulse through a material is related to dynamic modulus of elasticity, density, and Poisson's ratio of the material. Any changes in the modulus caused by deterioration, cracks, poor compaction, voids, joints, etc., would affect the velocity of ultrasonic pulses. Such defects and variations in the concrete increase the ultrasonic transit time, and thus results in a slower velocity.

The UPV testing equipment consists of a transmitter and receiver transducer coupled to a signal generator and a recording device displaying transit time. The piezoelectric transducers are placed against the dam to be examined in various strategic configurations. The signal generator produces electric pulses which cause the transmitter to vibrate at its natural resonant frequency, producing sound waves that pass through the concrete, reaching the receiver which will be detected by the recording device which will then display the transit time. The velocity is calculated from the time elapsed for the pulse to travel a predetermined length through the dam or a test specimen

$$UPV = \frac{Path\ Length}{Transit\ Time}$$

Unusually low velocities (less than 10,000 ft/sec) or a wide range of measured velocities, generally indicate deteriorated or poor quality concrete. Table 11-3.1 shows the general classification used in correlating the UPV with the quality of concrete. As shown in the table, normal quality concrete typically produce velocities in the range of 12,000 to 15,000 ft/sec.

Attempts to correlate pulse velocity data with concrete strength parameters have not generally been successful. Although UPV does not directly measure strength, it does indicate general condition and uniformity and can be used to complement and correlate with the information obtained by visual inspection and core sampling. The UPV works effectively, if both surfaces of the concrete dam are accessible and sound waves pass through minimum number of joints. Because with each pass through a joint, the wave front is dispersed and losses 50 to 70 percent of its amplitude.

Table 11-3.1 (Leslie and Cheesman 1949)

Ultrasonic Pulse Velocity, ft/sec	General Condition of Concrete
Above 15,000	Excellent
12,000 - 15,000	Generally good
10,000 - 12,000	Questionable
7,000 - 10,000	Generally poor
Below 7,000	Very poor

Sonic Coring Tests.

Sonic coring (sonic logging) tests work the same way as the UPV tests, except that the transmitter and receiver are sealed and placed in adjacent vertical core holes to check the quality and uniformity of concrete. During the tests, coring holes are filled with water to create acoustic coupling for transmission of ultrasonic pulses between transducers and the concrete. This method can be used in certain situations, such as underwater regions of the dam or when a more controlled spot check for establishing the quality of concrete is required.

11-3.3 Concrete Coring and Specimen Parameters

Concrete coring should be performed in conformance with ASTM C42. The purpose of coring is twofold. First, a random coring and testing program can be used to determine the uniformity of the concrete, and to locate problem areas. Second, once potential problem areas are discovered, coring can be concentrated in these areas to better define properties. While average values of strength and elastic modulus are of some value for structural analysis, investigations should focus on "weak links" since these problem areas are more likely to govern the safety of the dam, than the average properties.

Normally, concrete cores are extracted from the downstream face of the dam by drilling horizontally or from inside the dam galleries. When vertical drilling is done to extract samples, care should be taken to obtain samples with intact bond between construction lifts so that the strength of lift joints can be determined.

The condition of the entire core should be accurately logged during drilling. The impression of an experienced engineer during a visual inspection of the extracted core is very important in ensuring that the test results are indicative of the condition of the dam.

Concrete cores extracted from different locations generally show different strength depending on the batches of concrete placed at that location. They are also influenced by the aggregate sizes within a particular specimen and the local deterioration of the mass concrete. The material parameters from a testing program should therefore be based on the overall condition of all cores and deterioration of the dam concrete and not just on a selected “best” core samples.

11-3.4 Petrographic Examination of Concrete

Where there is evidence of concrete deterioration, a petrographic examination of concrete specimens should be carried out to ascertain the presence of any deleterious chemical re-

actions such as alkali-aggregate reactivity. This examination should be conducted in accordance with ASTM C856, Petrographic Examination of Hardened Concrete.

11-3.5 Elastic Properties

An estimate of the elastic modulus of concrete is necessary for calculating stresses induced in the dam by strains associated with loading. Poisson's ratio, which relates the lateral strain to axial strain within the elastic range, is also needed for arch dams.

The static modulus of elasticity (chord modulus) and Poisson's ratio should be determined in accordance with the standard test method described by ASTM C469. The modulus of elasticity and Poisson's ratio of concrete typically are measured in a compressive strength test of specimen that is loaded to failure in a period of about 2 to 3 minutes, and the modulus obtained in such a test may be called the short-term or instantaneous value. However, concrete is a material that exhibits considerable creep under prolonged loading, so the short-term modulus is not suitable for evaluating the deformations of a dam subjected to continuing static loads. The effects of creep resulting from such loads can be presented by using a reduced modulus of elasticity in the static displacement calculations. Typically the short-term modulus is reduced by 25 to 30 percent to obtain a *sustained modulus* value in prolonged loading. The elastic modulus is also affected by the rapid seismic loading, which is discussed in Section 11-3.8.

11-3.6 Thermal Properties

The basic properties required for performing a thermal stress analysis include coefficient of thermal expansion, specific heat, thermal conductivity, and thermal diffusivity.

Coefficient of Thermal Expansion. In general, concrete expands with heating and contracts with cooling. The strain associated with the change of temperature depends on the coefficient of thermal expansion and on the degrees by which temperature rises or drops. The coefficient of thermal expansion for concrete varies directly with the coefficient of thermal expansion of the aggregates, and typically the values range from 3.5 to 7×10^{-6} in./in./ °F. In the absence of measured data, an average value of 5×10^{-6} in./in./ °F may be used.

Specific Heat. Specific heat is storing heat capacity per unit temperature. Compared to a specific heat of 1.0 for water, specific heat of mass concrete typically varies between 0.20 and 0.25 Btu/lb-°F. In the absence of measured data, an average value of 0.22 Btu/lb-°F should be used.

Thermal Conductivity. Thermal conductivity is a measure of the ability of a material to direct heat flow. Typical values of thermal conductivity for mass concrete ranges from 13 to 24 Btu-in./hr-ft^2-°F.

Thermal Diffusivity. Thermal diffusivity is the rate of heat flow through a unit area divided by the product of the specific heat times the density times the gradient.

$$\frac{\text{Rate of heat flow through unit area } {}^{(BTU)}/_{(FT^2*HR)}}{(\text{Specific heat } {}^{(BTU)}/_{(\#*DEG)}) * (\text{Density } {}^{(\#)}/_{(FT^3)}) * (\text{Temp. gradient } {}^{(DEG)}/_{(FT)})} = \text{Thermal diffusivity } {}^{(FT^2)}/_{(HR)}$$

For mass concrete, it varies in the range of 0.02 to 0.06 ft^2/hr. In the absence of measured data, an average value of 0.04 ft^2/hr may be used.

11-3.7 Strengths of Concrete

11-3.7.1 Compressive Strength

The compressive strength of concrete shall be determined in accordance with ASTM 39.

11-3.7.2 Tensile Strength

While there are many methods of determining the tensile strength of concrete, this parameter has little significance in the performance of an arch dam. Core samples can be obtained and tested in a variety of ways, but the tensile strength of an arch dam is usually limited by the ability of horizontal lift joints, vertical contraction joints, and pre-existing cracks to resist tension. For this reason, the accurate determination of the tensile strength of the intact concrete may not be necessary.

Often, linear elastic analysis of arch dams will predict tensile stresses, and it can be helpful for the analyst and reviewer to have a tensile stress value that serves as a flag for performance evaluation of the dam. This flag has no real physical significance, but it can alert the analyst or reviewer that predicted tensile stresses are too high, and that the effect of tensile cracking should be incorporated into the model. For the linear-elastic analysis, helpful flag values are the apparent tensile strength proposed by Raphael (1984) for the static and dynamic loading conditions, as shown in Fig. 11-3.2.

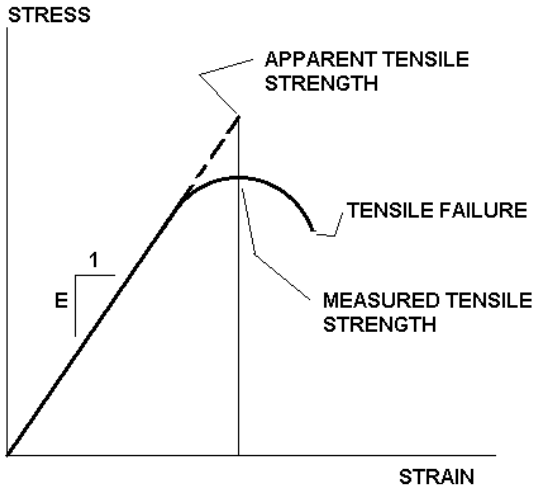

Fig. 11-3.1 Apparent tensile strength (From Raphael 1984).

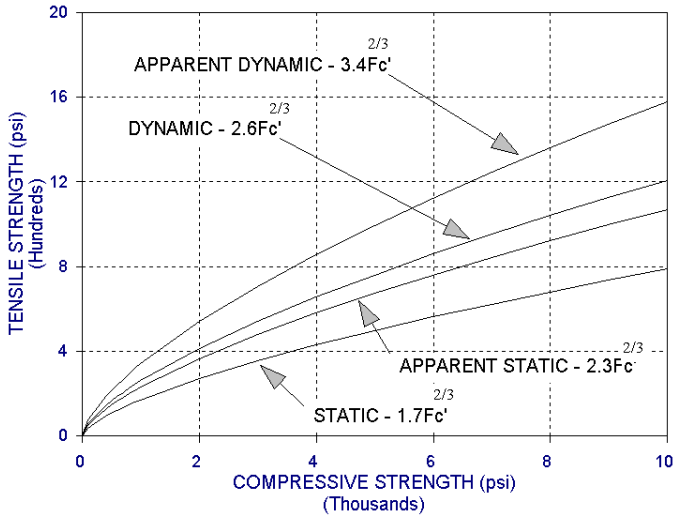

Fig. 11-3.2 Design chart for tensile strength (From Raphael 1984).

Several researchers, notably Raphael (1984), have recognized that the measured tensile strength of concrete should be augmented by a factor for comparison with results of the linear finite-element analysis. It is evident in the stress-strain curves from laboratory tests (Fig. 11-3.1) that the stress is not proportional to strain throughout the test. Thus, if the finite element model assumes a linear stress strain relationship, the apparent tensile strength which is the linear tensile stress at the failure value of tensile strain is considered to be more appropriate than the measured tensile strength. The modulus of rupture which is obtained on the principle of linear behavior provides an experimental method for measuring the apparent tensile strength. If only splitting tension tests are conducted, apparent tensile strength can be obtained from the measured tensile strength by multiplying

by 2.3/1.7 = 1.35 (two lowest plots in Fig. 11-3.2). The concept of apparent tensile strength also applies to seismic loading, which is discussed next.

It should be realized that the apparent tensile strength is not an "allowable" tensile stress value. If predicted tensile stresses are below this value but extend over large areas of the dam, the analyst should still suspect the results and re-run the analysis to account for re-distribution of tensile stresses due to joint and crack opening.

11-3.7.3 Shear Strength

Although arch dams are designed to resist load by compressive arch stresses, shear stress can be a problem on certain planes within the dam, especially near the foundation. The simplest criterion for failure for concrete under multiaxial stresses is based on the Mohr-Coulomb theory. The Mohr-Coulomb diagram shown in Fig. 11-3.3 represents a procedure for determining the failure under combined stress states from which an estimate of the shear strength can be obtained. In this figure, the point at which the failure envelope intersects the vertical axis represents the strength of concrete in pure shear, τ_o. Using this method the shear strength of the concrete has been found to be approximately 20% of the uniaxial compressive strength.

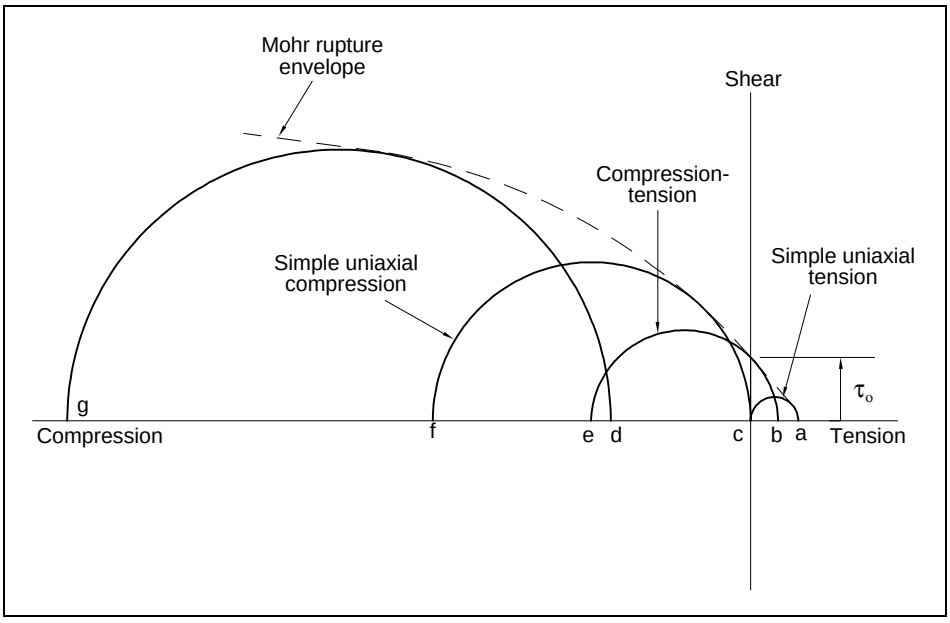

Fig. 11-3.3 Typical Mohr rupture diagram for concrete.
(From S. Mindess and J.F. Young, Concrete, 1981)

11-3.8 Dynamic Material Properties

During earthquake excitation, the rate of loading is much greater than in a short-term compression test. The strains in a typical concrete dam earthquake response are developed at frequencies of 2.5 to 25 Hz, which corresponds to times from zero to peak load of 10 to 100 milliseconds. Tests performed at such rapid rates of loading demonstrate that the dynamic modulus of elasticity is about 25 percent greater than that observed in short term tests, and this increased modulus should be used in the dynamic response analyses. Tests performed at loading rates typical of earthquake response, such as those mentioned above with regard to the dynamic modulus of elasticity, have shown that on average tensile strength is increased by about 50 percent at these high strain rates. Comparison of the lowest and highest plots in Fig. 11-3.2 shows that the apparent tensile strength of concrete under seismic loading is twice its splitting tensile strength under short-term loading. Similarly, the rapid rate of seismic loading increases the compressive strength but this increase is reported to be 30 percent as opposed to 50 percent for the tensile strength.

Since this measure of tensile strength has been developed without regard for any specific weakness in the mass concrete, such as the lift joints, and because the tensile strength across such joints may be 15 to 20 percent less than in the homogenous material, it would be judicious to assume the tensile strength for the lift joints is somewhat less than that for the homogenous concrete. In fact, the actual tensile strength across the poorly constructed lift joints of some older dams could be even drastically lower than that for the homogeneous concrete. Thus it is important that such weaknesses in the mass concrete are accounted for in the seismic safety evaluation, and that the actual reduced strength at lift joints is determined by material testing.

11-4 LOADING

Arch dams are subjected to various loads. Loads can be categorized into 2 basic types, static and dynamic. Static loads are sustained loads that do not change, or change very slowly compared to the natural periods of vibration of the structure. A dam's response to static loads is governed by its stiffness. Examples of static loads include dead load, hydraulic load from normal or flood conditions, forces from flowing water changing direction, uplift, forces from ice expansion, and internal stresses caused by temperature changes. Dynamic loads are transitory in nature. They are typically seconds or less in duration. Because of the speed at which they act, the inertial and damping characteristics of the dam as well as its stiffness affect the dam's behavior. Examples of dynamic loads include earthquake-induced forces, blast-induced forces, fluttering nappe forces, or forces caused by the impact of ice, debris, or boats.

11-4.1 Dead Load

Dead load in arch dams is the weight of the concrete plus appurtenant structures such as gates, bridges, and outlet works. The unit weight of the concrete is based on the laboratory test results of the mix design and/or physical measurements of concrete cores. However, mass concrete containing natural sand and gravel or crushed-rock aggregates generally weighs about 150 pounds per cubic foot (pcf). In the absence of measured data, this unit weight can be assumed for the concrete. Dead load is normally imposed on cantilever monoliths prior to the grouting of the contraction joints. This should be taken into account when analyzing then dam. (See section 11-5.2.2.)

Compared to the dam itself, the weight of appurtenances is typically negligible and may be ignored in the stress analysis. Massive outlet works and overflow-ogee-weir spillways, however, may have noticeable effects on the static and dynamic stresses and their weight should be considered.

11-4.2 Hydraulic Loading

11-4.2.1 Normal Water Loads

Normal water loads include hydrostatic pressures on the dam faces resulting from the reservoir and tailwater during the normal operation of the hydroelectric project. The reservoir levels should correspond to the maximum normal-high-water-level (NHWL), which is usually the level of the spillway crest for ungated spillways and the top of the spillway gates for gated spillways. Normal tailwater can be obtained from historical operation records.

For computation of normal water loads, headwater and tailwater pressures are considered to vary linearly with depth and to act normal to the dam surfaces. In addition to the dam surface, headwater pressures should also be applied on the foundation rock at the valley floor and flanks since reservoir water load causes foundation rock to deform and produce additional deformations and stresses in the dam. In computation of water loads, a constant unit weight of 62.4 pcf may be assumed for fresh water.

Acting in the opposite direction, tailwater generally produces stresses with opposite signs of those induced by the headwater. The effect of tailwater, therefore, is to reduce both tensile and compressive stresses below the tailwater elevations. This effect diminishes when the tailwater depth is less than 20% of the dam height. For these reasons, it is generally considered conservative to ignore tailwater loads in an arch dam stress analysis, and may be omitted for simplicity. If, however, tailwater effects uplift pressure on a failure plane on which sliding stability is being analyzed, uplift should be considered.

11-4.2.2 Flood Loads

The basic flood loads include hydrostatic pressures on the dam faces resulting from the reservoir and tailwater elevations which occur during the passage of the inflow design flood (IDF). Chapters 2 and 8 describe the methods to be used for defining the IDF and the probable maximum flood.

The water pressures due to flood are also assumed to vary linearly with depth and to act normal to the dam surfaces and to valley floor and flanks of the foundation rock.

11-4.2.3 Uplift

Uplift or pore water pressures develop when water enters the interstitial spaces within the body of an arch dam as well as in the foundation joints, cracks, and seams. Under static loading conditions, the effect of pore water pressure is to reduce normal compressive stresses within the concrete and to increase the corresponding normal tensile stresses should they exist (NRC 1990). A computer analysis of these effects on Morrow Point Dam, a 465-ft-high thin arch dam, and on a thick arch dam of similar height and crest length, showed a stress change of less than 20 psi -- i.e. about less than 5% of the tensile strength of the concrete. Because of this minor change in stress, the effects of pore water pressure on stresses within an arch dam may be ignored in the absence of any cracks.

When the stress results and field conditions for a gravity (thick) arch dam indicates that tensile cracking will develop at the dam-foundation interface, uplift should be considered and applied as external loads on both faces of the crack. Uplift does not need to be considered in the stress analysis for thin arch dams.

Uplift should always be considered in the sliding stability analysis of the potential failure planes within the foundation (Section 11-5.4) or along the dam-foundation interface (Section 11-5.6.1).

When required, distribution of uplift pressure at the contact surface between an arch dam and the foundation rock can be determined using the field data from piezometer readings or by performing seepage analysis. In general, the distribution of uplift pressure is influenced by the geological conditions of the foundation rock near the base of the dam, by location and length of drain, and by the crack length. When the field data and seepage analysis are not available, uplift on the average can be represented by the conventional linear or bi-linear approximation described in Chapter 3. When analysis or inspection indicate cracking, full uplift should be assumed to exist over the entire crack when it is exposed to the reservoir.

11-4.2.4 Silt Load

Existing arch dams are usually subjected to silt pressure due to sedimentary materials deposited in the reservoir over many years. However, the significance of silt pressure as an additional static load depends on the sediment depth. For U-shaped and broad base arch dams, sediment depth of less than 1/4 of the dam height produces negligible deformations (Fig. 11-4.1) and stresses (10 to 15 psi), and thus their effects may be ignored. For V-shaped dams the effects of silt pressure are even less and may be ignored if the depth of sediment is less than 1/3 of the dam height (Fig. 11-4.2). Both of these figures also show that the maximum deformations due to silt loading occur at locations below the silt level identified by dashed lines.

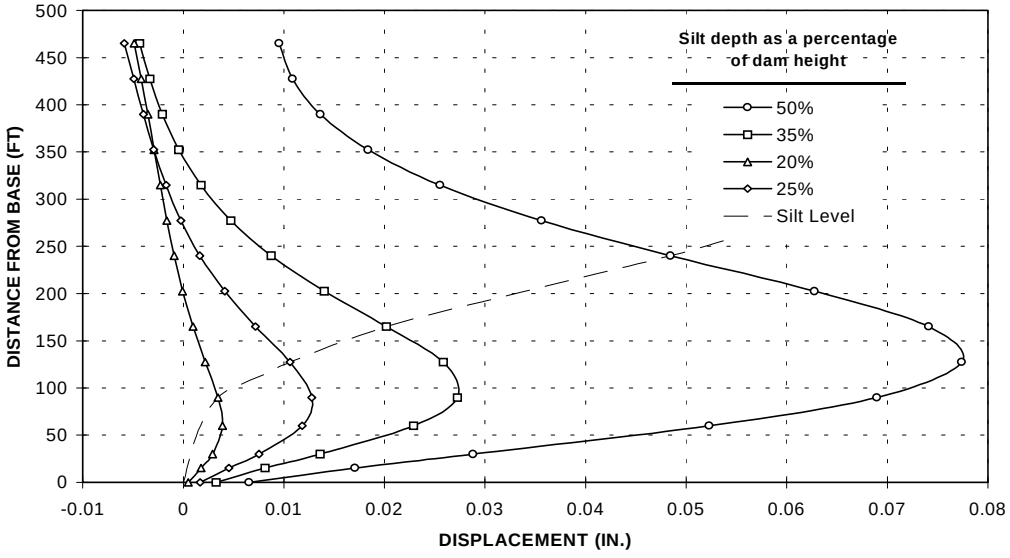

Fig. 11-4.1 Effect of silt on displacement (U shaped valley)

When silt depth is significant, silt load is treated as an equivalent fluid exerting hydrostatically varying pressures on the upstream face of the dam and on the valley floor. The equivalent fluid density for the saturated silt is assumed to be 85 pounds per cubic foot (pcf); that is 22.5 pcf in addition to 62.4 pcf for the water.

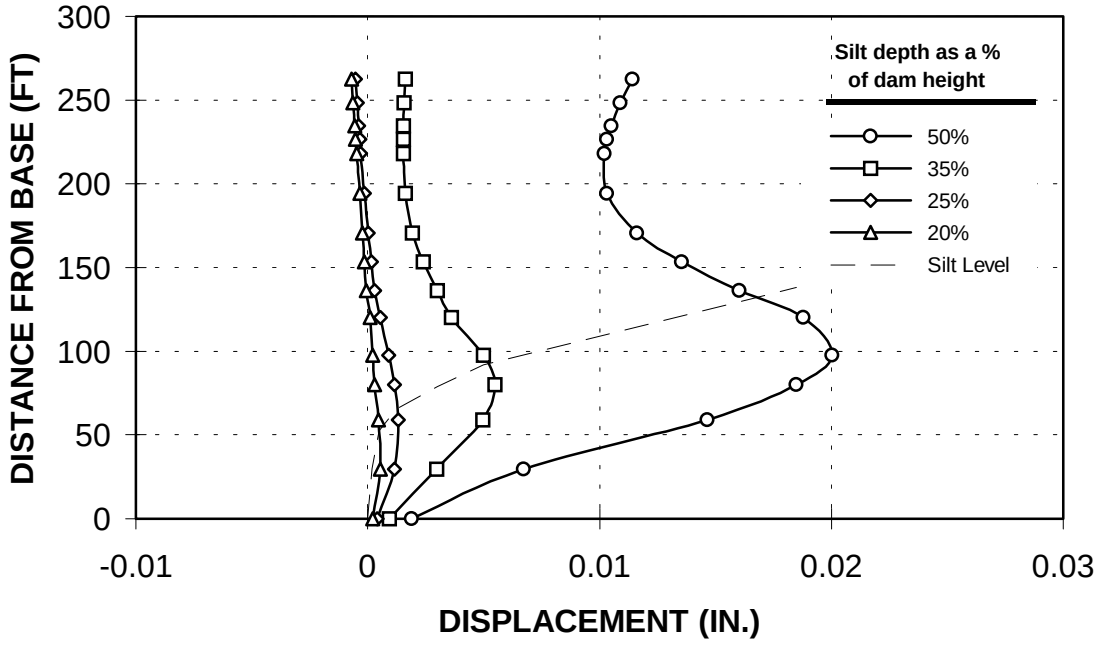

Fig. 11-4.2 Effect of silt on displacement (V shaped valley)

11-4.2.5 Ice Load

Ice can produce significant loads against the face of an arch dam. For this reason, ice load must be considered where reservoir freezing can be expected. Ice loads can be categorized into 2 different types; static loads, produced by the ice in contact with the dam when the reservoir is completely frozen, and dynamic loads, caused by the impact of large floating sheets of ice colliding with the dam.

Static load

This type of ice load is caused by the thermal expansion of the ice or by the wind and current drag. Pressures generated by the thermal expansion depend on the temperature rise and the ice properties. Wind drag depends on properties of the exposed surface and on the direction and velocity of the wind.

The magnitude of ice loading depends on the thickness of the ice cover. When actual measurements of ice pressure are not available, ice loading may be taken as 5 kips per square foot along the contact surface with the dam. For example, a 2-foot thick layer of ice would apply a 10 kip per linear foot load along the axis of the dam. The method of Monfore and Taylor (1954) can also be used to estimate ice pressure.

The radial distribution of ice pressure is of some concern, especially for thin arch dams. Arch dam design assumes that loads will be radially uniform. If this is not the case, large bending stress in the arch direction could result. Radial variation of the ice load could be caused by un-even heating, differences in thickness, or the absence of ice over part of the arch due to powerhouse intakes. In addition to the possibility of non-uniform loading, there is the fact that the ice itself interacts structurally with the dam, complicating the determination of the arch's response. The applied ice load must be representative of the site specific conditions.

Ice Impact

Another possible source of ice loading is ice impact. In many northern rivers, large ice sheets, sometimes weighing many tons, can float down river under the influence of high spring discharges. The force of these impacts can be roughly calculated by equating the kinetic energy of the moving ice sheet and the energy dissipated in crushing ice against the object that it impacts. Refer to the U.S. Army Corps of Engineers EM-1110-2-1612 "Ice Engineering" for additional guidance.

11-4.2.6 Hydraulic Loading of Spillways

The hydraulic loading induced by operation of the spillway is only of concern when the spillway is located on the dam. Forces produced by discharge are usually not significant and are typically ignored in the analysis of arch dams. However, if it is determined that hydrodyanmic forces could effect dam stability, methods for determining spillway pressures are outlined in Chapter 3 of this guideline, and in Corps of Engineers EM 1110-2-1602.

In rare instances arch dams with crest overflow spillways can be subject to forces produced by a "fluttering nappe". Nappe flutter is caused by resonance between air trapped in the cavity between the nappe and the downstream face of the dam. Vibrations induced by such a fluttering nappe could be of importance to the safety of tall and thin arch dams. In addition, if flow over the spillway is controlled by a flap or bascule gate, the fluttering

of the nappe can excite the gate to vibrate; the gate in turn could transfer an important dynamic load to the top of the dam. The phenomenon, and methods to prevent such vibrations, is thoroughly described in ICOLD Bulletin 102, Vibrations of Hydraulic Equipment for Dams (ICOLD 1996).

11-4.3 Thermal Loading

Temperature loads in arch dams result from the differences between the closure temperature when construction joints between cantilever monoliths are grouted or filled by concrete to bind them together, and the concrete temperatures during the operation of the dam. The closure or stress-free temperature is a design parameter selected such that to minimize thermally induced tensile stresses in the dam. In the case of an existing dam, the actual value(s) of closure temperature can usually be found in the construction or design records. If such records are not available, it can be assumed to be equal to either the mean annual concrete temperature or the mean annual air temperature that exists at the dam site. The concrete temperatures are determined from either computation of heat flow through the dam due to the air and water temperatures adjacent to the dam surfaces and exposure to the solar radiation, or from embedded instruments.

The following subsections provide a brief description of procedures and guidance for determining thermal loading for arch dams. Additional details are contained in Chapter 8 of EM 1110-2-2201 (1994).

11-4.3.1 Temperature Distribution

Variation of temperatures through the dam thickness primarily depends on the thickness of the dam. For relatively thin arch dams, a linear temperature distribution from the reservoir temperature on the upstream to the air temperature on the downstream face provides a reasonable approximation. The linear temperature distributions can be obtained by a simplified method (Section 11-4.3.5) or by the FEM (Section 11-4.3.5). Dams with relatively thick sections exhibit a nonlinear temperature distribution. In these cases, concrete temperatures near the dam faces respond quickly to the air and water temperatures, whereas temperatures in the center of the section remain near the closure temperature with minor fluctuations. The nonlinear temperature distributions for thick dams can be determined using the FEM (Section 11-4.3.5). For dams with reliable embedded temperature monitoring instruments, actual temperature should be used. An example of recorded temperatures in the interior of an arch dam is shown in Figure 11-4.3.

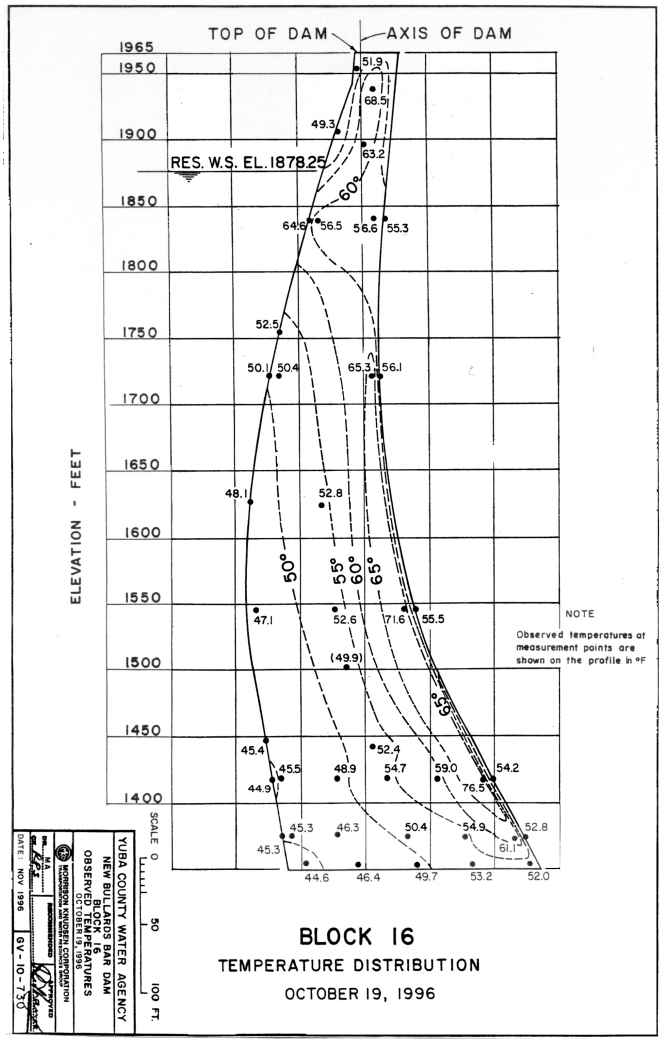

Fig. 11-4.3 Example of interior temperature distribution

11-4.3.2 Air Temperature

Estimates of air temperatures at a dam site are based on the past air temperatures measured at the dam site or at nearby locations. If not measured at the dam site, air temperatures near the dam site can be obtained from the US Weather Bureau, which collects weather data at many stations. Data from the nearby station should be adjusted for the differences in elevation and latitude that may exist between the station and the dam site. The actual air temperature data for a period of 5 years or longer is required to assemble a chart showing various mean temperatures as well as the maximum and minimum recorded temperatures (Fig. 11-4.4).

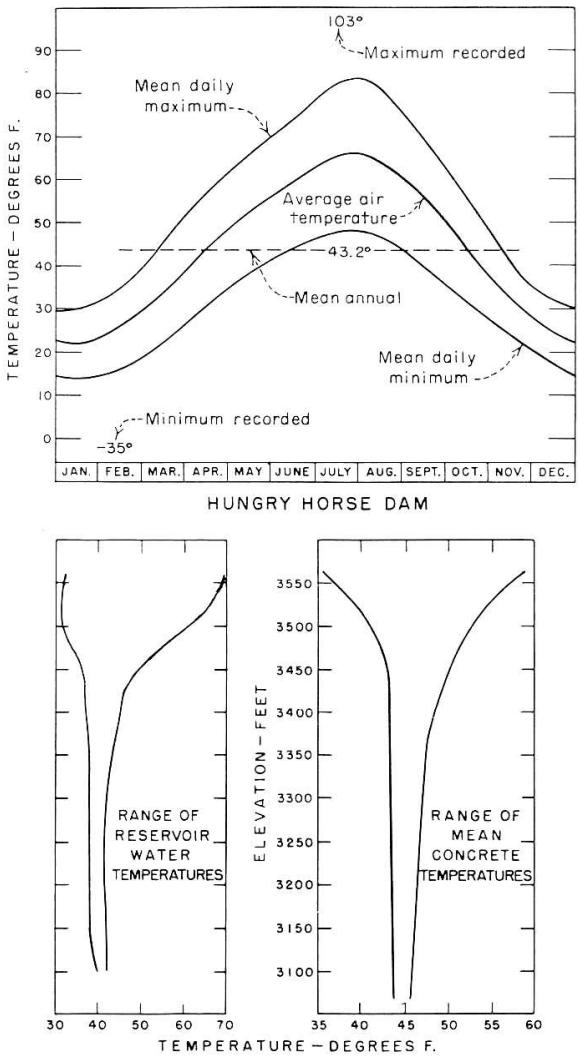

Fig. 11-4.4 Hungry Horse Dam – climatic and mean concrete temperatures (USBR, Townsend 1965)

11-4.3.3 Reservoir Water Temperature

The reservoir water temperatures vary with depth and season. Estimates of temperatures for the impounded water are obtained by measuring temperatures directly at and below the water surface at locations near the dam. Such data usually include one recording per month for several months each year and for a period of several years. When no direct data are available, the best estimate of the expected reservoir water temperature can be obtained from water temperatures recorded at nearby lakes and reservoirs of similar depth and with similar inflow and outflow conditions. These data are then used to estimate a range of reservoir water temperatures showing the mean annual high and the mean annual low temperatures for the impounded water (Fig. 11-4.4).

11-4.3.4 Solar Radiation

Solar radiation on the exposed faces of a dam increases the temperature of the structure. The solar radiation, therefore, has the net effect of reducing temperature loads for the winter conditions and increasing for the summer conditions. The mean concrete temperatures discussed in Section 11-4.3.5 should be adjusted for the effect of solar radiation on the downstream face and on the portion of upstream face not covered by reservoir water. The amount of temperature rise due to solar radiation depends on the slope and orientation of the exposed surface as well as the latitude. Knowing the slope and orientation of a point on the dam and the latitude, the solar temperature rise for that point can be obtained from a set of charts developed by USBR (Townsend, 1965). Since the sun's rays strike different parts of an arch dam at varying angles, values of the solar temperature rise should be evaluated at the quarter points.

11-4.3.5 Concrete Temperatures

The range or amplitudes of concrete temperatures arising from exposure to air and water can be determined by a simplified method or the finite-element method. In the simplified method assumed external sinusoidal temperature variations are applied to the edges of a theoretical flat slab, whereas in FEM they are applied to the faces of a finite-element model of the dam using a conductive boundary condition.

Simplified Method. Described fully by USBR (Townsend, 1965), this method is based on computation of heat flow through a flat slab of uniform thickness exposed to sinusoidal temperature variations on both faces. The method has been simplified by reducing the heat flow computation into a curve showing the ratio of the variation of the mean temperature of the slab to the variation of the external temperature as a function of an "effective" slab thickness. The simplified method can be used in the trail load method as well as the FEM.

Finite Element Method. Amplitudes of concrete temperatures can also be determined using the finite-element method. The FEM is especially suitable for dams with relatively thick sections that exhibit a nonlinear temperature distribution through the dam thickness. Since very little heat is transmitted along the axis of the dam, the finite-element heat-flow analysis of arch dams may be conducted on the basis of a 2-D model without significant loss of accuracy. Two-dimensional heat-flow model of an arch dam should be developed as a vertical section through the crown section with three or more elements through the thickness. For dams with varying arch thickness along the dam axis, an additional vertical section taken near the quarter point of the dam axis is recommended. Three-dimensional heat-flow analysis may be performed using the same 3-D model developed for the static stress analysis, provided that for relatively thick arch dams three or more

elements are included through the dam thickness. The water and air temperature cycles discussed previously are applied to the boundaries of the dam model and the foundation is either subjected to the mean annual air temperature or assumed to be adiabatic. Most computer programs with heat flow capabilities permit for both steady-state and periodic analyses. When performing these analyses, the periodic solution using sinusoidal temperature cycles should be employed. The closure temperature or the mean annual air temperature should be used as the initial temperature. The important factor in these analyses is to let the solution run long enough for the cycle to settle down to a final stable value. The effects of solar radiation, if important, can be estimated from the USBR charts (Townsend, 1965) and superimposed to the FE results. The temperature distributions obtained in this manner can then be applied directly to nodal points of the 3-D stress model (Section 11-5.2.2).

11-4.4 Earthquake Loading

Earthquake loading described in this section is required for arch dams located in seismic zone 3 and higher. Arch dams in seismic zone 2 may also require analysis for earthquake loading on a case by case basis.

11-4.4.1 Safety Evaluation Earthquakes and Associated Ground Motions

The safety evaluation earthquake for analysis of existing arch dams requiring earthquake loading is the maximum credible earthquake (MCE). The MCE is defined in Chapter 12.

11-4.4.2 Response Spectrum Earthquake Input

Site-specific response spectra of earthquake ground motions are required. (Fig. 11-4.5) The response spectrum must be smoothly enveloped to avoid the possibility of low energy notches in the response spectrum coinciding with the natural frequencies of the dam. Response spectra should be developed for both horizontal and vertical ground motions. Spectra should be developed consistent with the Guidelines contained in Chapter 12, Section 3. The spectra should be developed for 5% damping. In addition, relationships or factors should be provided to obtain response spectra for higher damping ratios (as high as 10%) if required for the analysis of the dam. These relationships or factors may be based on a documented site-specific study; alternatively, the relationships presented by Newmark and Hall (1982) may be used.

11-4.4.3 Acceleration Time History Earthquake Input

Acceleration time histories of ground motions should be developed consistent with the guidelines contained in Chapter 12, Section 3.3. Acceleration time histories should be

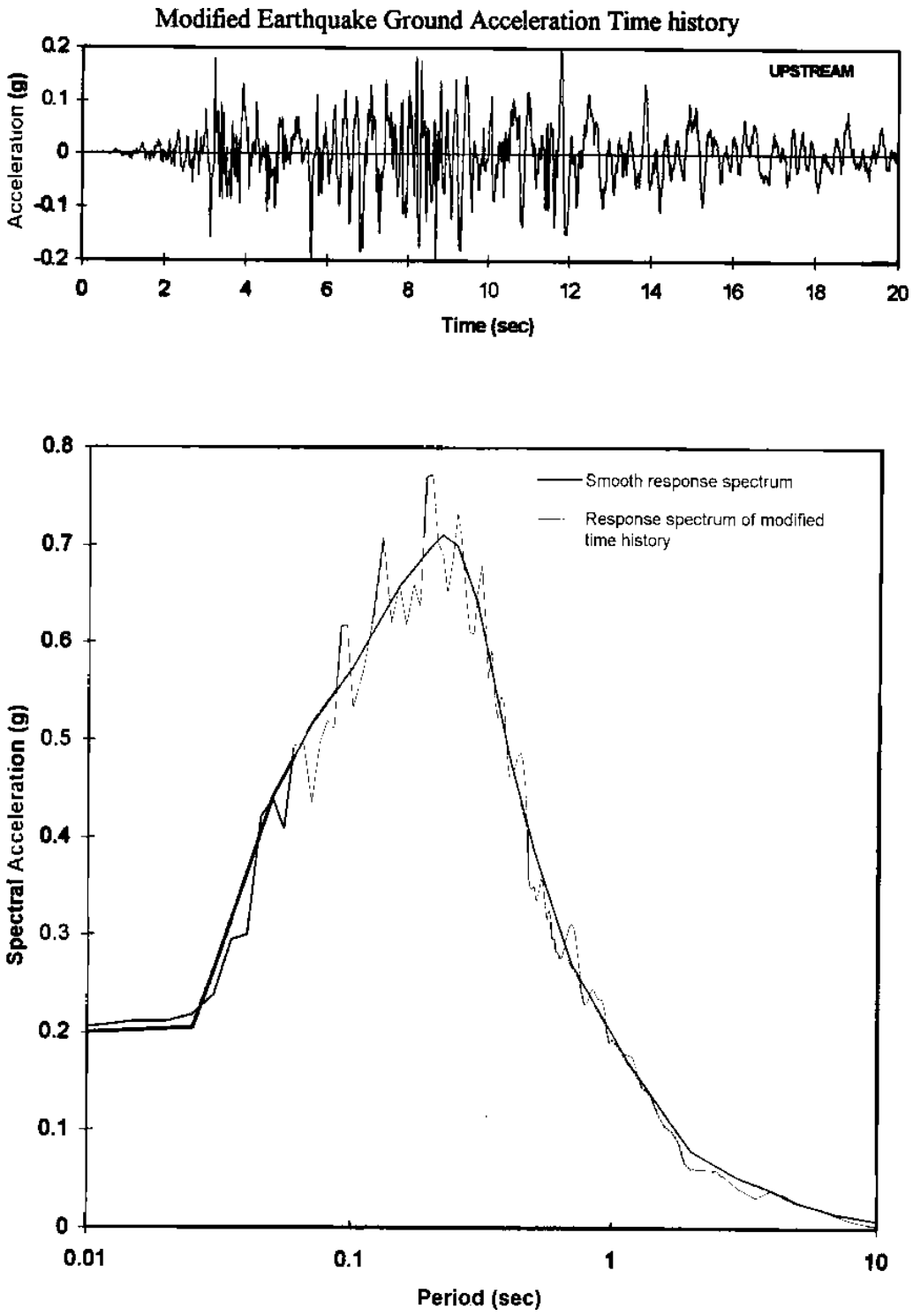

Fig. 4-5 Comparison of smooth response spectrum with spectrum modified acceleration time history, 5% damping.

developed for three components of motion (two horizontal and one vertical). Time histories may be either (a) recorded or simulated-recorded time histories or (b) response-spectrum matched time histories (Figs. 11-4.5 and 11-4.6), as described in Chapter 12, Section 3.3. For recorded or simulated-recorded time histories, three recordings should be used. Whereas for the response spectrum matched time histories, one set would be adequate for linear dynamic analysis.

11-4.4.4 Spatial Variation of Ground Motion

Recorded earthquake ground motions at Pacoima Dam during the 1994 Northridge earthquake (CDMG, CSMIP, 1994) indicated that the seismic input for arch dams should vary along the dam foundation interface. However, the recorded abutment motions at Pacoima Dam included contributions from both the canyon topography and the dam-foundation interaction. These motions, therefore, are not free-field accelerograms that would have been recorded if the dam were not there. Except for one recording at an arch dam in Taiwan, which included free-field motions at locations on the canyon slopes and valley floor away from the dam, other cases of measured free-field ground motions across the canyon suitable for analysis of arch dams have not been reported. At present time scarcity of data prevents a realistic definition of non-uniform free-field motions for arch dams, even though procedures for handling non-uniform input have been developed. In view of these difficulties, the use of standard uniform seismic input , while not as realistic as one may desire, will continue to be acceptable.

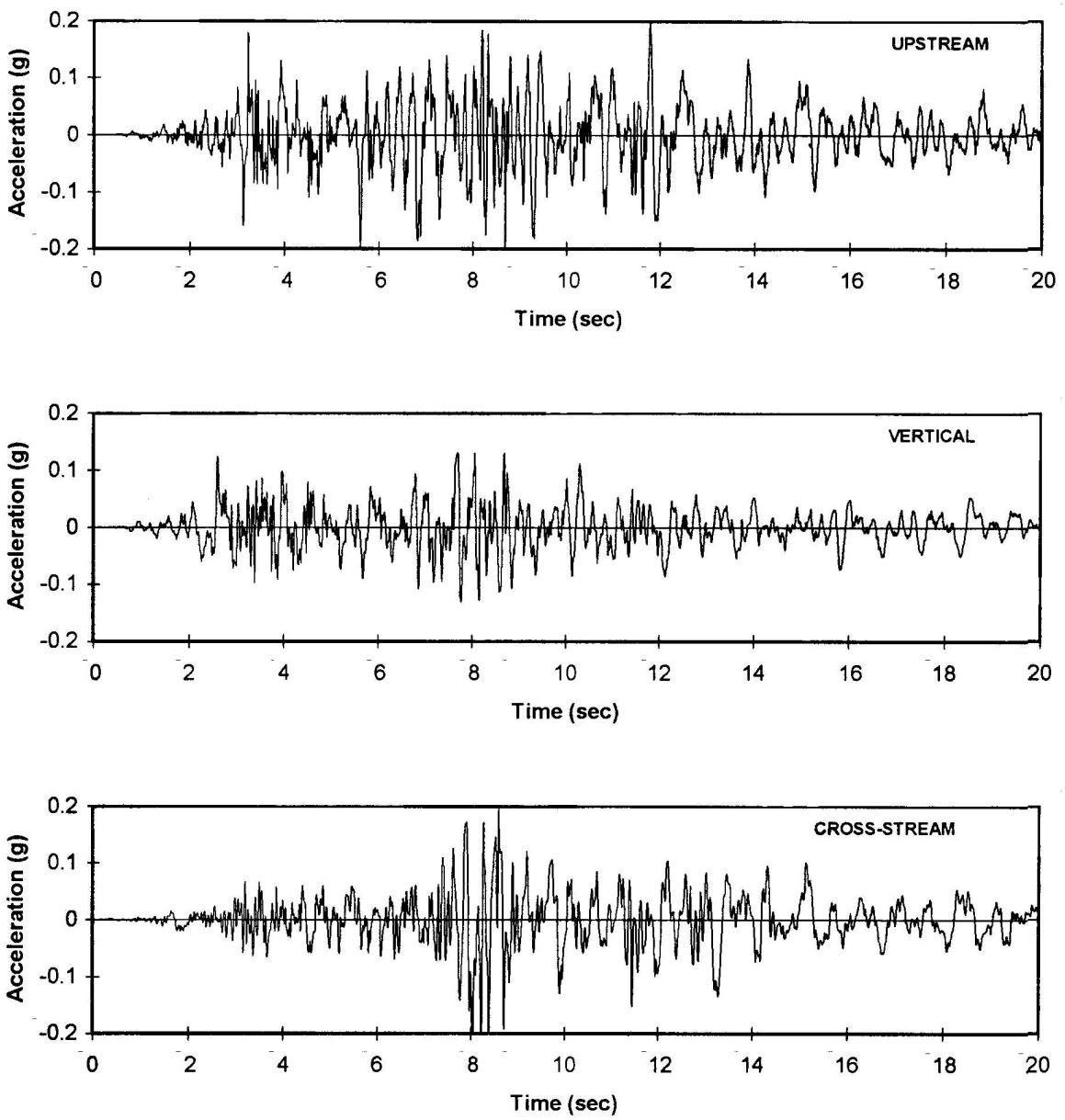

Fig. 11-4.6 Spectrum matched acceleration time histories foe excitation in upstream, vertical, and cross-stream directions.

11-4.5 Load Combinations

Arch dams should be evaluated for all appropriate load combinations using the safety factors prescribed in Section 11-1.4. Depending on their probabilities of occurrence, three basic loading combinations, *Usual*, *Unusual*, and *Extreme* should be considered. The usual loading combination considers the effects of all loads that may exist during the normal operation of the dam. The unusual loading combination refers to the loads acting on the dam during the flood stage. The extreme loading combination includes any of the usual loading combinations plus the effects of the Maximum Credible Earthquake described in Section 11-4.4. Rare loading conditions which have a remote probability of occurrence at any given time, have a negligible probability of simultaneous occurrence and should not be combined. When a very low water level or empty reservoir may be expected, its effects should be considered by a special loading combination described in Section 11-4.5.2. The loading combinations to be considered are as follows:

11-4.5.1 Usual Loading Combinations

Two usual loading combinations representative of the summer and winter temperature conditions should be considered. The reservoir water level is assumed to be at the normal high water level (NHWL) defined in Section 11-4.2.1 unless the most probable water level at the time of respective mean concrete temperatures can be established.

a. Summer Condition:

- Maximum mean concrete temperatures
- Normal high water level (NHWL), or the most probable water level occurring at the time of maximum mean temperature
- Dead load
- Silt load (if applicable)
- Tailwater (if applicable)

b. Winter Condition:

- Minimum mean concrete temperatures
- Normal high water level (NHWL), or the most probable water level occurring at the time of minimum mean temperature
- Dead load
- Silt load (if applicable)

- Ice load (if applicable)
- Tailwater (if applicable)

11-4.5.2 Unusual Loading Combinations (IDF)

Depending on the time of flooding, one or both of the following unusual loading combinations should be considered. The maximum mean concrete temperatures should be used with the summer flooding and the minimum mean concrete temperatures should be employed with the winter flooding, unless the most probable mean concrete temperatures at the time of respective flooding can be established.

a. Summer Flooding:

- Flood water level
- Maximum mean concrete temperatures, or mean concrete temperature occurring at the time of flood
- Dead load
- Silt load (if applicable)
- Tailwater (if applicable)

b. Winter Flooding:

- Flood water level
- Minimum mean concrete temperatures, or mean concrete temperature occurring at the time of flood
- Dead load
- Silt load (if applicable)
- Ice impact (if applicable)
- Tailwater (if applicable)

c. Special Loading Combination:

Special loading combinations correspond to the seasonal minimum water level (NLWL) or a complete reservoir drawdown condition. They are considered as a safeguard against possible instability conditions due to the reduced or lack of water pressures.

- Minimum (NLWL) or no headwater, whichever applicable
- Most probable mean concrete temperatures at that time
- Dead load
- Silt load (if applicable)

- Tailwater (if applicable)

11-4.5.3 Extreme Loading Combinations (MCE)

Extreme loading combinations include any of the usual loading combinations plus the effects of the maximum credible earthquake.

- Summer usual loading combination + MCE
- Winter usual loading combination + MCE

When more than one MCE ground motions governs, the effects of each MCE should be combined with each of the usual loading combinations described above.

11-5 STATIC ANALYSIS

11-5.1 Overview

This section describes analysis and evaluation procedures required for assessing the structural stability of arch dams and their abutment foundation under static loads. The acceptable methods of analysis for computing deflections and stresses developed in the dam include three dimensional finite element (FE) and in certain cases continuum solution procedures, as applicable. The FE stress analysis should be conducted by developing an accurate three-dimensional model of the dam-foundation system. The manner by which various static loads are applied should be described. The results of analyses should be presented appropriately in order to facilitate examination, interpretation, and evaluation of the findings.

11-5.2 Finite Element Analysis

The finite element procedure is the numerical method most often used for the structural analysis of arch dams. This guideline assumes that the reader is already familiar with the general theory of finite element analysis of elastic solids (Zienkiewics, 1971; Bathe and Wilson, 1976). The following remarks are intended only to point out some special considerations in the application of this technique to arch dam analysis.

11-5.2.1 Structural Modeling Assumptions

The finite element analysis of arch dams is based on the same assumptions that underlie all finite element analyses. This being the case, the basic principles that govern element formulation, mesh construction, and load application are as valid in the analysis of arch dams as they are anywhere in structural mechanics. There are, however, certain special considerations in the use of the finite element in arch dam analysis:

1. The body of the dam is typically assumed to be bonded to the foundation rock throughout its contact with the canyon. However, the validity of this modeling assumption is often what the analysis is seeking to determine. If this assumption results in excessive shear or tensile stresses on the foundation contact, this modeling assumption may require modification.

2. The dam is typically assumed to be a monolithic structure with linear elastic and isotropic material properties. In reality, the typical arch dam is divided by construction joints, con-

traction joints, and pre-existing cracks. In addition, concrete by its nature is not isotropic because its compressive strength is typically 10 times its tensile strength.

3. The foundation rock is assumed to be monolithic with linear elastic and isotropic material properties, when in reality it is jointed with non -linear characteristics. The use of a "deformation modulus" instead of the actual Young's modulus is an attempt to deal with the complex character of the typical foundation.

11-5.2.1.1 Dam Model

The basic geometry data for developing a 3D finite element mesh for the dam can be obtained from the construction drawings. In some situations, however, it may be necessary to confirm the accuracy of such data by visual inspection, and possibly by field surveys, to ensure that the existing conditions of the dam matches the as-built drawings. For example, a severely deteriorated layer of concrete near the dam surface may have lost its strength, suggesting that a reduced dam thickness or a reduced effective modulus of elasticity might better represent the actual conditions. In other situations, structural modifications may have increased both stiffness and mass of the dam. Critical gravity abutment thrust blocks that may exist at one or both ends of an arch dam should be included in the dam model. Smaller and less important thrust blocks may be considered as part of the foundation rock, and not modeled separately. The FE model developed for the dam should closely match the dam geometry and be suitable for application of the various loads.

Meshing

The type of FE mesh employed is highly dependent on the geometry of the dam and the ability of the displacement field of the element to capture the displacement and stress fields that one is attempting to model. For this reason, there is no "magic number" of elements that constitute a good FE mesh. In general, higher order elements such as 16 node shell and the thick shell (Ghanaat, 1993a), and the general 3D element (Bathe and Wilson, 1974) (See Fig. 11-5.1) can have relatively coarse meshes. The linear 8 node solid element requires finer meshing to accommodate the same displacements.

The size of elements sometimes may be dictated by the foundation profile. Highly irregular foundation profiles in general require smaller elements to match the dam geometry. In general, as elements get smaller, they become increasingly sensitive to geometric discontinuities, such as re- entrant corners found at the dam / foundation interface. The result can be large stress concentrations that are fictitious because of the formation of

cracks in the foundation material. The size of elements also affects how accurately the dynamic characteristics, and thus response of the dam to earthquake loading is being evaluated. Large thin arch dams such as Morrow Point Dam may have numerous vibration modes (Fig. 11-6.2). To account for the contribution of all significant modes, sufficient number of elements must be included in the finite element mesh. As a general rule, an FE mesh of an arch dam should include 5 or more element rows along the dam height with sufficient number of elements along the dam axis.

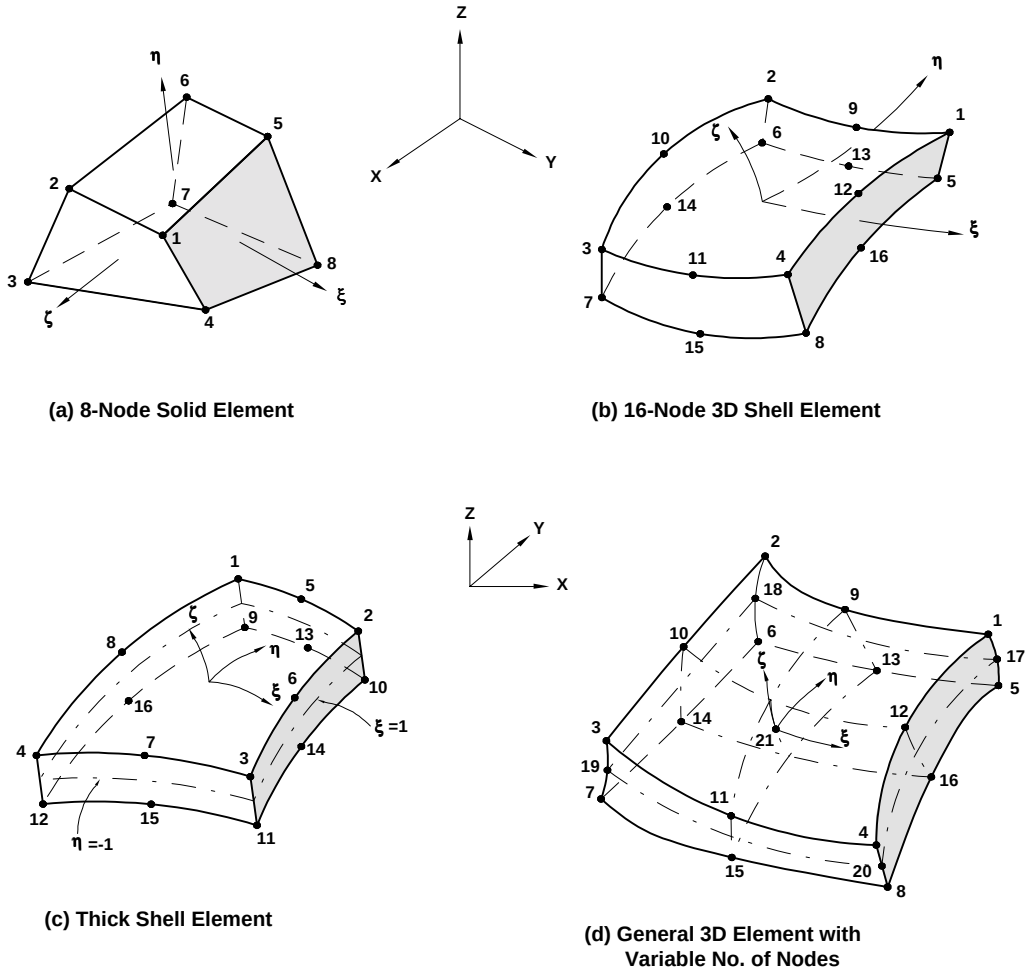

Fig. 11-5.1 Typical finite elements used in solid modeling.

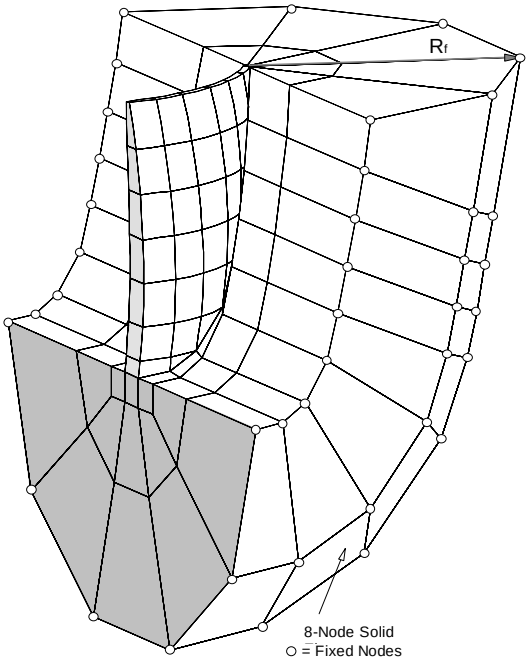

(a) Perspective view of dam-foundation

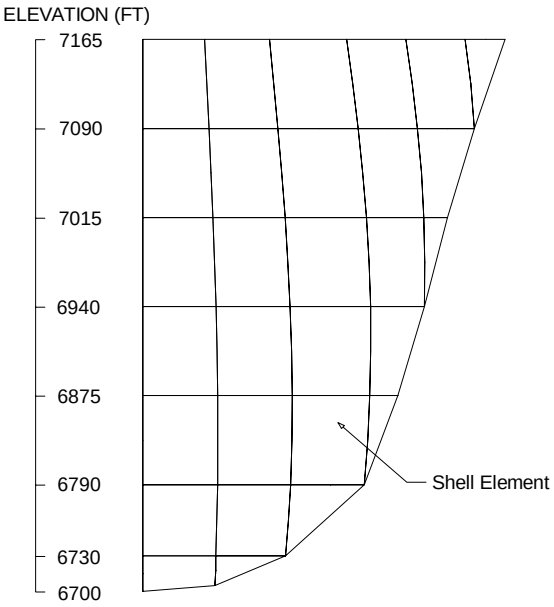

(b) Mesh Layout

Fig. 11-5.2 Dam modeled using single layer of shell elements with circular foundation mesh of 8 node solids.

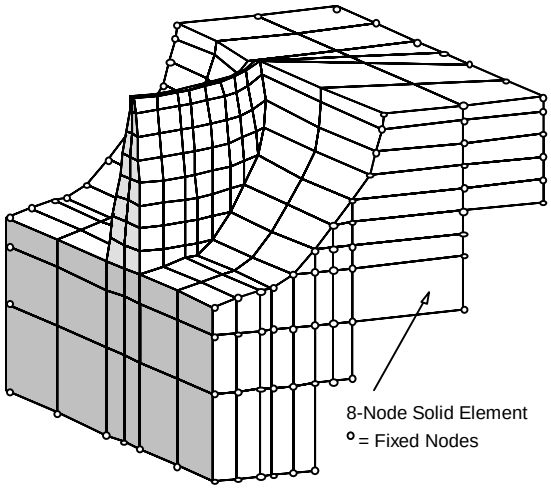

(a) Perspective view of dam-foundation model

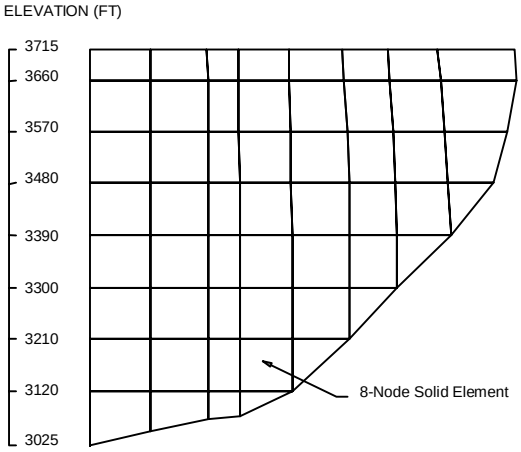

(b) Mesh Layout

Fig. 11-5.3 Dam modeled using 2 layers of 8 node solids with stepped foundation.

The number of elements along the dam axis are selected such that the elements have aspect ratios of less than 2. The Morrow Point Dam model shown in Figure 11-5.2 is an example of a fine mesh for the quadratic shell elements. The Glen Canyon Dam model in Fig. 11-5.3, shows an example of a fine mesh for the 8-node solid elements.

11-5.2.1.2 Foundation Model

An appropriate volume of the foundation rock should be included in the dam model to account for the effects of foundation flexibility on the static deflections and stresses of the dam. The foundation model should extend to a large enough distance beyond which its effects on deflections and stresses of the dam become negligible. Although finite element mesh for the foundation rock can be developed to match the site topography, such an elaborate model is not required in practice. Instead, a prismatic foundation mesh constructed on semi-circular planes (Fig. 11-5.2), or developed by simple projection along the global coordinate axes (Fig. 11-5.3) may be employed. Typically, smaller elements are employed near the dam-foundation contact region where the largest deformations and stresses occur, whereas larger elements are used away from the dam, where the interaction with the dam is reduced.

The size of the foundation model should be determined based on the ratio of the foundation deformation modulus to the concrete modulus of elasticity (Ef /Ec). For a competent foundation rock with Ef /Ec equal or greater than 1, a foundation mesh extending one dam height in the upstream, downstream, and downward directions should suffice. For a very flexible foundation rock with Ef /Ec in the range of ½ to ¼ , the foundation model should extend twice the dam height in all directions and include more number of elements.

11-5.2.2 Application of Loads

In FE analysis, internal and external static loads are computed for each individual finite element and are applied as equivalent forces at nodal points of the dam model.

Dead Load

As described in Section 11-4.1, dead loads in arch dams are the weight of the concrete plus appurtenant structures. The application of dead load should consider the manner in which the dam was constructed. For example, arch dams are often constructed as independent cantilever blocks separated by vertical joints. Since these joints are not capable

of transferring dead load horizontally until they are grouted, dead loads should be applied to individual cantilevers to simulate this condition. This may be accomplished by performing dead load analysis in two steps. First, dead loads are applied to alternate cantilevers (Set-1) by assuming a zero modulus of elasticity for the remaining cantilevers (Set-2). In the second analysis, the modulus of elasticity is switched on for the Set- 2 cantilevers, and set to zero for the Set-1. If the dead load is applied to the dam all at once, without taking into account the fact that horizontal load transfer can not occur before the dam is complete, fictitious stresses will be indicated.

The sequence of construction for some dams may significantly differ from the independent cantilever blocks. It may involve staged construction and sequence of grouting and partial reservoir filling that can have a major effect on the distribution of dead loads. In these situations the alternate cantilever loading discussed above is not appropriate, instead the actual sequence of construction should be considered in the application of dead load.

Water Load

Water loads due to hydrostatic pressures of the normal water level or flood, are external forces acting on the surfaces of all finite elements in contact with the impounded water. These include dam elements having faces coincident with the upstream face of the dam and foundations having surfaces at the reservoir floor and sides.

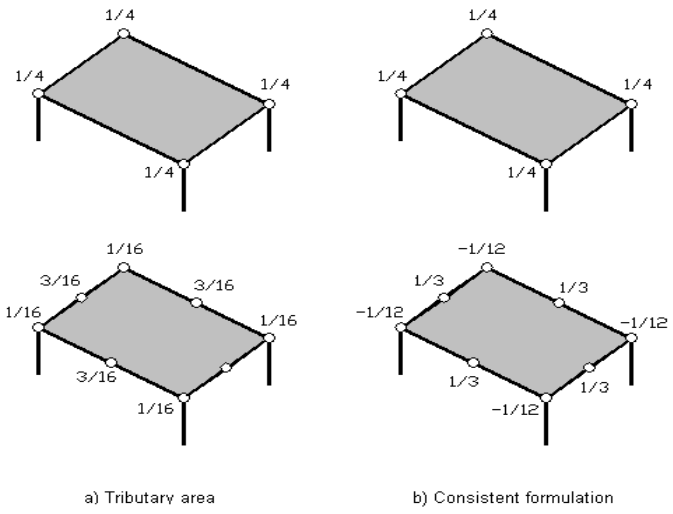

Fig. 11-5.4 Tributary area and consistent lumping of nodal forces due to a uniform surface pressure acting on linear and quadratic 3D elements.

Water loads are lumped at discrete nodal points as equivalent nodal forces. They are applied to the monolithic arch structure after the contraction joints are grouted. The hydrostatic pressures are lumped into equivalent nodal forces using the "consistent" or approximate tributary area lumping process. For linear elements, the equivalent nodal forces computed using either the tributary area or consistent formulation will be the same, as shown in Fig. 11-5.4. For higher order elements, however, the consistent nodal forces completely differ from those obtained on the basis of the tributary area. As shown in the lower graphs of Fig. 11-5.4, the consistent nodal forces are even negative for the corner nodes, a fact not so obvious. It should be noted that the tributary area lumping of nodal forces would converge to accurate results for a very fine mesh. However, since the use of higher-order elements implies a relatively coarse mesh, this kind of error can be very significant and should be avoided.

Temperature Load

Temperature loads arise from the differences between the closure (stress free condition) temperature and concrete temperatures expected during the operation of the dam. Temperature loading should be applied in accordance with section 11-4.3

Silt Load

Similar to the impounded water, silt load is applied to the monolithic structure as an equivalent fluid exerting hydrostatically varying pressures on the upstream face of the dam and on the valley floor.

Ice Load

Ice loads are applied radially (normal to the upstream face) to the monolithic structure. Ice loads in the form of distributed surface pressures may be applied on the upstream faces of a horizontal layer of elements included in the model at the ice level. Loading should be in conformance with the guidance given in section 11-4.2.5

Uplift load

Ideally uplift in FE analysis should be introduced as pore water pressures at element nodes throughout out the dam-foundation model, if the program used has this capability. In the absence of such capability, uplift pressures at the base of thick arch dams may approximately be applied as distributed pressures or equivalent nodal forces on the faces of a thin pervious layer placed between the dam and the foundation rock (Fig. 11-5.5). In

this approach the pressures or nodal forces due to uplift are transferred to the dam and to the foundation one row of elements away from the interface, so that the equal magnitude uplift pressures along the uncracked portion of the interface are not canceled out. The resulting stress output from these elements will include the effect of uplift pressure. This procedure can also be used to model uplift in an abutment rock joint.

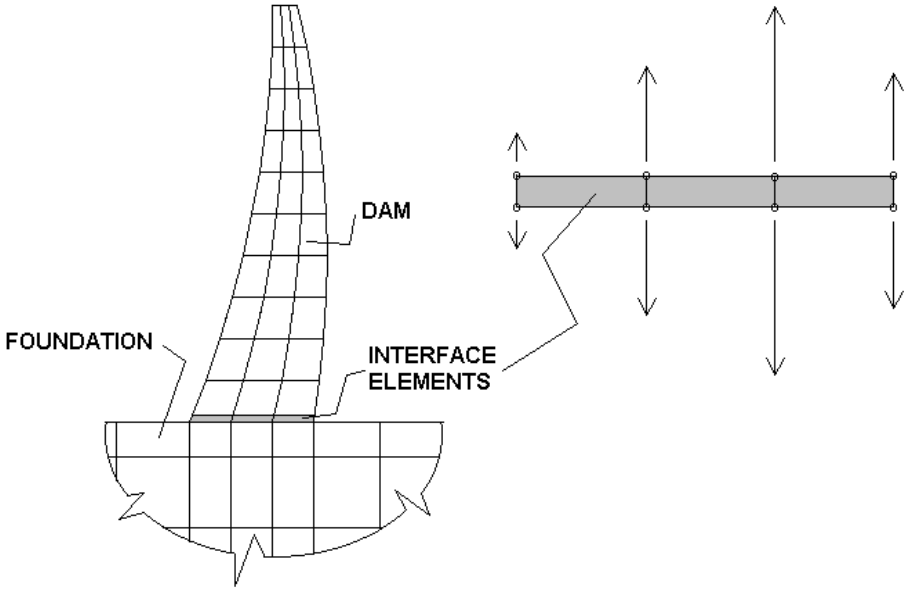

Fig. 11-5.5 Procedure for application of uplift.

11-5.2.3 Presentation of Results

The basic results of a finite element analysis include nodal displacements and element stresses. As a minimum, nodal displacements and surface stresses should be presented for the static loading combinations described in Section 11-4.5 in clear graphical form. Surface stresses should be presented in the local arch and cantilever directions. Additionally, since nodal loads can be obtained from finite element analyses on an element by element basis, dam thrust needed for the rock wedge stability analysis (Section 11-5.4) can be determined from loads acting on elements having a common surface or a common edge with the dam/foundation contact surface.

Although displacements are not directly used in evaluation of dam safety, they provide a visual means by which acceptability of the analysis results can be assessed. Nodal displacements may be displayed as simple deflected shapes across selected arch and cantilever sections or presented in the form of 3D plots for the entire dam structure. Fig. 11-5.6 is an example of the static deflections displayed across the crest and crown cantilever

sections. As expected, hydrostatic loads push the dam in the downstream direction; contraction due to temperature drop below the grouting temperature produces downstream deflections; and expansion of the concrete due to temperature rise above the grouting temperature results in the upstream deflections of the dam.

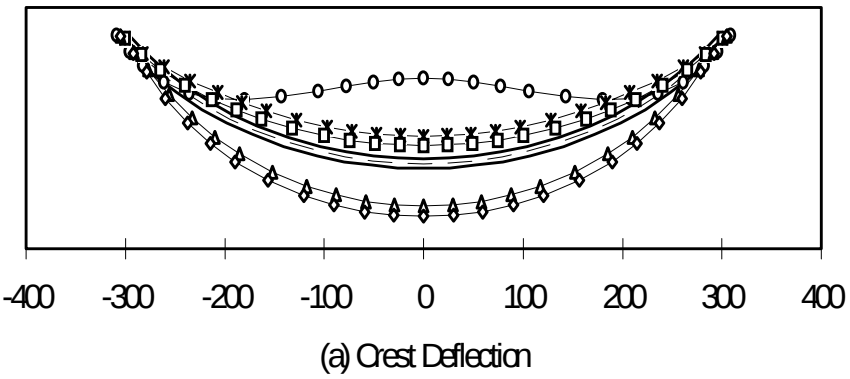

(a) Crest Deflection

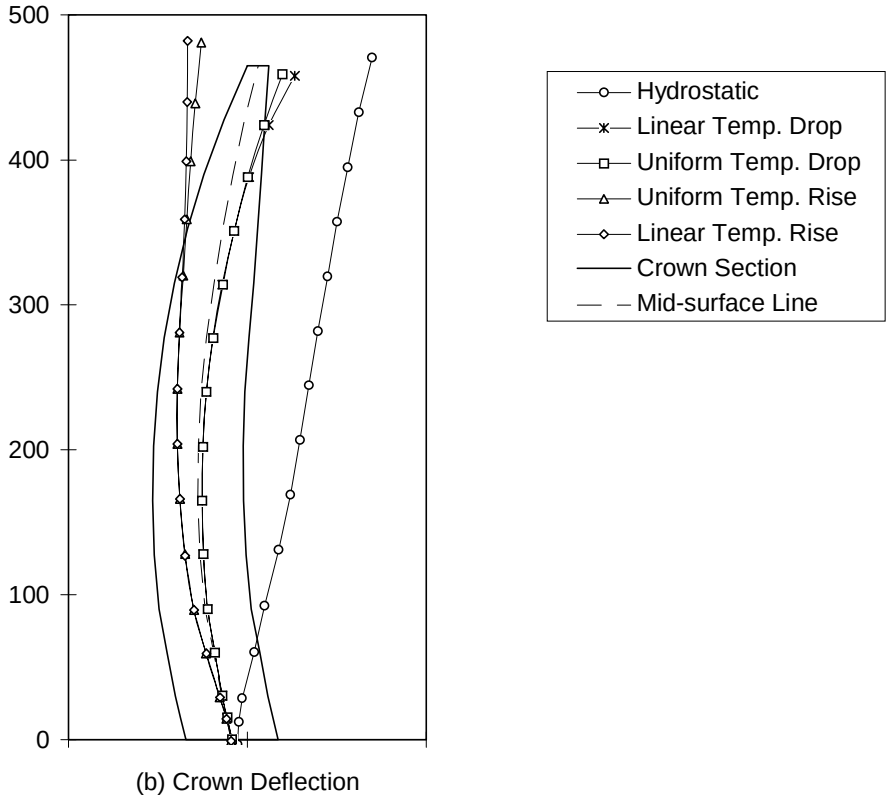

(b) Crown Deflection

Fig. 11-5.6 Static deflection due to various load conditions.

Maximum tensile and compressive stresses in an arch dam usually occur at the faces of the dam, therefore evaluation of stresses on the faces of the dam is required. The surface

stresses resolved into arch and cantilever stresses are usually presented in the form of stress contours on each face of the dam, while surface principal stresses are displayed in the form of vector plots, as illustrated in Fig. 11-5.7.

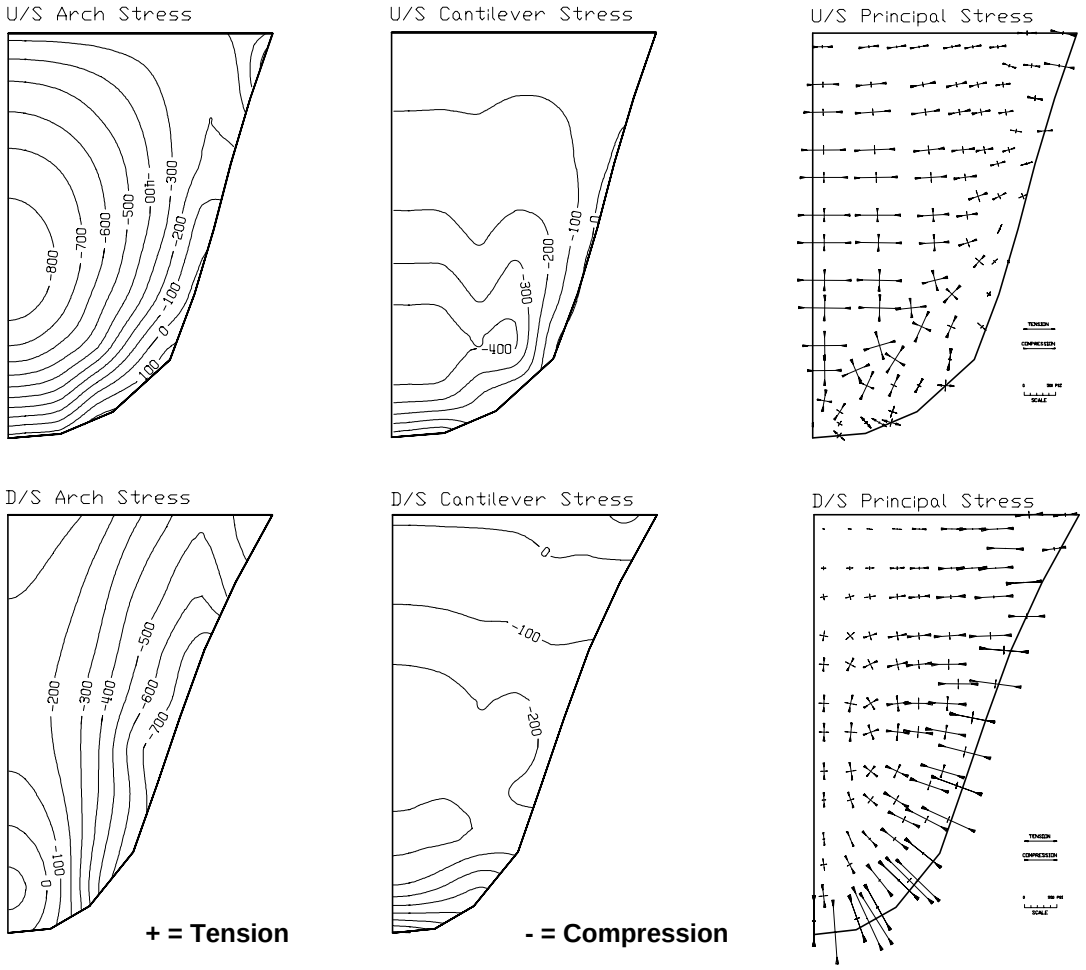

Fig. 11-5.7 Arch and cantilever stress contour and principle stress vector plots.

In addition to the arch and cantilever stresses, the magnitudes of the shear stresses caused by the bending and twisting moments should be examined, especially for very thin arch dams and those with cracked sections. These include radial cantilever shear stresses acting radially on a horizontal plane and radial arch shear stresses acting radially on a vertical plane. Also, excessive tangential shear stress acting on the foundation can be a cause for concern. (See 11-5.6.1)

11-5.2.4 Evaluation of Stress Results

Evaluation of the computed stresses should begin with validation of numerical results by careful examination of the deflected shapes and stress distributions due to individual loads. Such data should be inspected for unusual deflected shapes, exceptional high or low displacement and stress magnitudes, and unexpected stress distributions that differ significantly from the results of other arch dams and cannot be explained by intuition. Force equilibrium should also be verified by comparing the sum of reaction forces to the sum of applied loads. Problems usually arise from the input data and modeling errors and should be corrected. After the numerical results have been validated for accuracy, the stress results are used to evaluate the dam performance for each static loading combination in accordance with the criteria set forth in Section 11-1.4.

A concrete arch dam under static loading conditions is considered to be safe from over stressing failure if the allowable stresses are not exceeded in any extensive area. Allowable stresses of concrete are obtained by dividing the strength capacities (Section 11-3.7) by the appropriate safety factors given in Table 11-1.1. This requirement is easily satisfied for a well designed arch dam which resists the loads by developing essentially compressive stresses with very little tension (Fig. 11-5.7). In other cases compressive stresses usually meet the criteria but tensile stresses caused by temperature loads, or other unfavorable situations may be significant. When significant tensile stresses are indicated, sections of the arches and cantilevers subjected to excessive tension are assumed to be cracked. This cracking will result in the re-distribution of stresses and loads. For example, localized loss of cantilever action caused by cracking at the base of the dam can be compensated by increased arch action. If cracking appears to be significant, non-linear analysis or linear analysis of the "as cracked" model may be required.

In general, areas of high indicated tensile stress should correspond to observable cracks in the dam, however this is not always the case. It is not unheard of to observe cracking in the dam in an area which the FEM model indicates is in compression. This may indicate an error in the FEM model. It may also be a result of some past loading condition, such as high thermal loads during curing. If the crack is not an indication of a modeling error, it is not necessarily important to determine the cause of the crack if it can be shown that the dam is stable without requiring tensile strength across the crack.

Judgement is required in deciding when tensions indicated by a linear elastic model are in-significant enough to be overlooked, and when re-analysis must be done. Tensile stresses on the upstream face normal to the foundation are often indicated. If tensile normal stresses at the base of the dam are confined to a small region of the dam surface

area, and all other stresses are low and well within the allowable values, then it can be assumed any cracks formed under this condition would be shallow cracks limited to the dam-foundation interface with no serious consequences. However, if high tensile stresses persist over a large area, then an analysis considering the effects of cracks is required to demonstrate that the stress redistribution, as described above, would take place safely.

As cracks form at the base of the dam, the modulus of elasticity for the elements in the cracked portion of the interface must be reduced in the finite element method so that the indicated tensile stresses can be effectively eliminated. If a crack occurs at the upstream face of a cantilever below the water surface, the uplift pressure as described in Section 11-4.2.3 should be considered in the analysis.

Shear stresses in excess of the shear capacity of the concrete/foundation interface can also be of concern. Massive shear failures of the type treated in section 11-5.6 are rare, however local shear over stress is more common. Situations of shear over stress should be evaluated in a manner similar to indicated tensile overstress. If stress can be relieved by re-distribution without overstressing other areas, local shear failure can be tolerated. Elements may have to be allowed to "slide" by reducing their elastic modulus or disconnecting them. Many FE programs also have non-linear gap friction elements which can be used.

11-5.3 Alternative Continuum Models

The finite element method outlined in the previous sections may not be required if the dam has a simple geometry and its performance only due to the static loads is to be evaluated. In these cases, if the dam geometry can be represented by one-, two-, or three-centered layouts and if uniform material properties can be assumed for the concrete and for the foundation-rock, the dam may be analyzed using the trial load method.

A complete description of the trial load method and its computerized version known as Arch Dam Stress Analysis System (ADSAS) is given by the USBR (1977). Following iss a brief overview of the method and the conditions under which it can be applied to analysis of existing arch dams.

11-5.3.1 Trial Load Method

The trial load method is based on the assumption that an arch dam is made of two systems of structural members: horizontal *arch units* and vertical beams or *cantilever units*

(Fig. 11-5.8); that the waterload is divided between the arch and cantilever units in such a way that the resulting arch and cantilever deflections and rotations at any point in the dam are equal (Fig. 11-5.9). The preceding agreement is accomplished by subjecting arch and cantilever units to a succession of self-balancing trial-load patterns and solving the simultaneous equations involved. The solution is normally obtained by computers using a trial load program such as ADSAS developed by the US Bureau of Reclamation. The resulting load distributions required to achieve geometric continuity are then used to compute stresses in the dam.

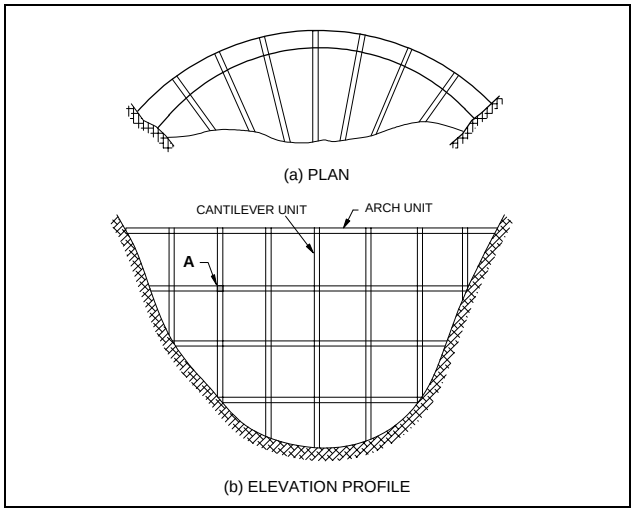

Fig. 11-5.8 Arch and cantilever units in Trial Load Method

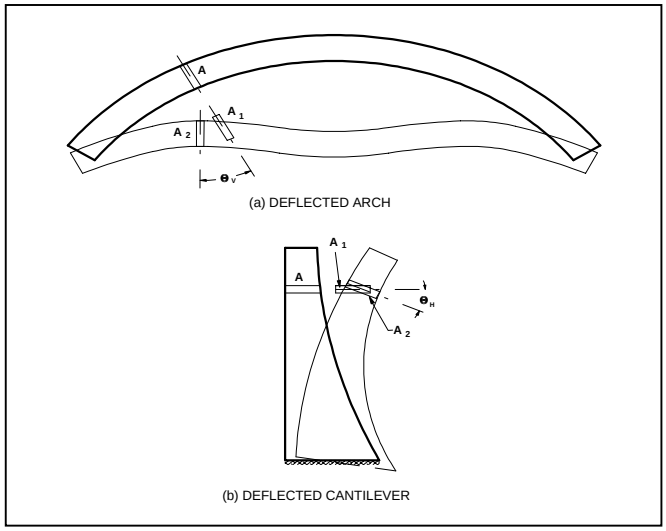

Fig. 11-5.9 Translations and rotations of arch and cantilever units.

Progressing from the simplest to the most comprehensive, a trial load analysis may consist of crown-cantilever adjustment, radial deflection adjustment, or the complete adjustment, which includes adjustments for the radial and tangential translations as well as ro-

tations. The crown-cantilever and radial deflection analyses are usually used for the preliminary and feasibility studies of new dams. For safety evaluation of existing arch dams only the complete trial load analysis should be attempted.

Many comparisons with measurements from actual dams and scale models as well as with 3D fintite element analyses have shown that ADSAS gives reliable results for one-, two- or three-centered dam layouts, subjected to standard static loads. It has been used successfully in the design of new dams over many decades, but its use in the evaluation of existing dams is limited to the geometry configurations just described and to static loading only. Complex geometry and material property variation, the effects of openings within the body of the dam, and nonradial abutments cannot be analyzed by ADSAS. Unlike FEM, ADSAS does not permit analysis of the effects of rapid changes in the dam geometry where detailed stress information may be required. Analysis of the effects of unusual loads, special boundary conditions, and seismic loading is not possible.

The use of trial load method and ADSAS should be limited to the geometry configurations described above so far as the computed static stresses are not excessive. Existing dams located in seismic regions requiring dynamic analysis should be evaluated by the finite element method.

11-5.3.2 Other Methods

Other mathematical formulations and approaches can also be applied to the analysis of arch dams. Finite difference solutions and global variational energy methods, etc. may all be acceptable provided force equilibrium is satisfied and realistic constitutive relationships are enforced.

Small single-centered (circular) arch dams located in seismic Zone 1, where seismic loading does not control, may be analyzed using the cylinder theory. In the cylinder-theory analysis of arch dams, the stresses at each elevation are assumed to be the same as in a cylinder of equal outside radius. That is, water loads are resisted entirely by individual arch sections acting independently. If average stresses from this approximate solution provide large allowance for stress uncertainties and meet the criteria, then no further sophisticated analysis will be required.

11-5.4 Rock Wedge Stability

Stability of the abutments of an arch dam is crucial to the safety of the dam. The abutments are required to resist the majority of the thrust imposed upon the dam by the impounded reservoir. Design of a new arch dam or inspection of an existing arch dam must

incorporate a careful evaluation of the stability of the abutments. Since rock failures almost always occur along preexisting discontinuities in the rock mass, abutment stability analysis must focus on an evaluation of any wedges of the abutment foundation which could fail under the loads applied naturally and by the dam and reservoir. As described in Section 11-8.2.1, the first failure of a thin arch dam occurred in 1959 with Malpasset Dam in France and resulted from the displacement of a large wedge of rock in the left abutment. Extensive post failure investigations and analysis led to the conclusion that the wedge was formed by the interaction of a downstream fault with the gneissic foliation in the rock and that it was displaced by arch thrust assisted by abnormally high seepage uplift forces. The primary lesson learned from this experience was the importance of performing a careful geologic investigation of the abutments of an arch dam followed by stability analysis of any kinematically capable wedges of rock identified.

11-5.4.1 Identification of Kinematically Capable Potential Failure Planes and Wedges

The first step in an abutment analysis is the identification of any wedges of rock that have the possibility of sliding under the loads expected to develop during construction and operation of the dam. This is initiated by a geologic investigation of the abutments designed to identify those discontinuity patterns that could contribute to the development of kinematically capable failure wedges. Discontinuities include such features as joints, faults, shears, foliation, schistocity, bedding planes, clay seams, coal beds, shale partings and any other planar weaknesses that may be present in the rock mass.

This is accomplished by first mapping the discontinuity pattern existing in each abutment. Some of the structural geologic features are mapped individually such as faults, shears, clay seams, and coal beds while others which are more ubiquitous such as joints are mapped as sets and are assumed to be capable of occurring anywhere in the rock mass. Bedding, schistocity, and foliation may be ubiquitous, but their orientation may vary from one part of an abutment to another due to folding and this must be identified during the mapping.

The joint system in a rock mass normally will consist of from two to six individual joint sets. A joint set is defined as a series of essentially parallel planar fractures which have not experienced translational movement. Joint sets are usually identified by plotting the results of a large number of field joint orientation measurements on a stereonet and contouring the density of the pole positions to locate the orientation of the largest concentrations. Detailed instructions for performing a joint system analysis are contained in most

structural geology texts, such as Billings (1954). Software programs are available which facilitate stereographic analysis by use of computers.

The geological investigation then uses the assembled data to locate any and all kinematically capable wedges of rock. This means the location of any rock mass which can fail by sliding on one or more preexisting fractures with out the necessity of shearing through a large mass of intact rock. The intact shear strength of most rock is sufficient to prevent sliding failure except on daylighting discontinuities. Such a daylighting discontinuity may be a single plane subparallel to a slope with a slightly lower dip angle than the slope, or it may be a combination of two or more intersecting discontinuities whose trend of intersection daylights on the slope at an angle of dip slightly lower than that of the slope.

11-5.4.2 Analysis by Stereographic Projection Procedures

The step by step procedures for performing a graphical slope stability analysis by use of stereonets is presented in Chapter Four of Hendron, Cording and Aiyer (1971) or Chapters 7 and 8 of Hoek and Bray (1981).

11-5.4.3 Vector Analysis

Vector analysis procedures have been developed for three dimensional analysis of potentially unstable wedges of rock in both natural and cut slopes. The failure of Malpasset Dam in 1959 provided much motivation to develop this procedure. Early researchers were Wittke and Londe. More recent developments have been documented by Hendron, Cording, and Aiyer (1971), and Hoek and Bray (1981). Procedures for performing this analysis are outlined and explained in great detail in each of these last two references. These publications are recommended as acceptable guides for performing the analysis. Computer programs have also been developed for performing the rigid block three-dimensional vectorial analysis. The Bureau of Reclamation publication by Scott and Von Thun (1993) describes one such program RIGID, which performs rigid block limit equilibrium analyses utilizing three dimensional vector procedures. Hoek, Carvalho, & Kochen (1995) have developed a rock wedge stability software program called SWEDGE.

OABC = Rock wedge or tetrahedron
P1, P2, P3 = Rock discontinuities or geological surfaces of separation
U1, U2, U3 = Water pressure forces
W = Weight
Q = Dam thurst

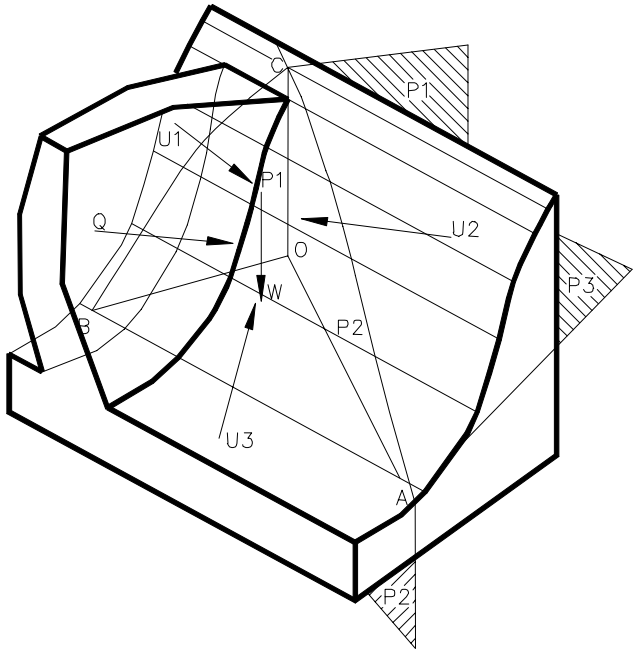

Fig. 11-5.10 Three dimensional representation of an arch dam acting on an abutment showing the planes of three discontinuities forming a rock wedge or tetrahedron and the vectors of forces acting upon the rock.

A vector representation of a tetrahedral rock wedge with the kinematic capability of failing under loads imposed by its own weight and the thrust and water pressure forces imposed by an arch dam is illustrated in Fig. 11-5.10 after Londe (1993). This illustration shows a three dimensional picture of the left abutment of an arch dam underlain by a large rock wedge formed by the intersection of three rock discontinuities or fractures. The vectors representing the water pressure on each of the fractures, the weight of the rock mass, and the thrust of the dam are shown. Forces resisting failure of the wedge of rock may include both friction and cohesion. The analytical procedures described in the above references provide for inclusion of cohesion in addition to friction where it is appropriate.

11-5.4.4 Loads to be Considered

Refer to section 11-4.5, Load Combinations, for detailed discussion of the loading combinations to be evaluated. These include summer and winter conditions for each of the following loading combinations:

1. Usual (normal operating conditions)

2. Unusual (flood condition)

3. Extreme (seismic)

The loads that must be considered in the analysis of abutment rock wedges include the weight of the rock wedge, thrust from the dam, uplift from hydrostatic forces applied on each plane which defines the wedge, and dynamic forces applied by the design earthquakes. The weight of the rock wedge is obtained by calculating the volume of the wedge times the unit weight of rock. The thrust from the dam is obtained from the structural analysis either by direct computation of nodal forces acting on the dam-foundation interface or from integration of element stresses in contact with the foundation. In determining the dam thrust, the effects of load redistribution due to possible joint opening and tension cracks should be considered. The following assumptions are made in calculating uplift on the various wedge defining planes in the absence of actual piezometric measurements:

(a) Fractures are open over 100 percent of the wedge area and are completely hydraulically connected to the surface.

(b) Head varies linearly from maximum at backplane to zero at daylight.

(c) Planes acted upon directly by the reservoir receive full hydrostatic force.

Dynamic loads are obtained from the design earthquake studies that specify the ground motions anticipated from the Maximum Credible Earthquake (MCE). Approximate dynamic loads may be incorporated into stability analysis of individual rock wedges by use of acceleration values represented by an equivalent static force as described by Hoek and Bray (1981) or by a seismic coefficient as described by Hendron, Cording, and Aiyer (1971) for the Extreme Case of load combinations.

Rock wedge stability can also be modeled directly by including element layers aligned along shear planes in the foundation. Refer to Sections 11-4.4 and 11-6 for further guidance on earthquake loading and finite element analysis.

11-5.4.5 Appropriate Factors of Safety

There is considerable debate among arch dam design professionals with regard to how safety factors should be applied. For instance, Londe (1993) discusses the safety factor in the light of applying a unique safety factor individually to each different property in the analysis depending upon the degree of uncertainty associated with that material rather than a single safety factor applied to the final computation. He also develops the case for the use of the probabilistic approach rather than the deterministic approach required by this guideline.

The safety factors to be used on projects under the jurisdiction of the FERC are based on a deterministic approach and the safety factors are applied to the final computation rather than to individual properties in the stability analysis. The assumption is made that the strength parameters and uplift forces assumed for the analysis will be conservatively selected. They must be based upon a comprehensive field investigation and testing program as described in Section 11-2, Foundation Considerations, which provides a high degree of confidence in the definition of geologic conditions and shear strength parameters. In the absence of such detailed foundation knowledge, much more conservative safety factors must be employed. These will be established for individual projects in consultation with and as approved by the FERC.

Following are the safety factors to be used where foundation conditions are well defined:

(a) Worst Static Case ---------- FS = 1.5

(b) Extreme (Seismic) ---------- FS = 1.1

It is important to understand that meeting an acceptable safety factor, as part of a stability analysis does not necessarily assure a safe structure. Assurance only comes when sound engineering and geologic judgement are applied at every step of the investigation, analysis and review to preclude the existence of undiscovered conditions which could defeat the stability analysis. An example again was the failure of Malpasset Dam in 1959 which was designed by one of the world's preeminent arch dam designers.

11-5.5 Parameter Sensitivity

11-5.5.1 Effects of foundation modulus on dam stresses

Considering that an arch dam resists a large portion of water pressures and other loads by transmitting them through arch action to the abutments, foundation deformations caused by the dam loads are likely to significantly affect stress distributions within the dam. Proper evaluation of stresses within the dam, therefore, requires an adequate determination of the foundation deformation characteristics. As described in Section 11-2, deformability of the foundation rock is characterized by the modulus of deformation. Depending on the type of material and discontinuities present in a foundation, values of the modulus of deformation may vary significantly from abutment to abutment, or with the elevation (depth). It is also possible that the differences are small or rock masses are of such a high quality that a uniform average modulus of deformation can be assumed for the entire foundation contact region.

A comprehensive field investigation to provide extensive definition of the variation of modulus of deformation is costly and may not be necessary, for example when the deformation modulus of foundation is much higher than the modulus of the concrete. Instead, the minimum field investigations and laboratory tests described in Section 11-2 should be supplemented by parameter sensitivity studies to account for the uncertainties and extrapolation to untested areas when necessary. The results of a parametric study of Morrow Point Dam in Figs. 11-5.12 to 11-5.22, are provided to demonstrate the relative importance of the foundation modulus on the dam response. The cases presented include:

a) $E_r / E_c > 1$
b) $E_r / E_c < 1$
c) Variable foundation modulus with abutments
d) Variable foundation modulus with elevation

where E_r is an effective modulus of deformation for the foundation and E_c is modulus of elasticity of the mass concrete. The results presented are for water pressures only, applied to upstream face of the dam as well as to the floor and flanks of the flexible foundation. Hydrostatic deflections along the crown section for various uniform rock to concrete modulus ratios (Cases a and b) are displayed in Fig. 11-5.11, whereas the variation of crest and heel deflections as a function of E_r / E_c are given in Fig. 11-5.12. These graphs demonstrate that the dam deflections are more sensitive to modulus ratios of less than 1, and that they especially increase dramatically when E_r / E_c becomes less than 0.5. While dam deflections for stiffer foundation rock ($E_r / E_c > 1$) change only slightly from

those for a rigid foundation. The effects of foundation flexibility on the dam response essentially diminish for $E_r / E_c > 2$.

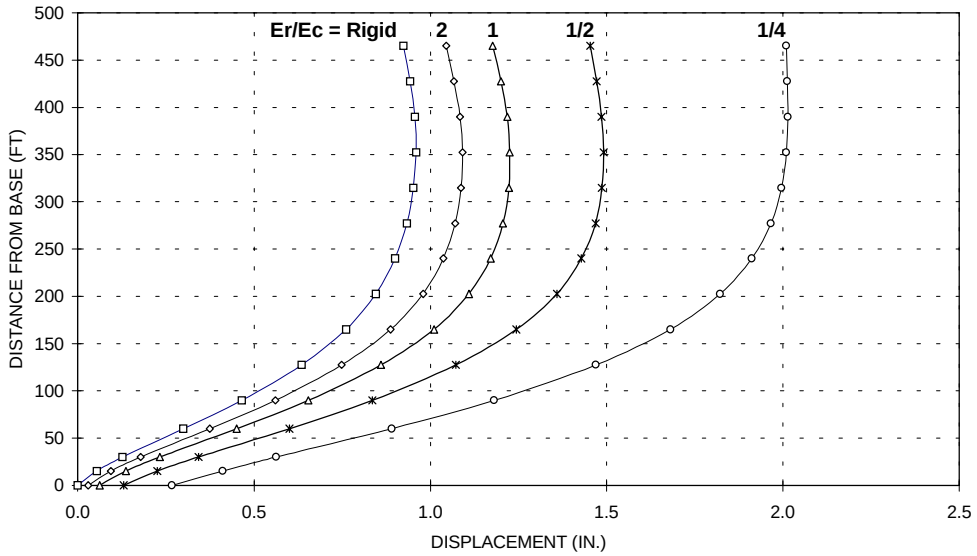

Fig. 11-5.11 Hydrostatic deflections of dam crown section for E_r / E_c = rigid, 2, 1, 1/2, and 1/4.

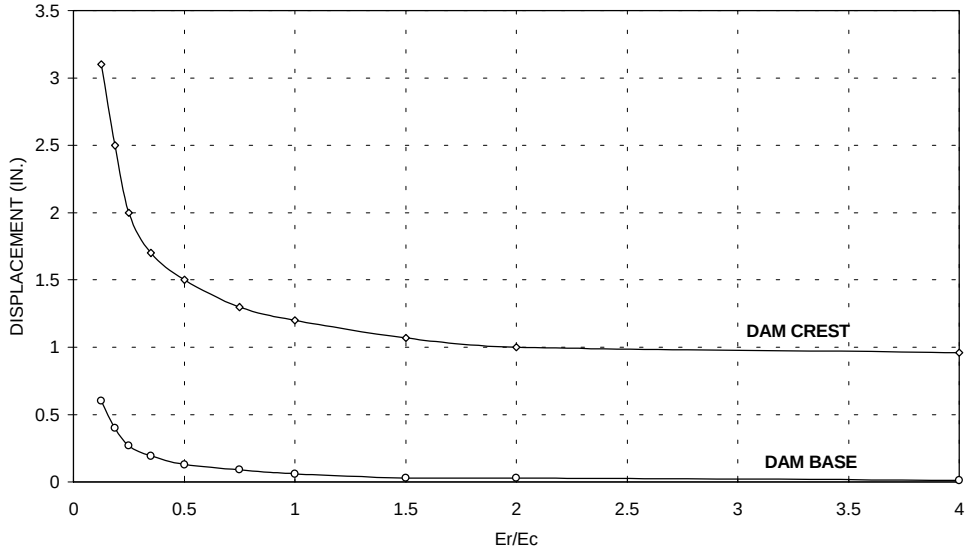

Fig. 11-5.12 Hydrostatic deflections of dam crest and dam base as a function of E_r / E_c.

Similarly, the values of arch and cantilever stresses are more sensitive to modulus ratios of less than 1, and only slightly differ from those for the rigid foundation when E_r / E_c exceeds 2 (Figs. 11-5.13 and 11-5.14). For Morrow Point Dam subjected to hydrostatic loading, foundation flexibility increases arch stresses mostly in the central part of the up-

stream and on the lower part of the downstream face of the dam (Fig. 11-5.14), while cantilever stresses are primarily increased in the lower 1/3 portion of the dam, as shown in Fig. 11-5.14.

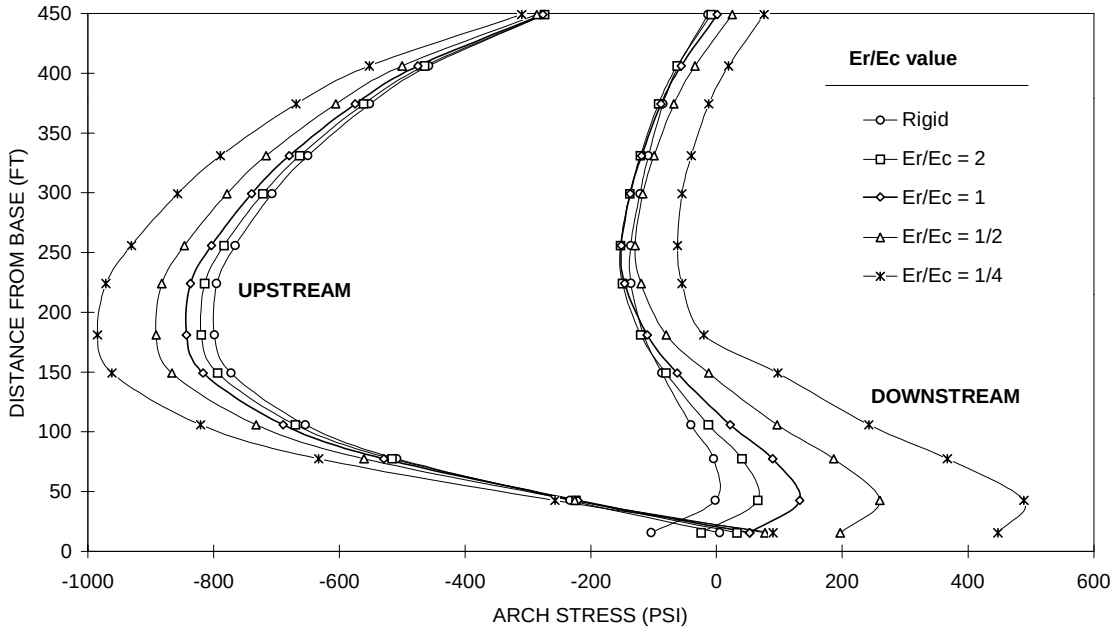

Fig. 11-5.13 Hydrostatic arch stresses at dam crown section for E_r / E_c = rigid, 2, 1, 1/2, and 1/4.

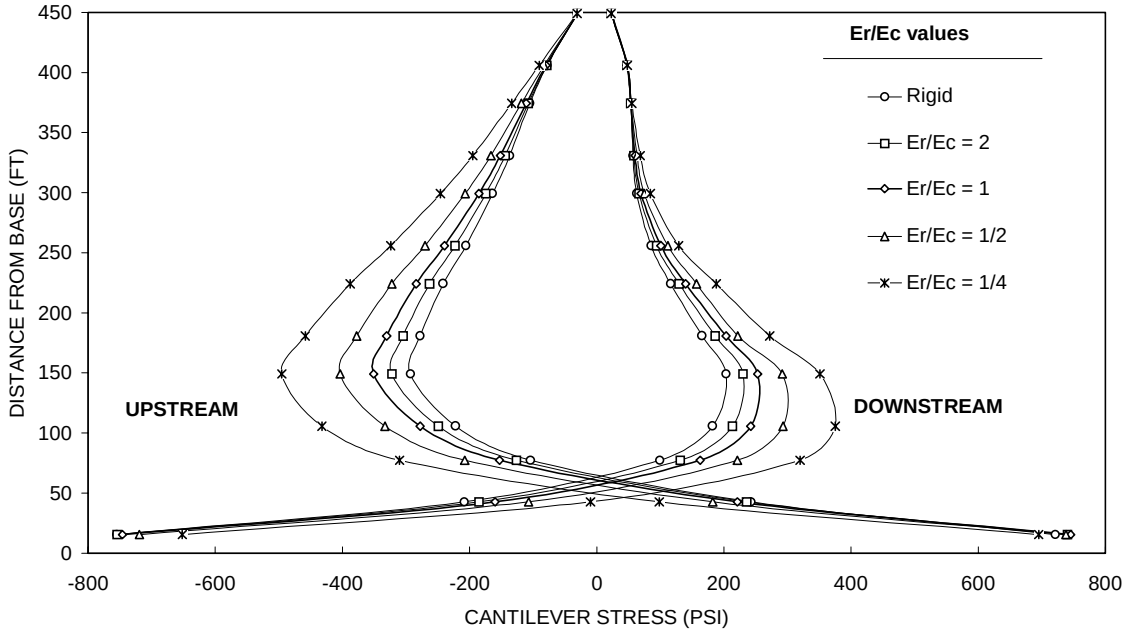

Fig. 11-5.14 Hydrostatic cantilever stresses at dam crown section for Er_f/E_c = rigid, 2, 1, 1/2, and 1/4.

Variable Foundation Modulus with Abutments. Variation of foundation modulus with abutment tends to skew dam deflections and stress distributions towards the weaker abutment, increase stresses within the body of the dam, and cause stress concentrations near the base of the dam (Figs. 11-5.16 and 11-5.17). The amount of distortion in deflections and stress distributions and increase in stress values depends on the modulus ratios between the abutments and between the abutments and the concrete. Softer foundation rock with greater differences between the abutment moduli, produce larger distortions and higher stresses. Whereas compared to the uniform foundation with $E_r / E_c = 1$, stiffer foundation rock with both abutment moduli higher than that of the concrete, cause negligible distortions with slightly more stress concentrations, even if the differences between the abutment moduli are significant.

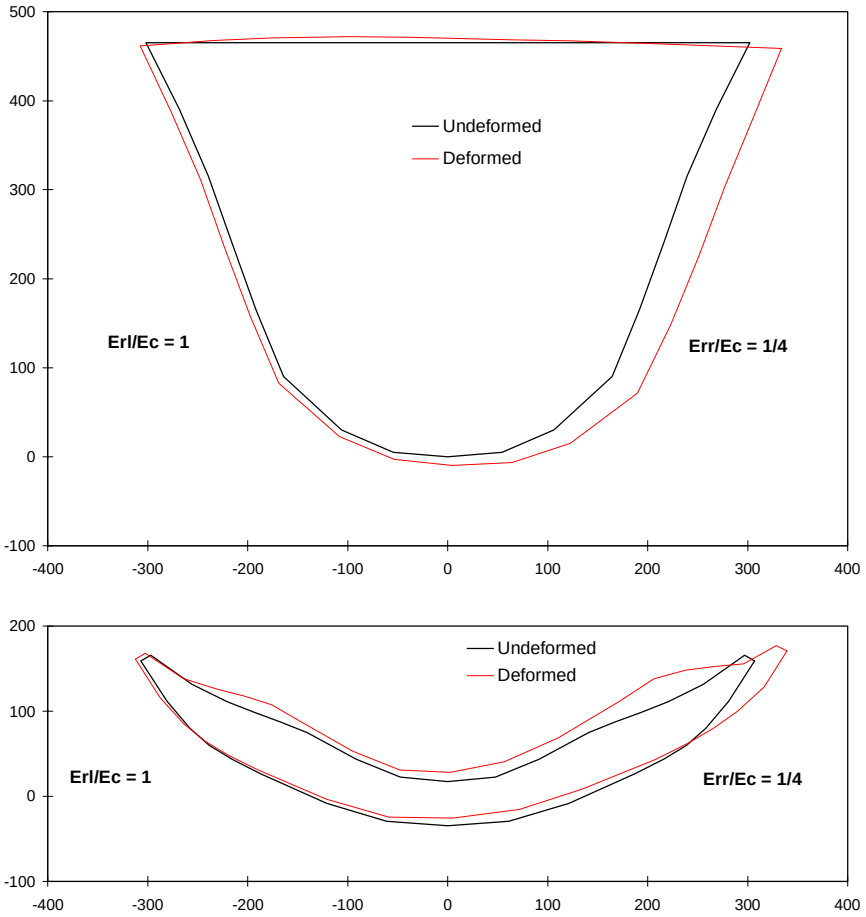

Fig. 11-5.15 Hydrostatic deflections of Dam/foundation contact for E_{rr}/E_{rl} = ¼.

Sensitivity analyses of Morrow Point Dam with assumed foundation-to-concrete modulus ratios of 1 for the left abutment and 1, 1/2, and 1/4 for the right abutment clearly demonstrates the behavior discussed above, as shown in Figs. 11-5.16 to 11-5.18. The results

indicate that while hydrostatic cantilever stresses increase on the weaker abutment side (right), their values on the left side only slightly differ from those obtained for the uniform foundation (Figs. 11-5.17 and 11-5.18). Cantilever stresses also increase at the base of the dam due to abrupt change of the foundation modulus at this location, with the stress concentration shifted toward the stiffer abutment side.

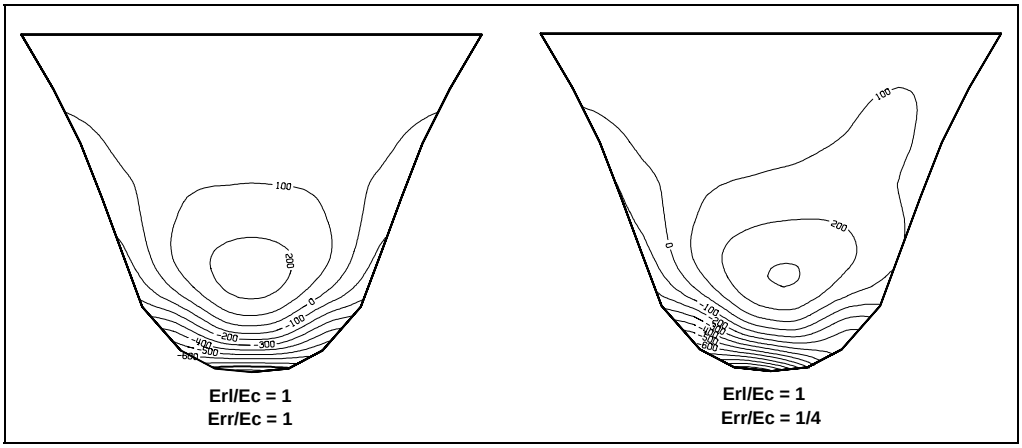

Fig. 11-5.16 Downstream hydrostatic cantilever stresses for uniform and varying foundation moduli with abutments.

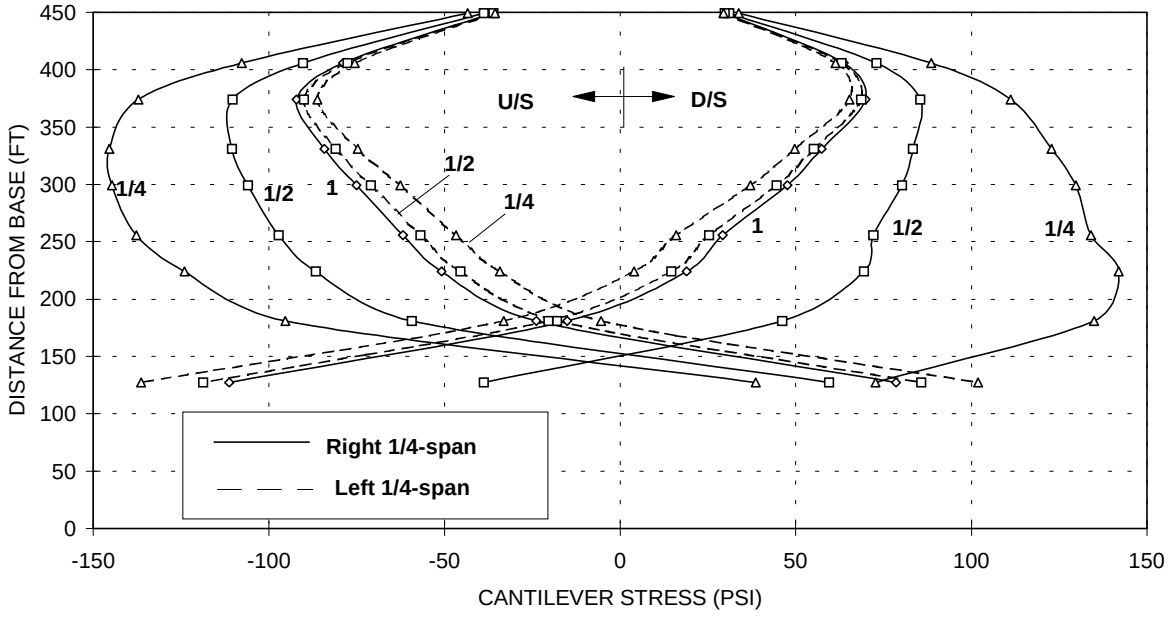

Fig. 11-5.17 Hydrostatic cantilever stresses at 1/4-span locations for E_{rl}/E_c = 1 and E_{rr}/E_c= 1, 1/2, and 1/4.

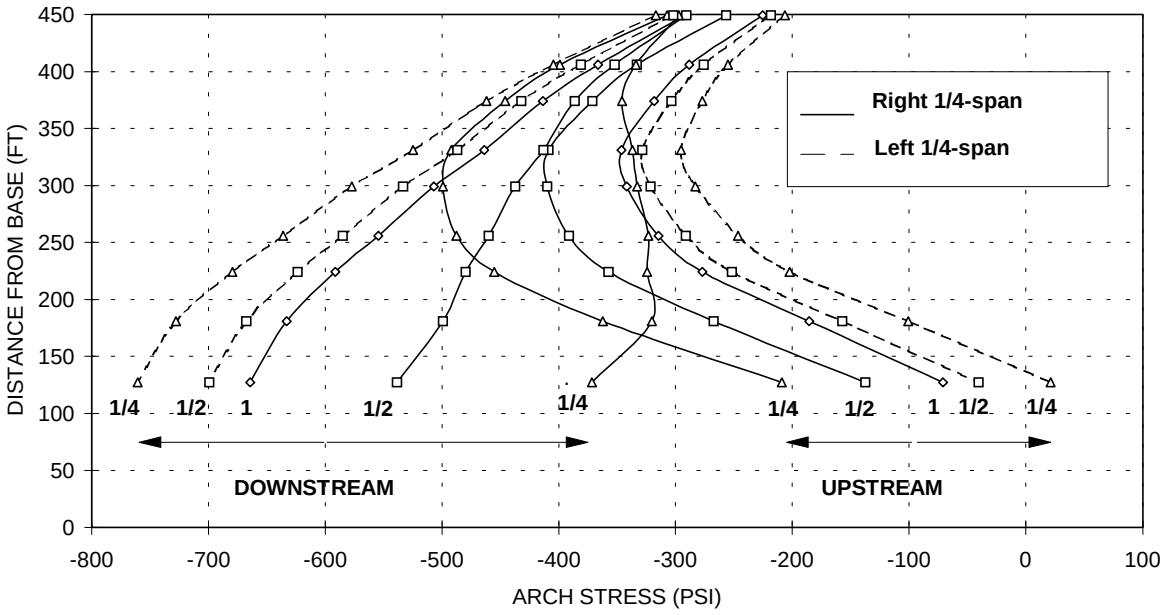

Fig. 11-5.18 Hydrostatic arch stresses at 1/4-span locations for $E_{rl}/E_c = 1$ and $E_{rr}/E_c = 1$, 1/2, and 1/4.

Hydrostatic arch stresses for the case of uniform foundation modulus are generally compressive in the entire dam, except for minor tensile stresses near the base. Compared to the uniform foundation case, compressive arch stresses in the weaker abutment side tend to increase on the upstream and decrease on the downstream face of the dam (Fig. 11-5.18). The variation of foundation modulus with abutment also increases tensile arch stresses near the base of the dam, with larger values on the upstream face concentrating on the stiffer abutment side and those of the downstream face on the weaker abutment side.

The effects of variation of foundation modulus with abutment are most significant when the modulus of the weaker abutment is substantially (factor of 2 or more) less than the modulus of the concrete, and should be considered in the analysis. As the modulus of the weaker abutment approaches the modulus of the concrete, its effects on the dam response diminishes and may be ignored. Variation of the foundation modulus with abutment may also be ignored when foundation moduli for both abutments are greater than that for the concrete. In these situations, if the variation of foundation modulus is ignored, the modulus of the weaker abutment should be applied to the entire foundation.

Variable foundation modulus with elevation. At some dam sites, the foundation modulus may vary significantly with the elevation. A situation in which the modulus of the highly

weathered and fractured upper abutment regions could be much lower than that of the lower foundation regions. The effects of weaker upper abutments on the dam response are most significant when they extend to large depths and their moduli are substantially less than the modulus of the concrete. Sensitivity analyses of Morrow Point Dam with the foundation rock overlain by one or two weaker zones, indicate that the variation of foundation modulus with elevation generally increases dam deflections and stresses. Figs. 11-5.19 to 11-5.21 show that, the larger the weaker abutment regions and the smaller their moduli, the greater would be the dam deflections and stresses. The increase in deflections and stresses for this case, however, is much less than those cases where one abutment or the entire foundation consist of low modulus materials as discussed previously. Nevertheless, the effects of variable modulus with elevation should be considered when the area the weaker zone is substantial and its modulus is less than the modulus of concrete. In situations where the moduli of the entire foundation including the weaker zones are higher than the modulus of the concrete, the effect of variation of modulus with abutment may be ignored and the smallest modulus employed for the entire foundation.

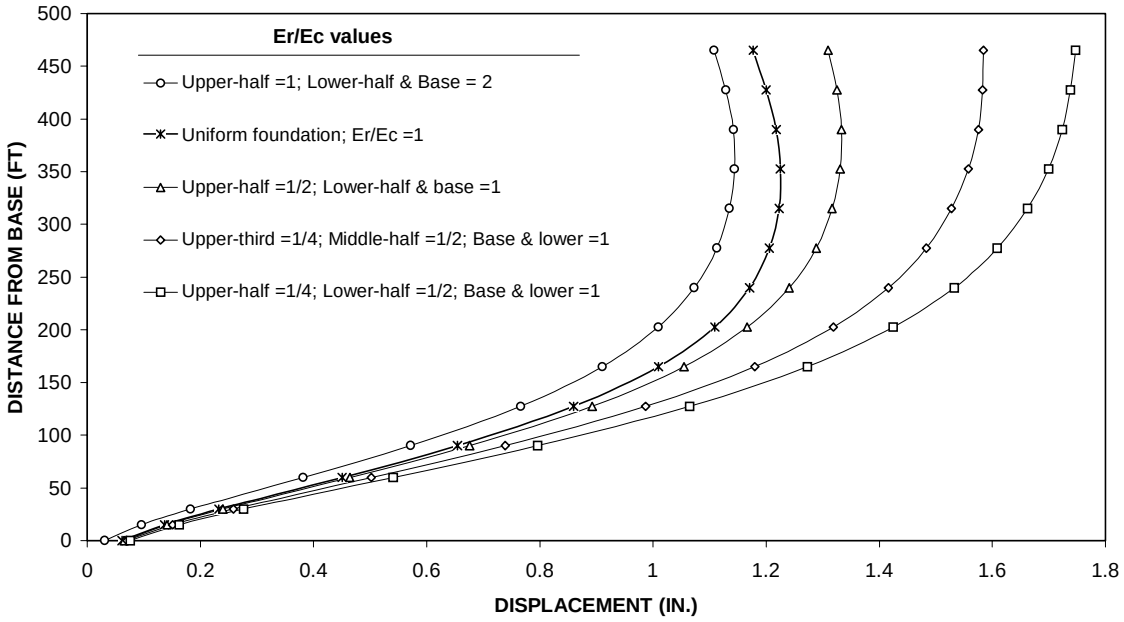

Fig. 11-5.19 Crown-section hydrostatic deflections for varying foundation modulus with elevation.

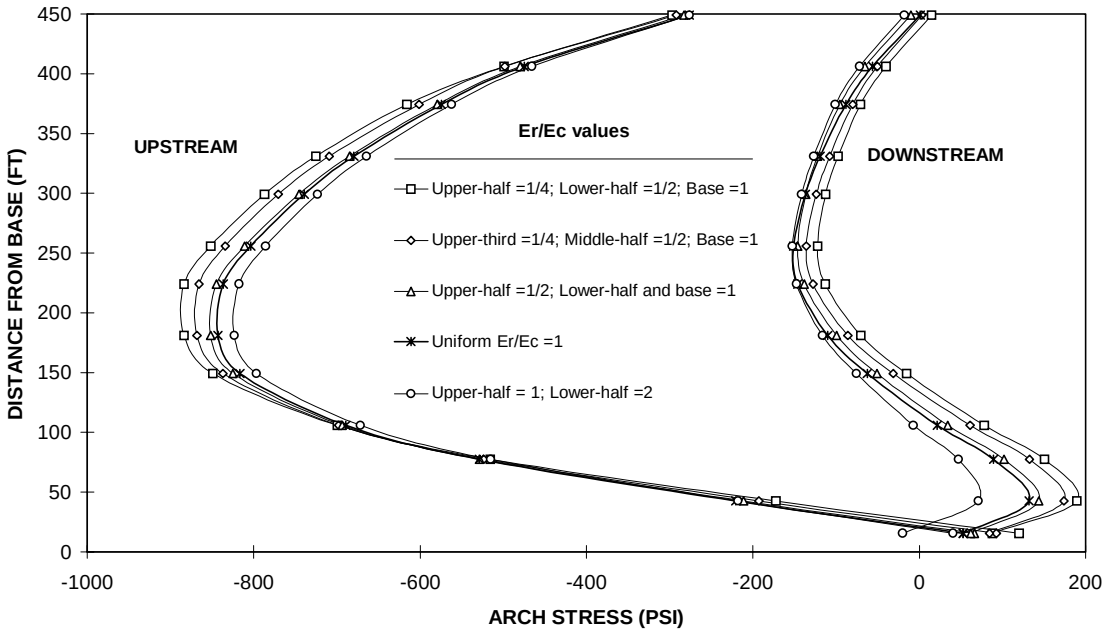

Fig. 11-5.20 Crown-section hydrostatic arch stresses for varying foundation modulus with elevation.

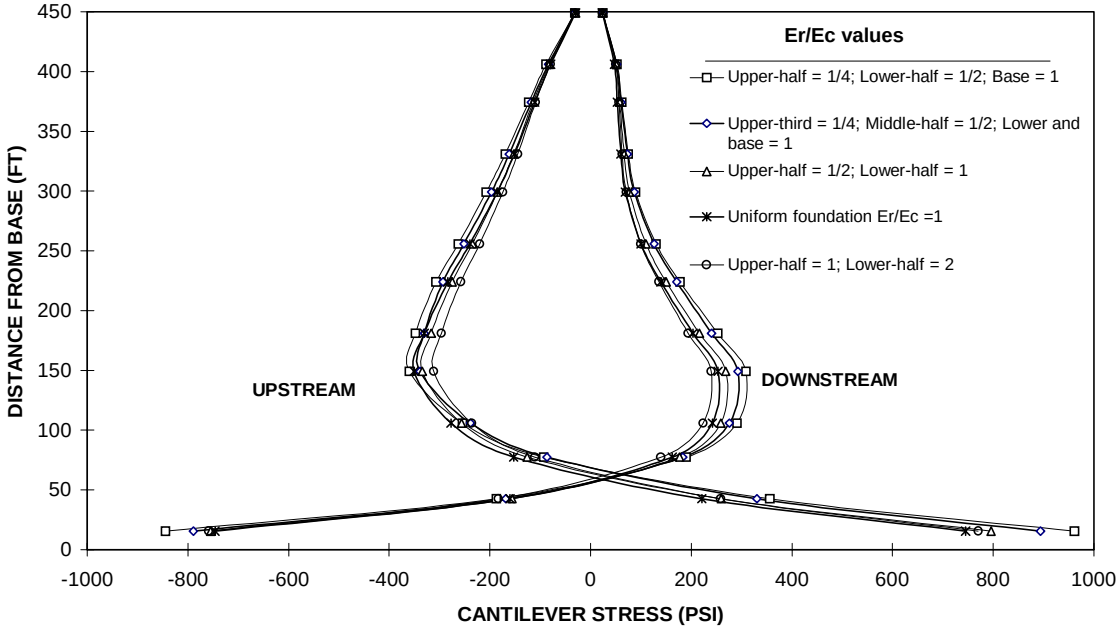

Fig. 11-5.21 Crown-section hydrostatic cantilever stresses for varying foundation modulus with elevation.

11-5.6 Limit State Analysis

In addition to failures resulting from exceeding the load-resisting capacity of the concrete and potential foundation instability, other possible types of failure should also be considered in the evaluation of arch dams for static loads. The analyses presented below are examples of the process of ruling out failure mechanisms. The purpose of this section is to call attention to the fact that computation of the stress within the body of the dam may not be the sole indicator of the dam's stability. Although the failure modes considered here are highly unlikely for majority of exiting arch dams, they cannot be completely ruled out for dams with unusually gentle abutment slopes and for very thin dams.

11-5.6.1 Sliding on the Abutment Contact

Usually, sliding stability along the dam-foundation contact of a concrete arch dam is unlikely because of the wedging produced by arch action. However, arch dams with relatively flat abutment slopes such as Dike "F", FERC project # 1759, shown in Fig. 11-5.22, or in cases where the concrete is not thoroughly bonded to the foundation rock and adequate drainage is not provided, the benefit of wedging will be reduced. In these situations the possibility that a portion of the dam might slide along the dam-foundation contact should be evaluated. A failure of this type did occur at Plum dam, located in southeast China. (See 11-8.3.2)

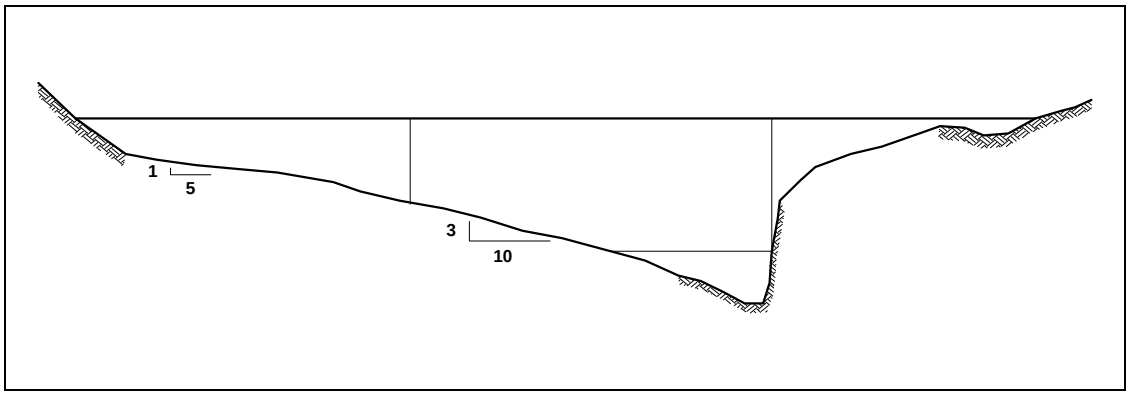

Fig. 11-5.22 Arch dam with relatively flat abutment slopes.

The potential for sliding can be evaluated by comparing computed shear forces with the shear resistance along the dam-foundation contact surface. An example of limit state analysis is shown below. In this example, non-linear finite element analysis first allows for the elimination of tensile stress normal to the dam/foundation contact through cracking. Then, the shear strength of the contact is reduced by allowing local sliding until the

non-linear finite element solution fails to converge. The direction of impending failure is depicted in figure 11-5.23

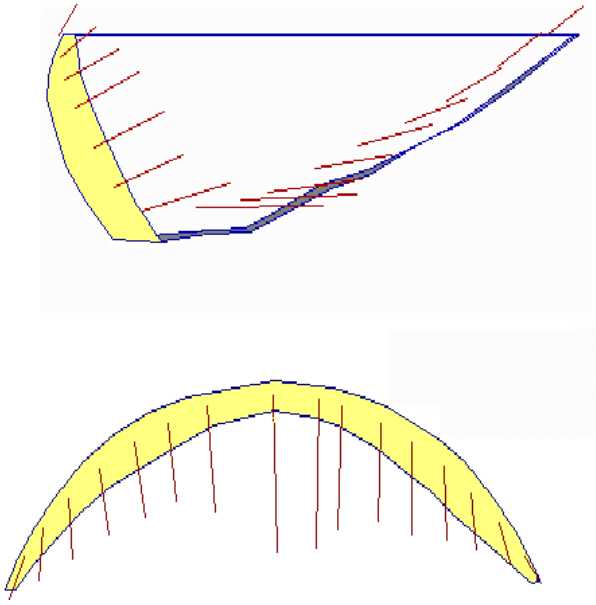

Fig 11-5.23 Direction of Impending Motion with Base Shear Failure.

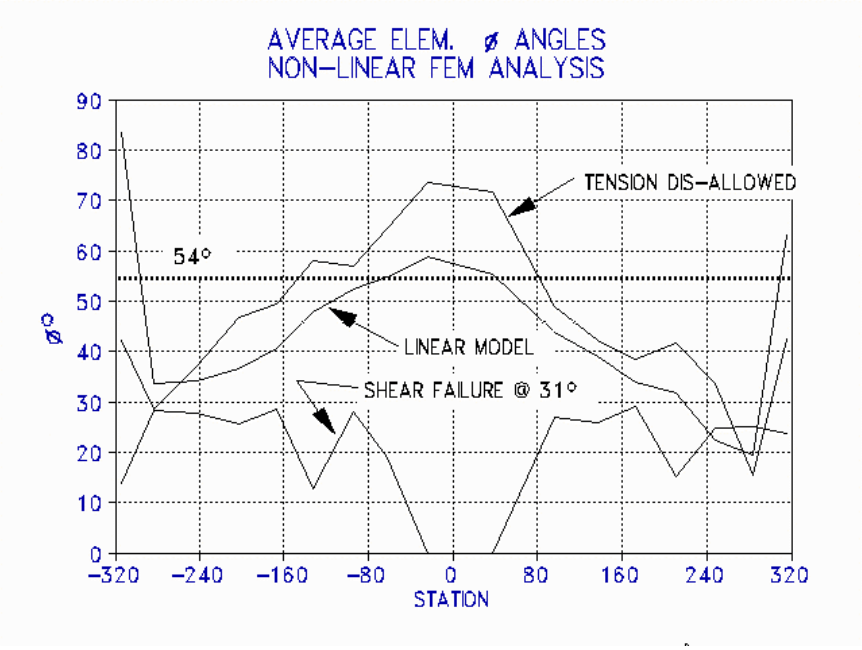

Fig. 11-5.24 Angle "ϕ" between forces applied to the foundation and outward directed normal to foundation under various modeling assumptions.

Figure 11-5.24 depicts the friction angle mobilized at the dam foundation contact under various modeling assumptions. The linear model indicates that shear strength require-

ments are highest near the center of the dam (Sta. 0). When tensile stress normal to the dam/foundation contact is disallowed, the shear strength required on the portion of the dam/foundation contact that is not cracked increases. The shear strength of the portion of the dam foundation contact that is cracked is assumed to be 0. Finally, shear stress re-distribution is allowed and load is transferred up the abutments. When the shear strength is reduced to 31° and no cohesion, the non-linear finite element solution fails to achieve force equilibrium.

11-5.6.2 Buckling Failure Modes

Over and above the determination of stresses and displacements in arch dams, under some extreme dam geometries such as thin, single curvature dams with large radii, the question of buckling stability of an arch dam structure may arise. Figure 11-5.25 and the corresponding equation describe the buckling mechanism of circular arches subject to uniform compressive load, q_{cr}

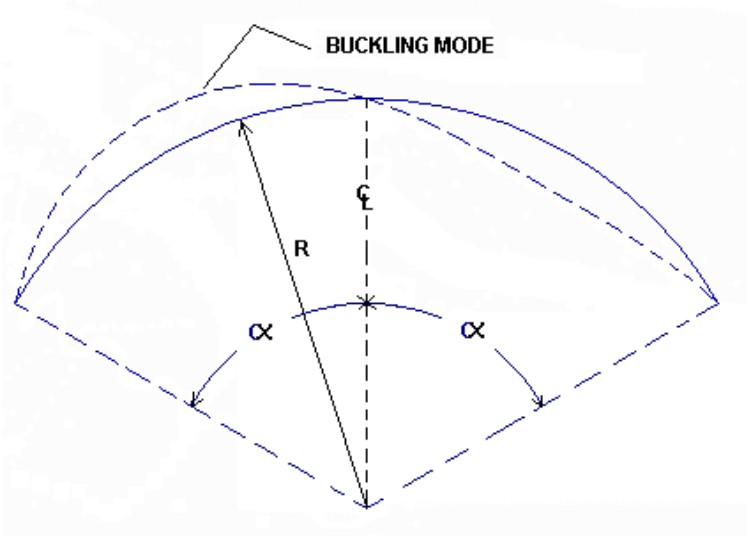

Fig. 11-5.25 Snap through buckling of a simply supported circular arch under uniform load.

$$q_{cr} = \frac{EI}{R^3}\left(\frac{\pi^2}{\alpha^2} - 1\right)$$

The critical uniform load in the above equation can be related to the average compressive arch stress σ_{cr} given by

$$\sigma_{cr} = \frac{EI}{R^2}\left(\frac{\pi^2}{\alpha^2} - 1\right) \qquad (11\text{-}5.1)$$

General formulas for different types of arches with different boundary and load conditions can be found in “The Theory of Elastic Stability” by Timoshenko and Gere.

While this arch analogy provides some insight into how arch dams could fail in buckling, it is overly simplistic since it treats the problem in only two dimensions. It also ignores the cantilever resistance of an arch dam and thus is very conservative. If the dam has double curvature, equation 11-5.1 is even more conservative. The equation is of some value however, since if the average computed compressive arch stress is less than σ_{cr} predicted by the equation, buckling failure can be ruled out.

Rigorous determination of the buckling stability of a general shell under variable load such as a double curvature arch dam requires the use of non-linear finite element analysis. If buckling instability is a concern, simple conservative analysis techniques such as that discussed above should be used if possible.

11-6 DYNAMIC ANALYSIS

11-6.1 Overview

All dams in seismic zone 3 and higher should be evaluated using dynamic analysis techniques. Dams in zone 2 may also require dynamic analysis on a case by case basis. Currently, three-dimensional linear-elastic finite-element analysis is the most common technique used for dynamic analysis.

A linear-elastic dynamic analysis of arch dams typically consists of the following four basic steps:

1. Determination of design or evaluation earthquakes and the associated ground motions;
2. Development of appropriate three-dimensional finite-element models including dam-foundation and dam-water interaction effects;
3. Specification of dynamic material properties, damping, and reservoir-bottom absorption, if applicable; and
4. Computation of the earthquake response and presentation, interpretation, and evaluation of the results.

The requirements for development of design or evaluation earthquakes and earthquake ground motions are discussed in Section 11-4.4. The design or evaluation earthquake for arch dams is the maximum credible earthquake (MCE). The earthquake ground motions include the horizontal and vertical response spectra, or three components of acceleration time histories. They are applied uniformly at the fixed boundaries of the foundation model.

Three-dimensional finite-element models for the arch dam and the foundation rock are essentially identical to those described for the static analysis (Section 11-5.2), except that the dam-water interaction effects should also be represented by the added hydrodynamic mass models or by the frequency-dependent hydrodynamic terms, as appropriate (Section 11-6.5.1).

A seismic safety evaluation of an arch dam should be based on the dynamic material properties of the dam concrete, foundation rock, and the energy loss at the reservoir bottom, if applicable. Dynamic modulus of elasticity and dynamic strength of the concrete for earthquake excitation are determined as described in Section 11-3. Damping associated with dissipation of energy in the concrete arch structure and the foundation rock must be consistent with the level of ground shaking, amount of non-linear responses developed in the dam and foundation, and the properties of the foundation rock. For the purpose of safety evaluation, a damping value of 5% or 10% should be used. A 5% damping should be applied to stress and sliding stability analysis of all dams. The in-

crease to a 10% is acceptable for stress analysis of those dams showing energy dissipation through joint opening and tension cracking. The sliding analysis of thrust blocks and abutment wedges, however, should always be conducted using a 5% damping.

The linear-elastic response of arch dams to earthquake loading is computed using the response-spectrum mode-superposition and the time-history method. The response-spectrum method of analysis gives only the maximum displacements and stresses. The response-spectrum method may be sufficient in most cases, especially when the dam response remains mainly within the linear elastic range of behavior. Linear time-history analysis is recommended when tensile stresses significantly exceed tensile strength of the concrete and consideration of time-dependent nature of the dynamic response is essential to assessment of dam safety, or when the frequency-dependent dam-water and dam-foundation interaction models are employed.

Evaluation of earthquake performance of an arch dam should consider many modeling, material properties, and seismic parameter assumptions commonly made in dynamic analysis of the dam. Whether the time-history or response-spectrum method of analysis is employed, the results are still influenced by such assumptions and cannot always be viewed as conclusive in itself. Rather than just checking stress contour plots to see if the apparent dynamic tensile strength of the concrete has been exceeded, evaluation of a dynamic analysis should also be aimed at answering the following questions:

1) How do the dynamic stresses compare in magnitude with the static stresses that the dam is currently bearing? Does the dynamic load represent a substantial increase over the static load?

2) Where do the major natural periods of the dam fall on the earthquake response-spectrum curve? As the earthquake shaking progresses, contraction joints may open and tension cracks develop. The joint opening and cracks increase the periods of vibration of the dam, possibly shifting the periods into different region of response spectrum, and hence changing the maximum response. If the natural periods of the dam fall in the ascending region, the dynamic response of the dam will increase as joint opening and cracks develop, as long as the modified periods still remain in this region. If the natural periods of the dam are in the descending region, the dynamic response of the dam will decrease as joint opening and cracks develop. This kind of evaluation can therefore indicate whether the assumption of an uncracked linear-elastic structure is conservative or unconservative with respect to the dynamic loading. If the primary natural periods fall far from the peak of the earthquake response spectra , the analyst must make sure that a change in the value of uncertain parameters will not greatly increase the response.

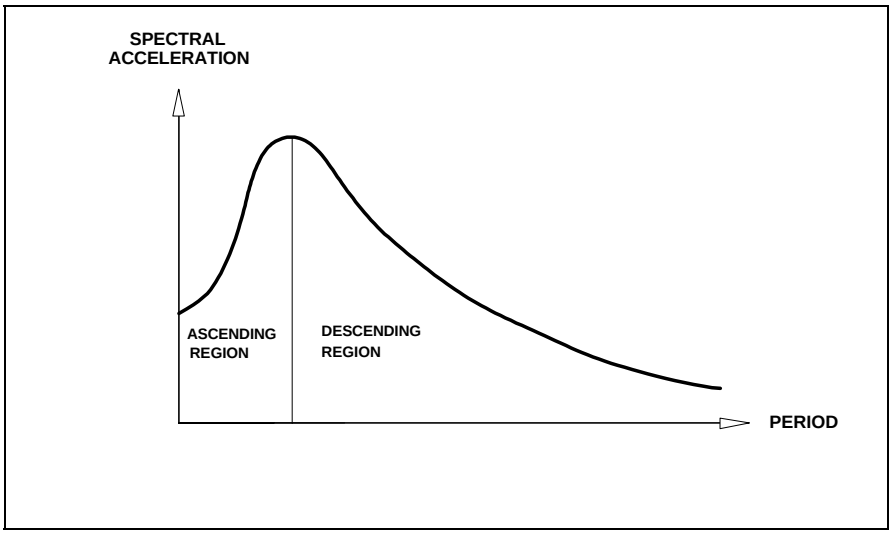

3) Contraction joints are known to have very little or no tensile strength, and the tensile strength across the lift joints, especially in older dams, is expected to be less than that for the intact concrete. Consequently, the contraction joins may open and close repeatedly and some of the lift joints crack regardless of the tensile strength of the "intact concrete" being exceeded or not. The question to be answered, then, is whether or not such joint opening and cracks will lead to failure mechanisms.

11-6.2 Finite-Element Response Spectrum Analysis

The response-spectrum analysis uses earthquake response spectra as the seismic input to compute the maximum response of an arch dam due to earthquake loading. The seismic input includes the two horizontal and the vertical response spectra of the MCE earthquake ground motions discussed in Section 11-4.4. The finite-element model of the dam system, including the dam-foundation and the dam-water interaction effects, is developed as described in the following section. Dynamic material properties are used for the dam concrete and the foundation rock, and a constant damping ratio as specified above is employed for all modes of vibration. The maximum nodal displacements and element stresses are computed separately for each individual mode of vibration, and are then combined to obtain total maximum response values due to all significant modes and all three components of the ground motion.

11-6.2.1 Structural Models

The finite-element model of the dam system for the response-spectrum mode-superposition method is essentially identical to that developed for the static analysis, except that the effects of the dam-water interaction must be also included.

The arch dam is modeled as a monolithic structure represented by a single or more layers of finite elements of appropriate types and sizes in accordance with the guidelines provided in Section 11-5.2. In addition, sufficiently small finite elements must be used, so that the contribution of all significant vibration modes with higher harmonic deflected shapes are represented accurately. The interaction effects of the power intakes and other appurtenant structures attached to the dam, if significant, must be considered by a lumped mass representation or by direct modeling of the appurtenant structure as part of the dam model, as appropriate.

Dam-foundation interaction effects are represented by a foundation model as described in Section 11-6.5.2.

Dam-water interaction effects are represented in accordance with the guidelines given in Section 11-6.5.1.

11-6.2.2 General Principles

The linear-elastic dynamic response of arch dams to earthquakes can be obtained by the mode-superposition response-spectrum method. This method provides estimates of the maximum response directly from the earthquake response spectrum.

The modal or mode-superposition method is based on the fact that for certain forms of damping, the response in each natural mode of vibration can be computed separately, and then combined to obtain the total response. Each mode responds with its own particular pattern of deformation or mode shape ϕ_n; with its own natural frequency of vibration ω_n; and with its own modal damping ratio ξ_n. Considering that the response of structures including dams to earthquakes is essentially due to the lower modes of vibration, only the response in the first few modes need be considered.

The response of the *n*th mode of vibration for an idealized arch dam structure can be obtained from the analysis of a single-degree-of-freedom (SDOF) system expressed as

$$\ddot{y}_n + 2\xi_n\omega_n\dot{y}_n + \omega_n^2 y_n = -\frac{L_n}{M_n}\ddot{u}_g(t) \qquad 11\text{-}6.1$$

with natural vibration frequency ω_n and damping ratio ξ_n, excited to the degree L_n/Mn (participation factor) by the ground acceleration $\ddot{u}_g(t)$. The earthquake excitation factor L_n and the modal mass M_n are given by:

$$L_n = \sum_{j=1}^{N} m_j\phi_{jn} + \sum_{i=1}^{M} m_{ia}\phi_{in} \qquad 11.6.2$$

$$M_n = \sum_{j=1}^{N} m_j \phi_{jn}^2 + \sum_{i=1}^{M} m_{ia} \phi_{na}^2 \qquad 11.6.3$$

where m_j is the dam nodal mass, N is total number of degrees-of-freedom, m_{ia} is the water added-mass defined at the dam-water interface nodes, and M is number of the dam-water interface degrees-of-freedom.

In the response spectrum method, the maximum response for the nth mode expressed by the above equation is obtained directly from the earthquake response spectrum. As illustrated in Fig. 11-6.1, for a natural period T_n, and modal damping ratio ξ_n the maximum modal displacement due to response spectrum of the k component of earthquake ground motion is:

$$Y_{n,\max}^k = \frac{L_n}{M_n \omega_n^2} S_{an}\left(T_n, \xi_n\right) \qquad 11\text{-}6.4$$

where S_{an} is the spectral acceleration, and is related to pseudo-velocity, S_v, and relative displacement, S_d, by

$$S_{an} = \omega S_v = \omega^2 S_d \qquad 11\text{-}6.5$$

Alternatively, the maximum modal displacement may be computed by using any of these response spectrum ordinates.

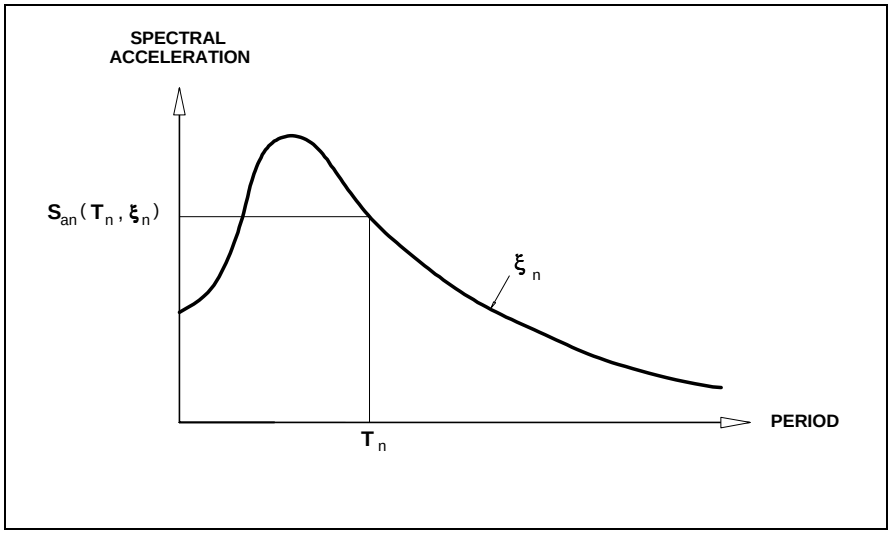

Fig. 11-6.1 Acceleration response spectrum illustrating how spectral acceleration for at a given period and damping ratio is obtained.

Finally, the maximum displacement vector for the dam nodal points is

$$u^k_{n,\max} = \phi_n Y_{n,\max} \qquad 11\text{-}6.6$$

Knowing the maximum nodal displacements, the maximum element stresses for each mode are obtained from the displacement-stress relationship.

Number of modes required.

In general, only a few lower modes of vibration are needed in the response spectrum analysis of arch dams. The actual number of modes to be included in the analysis depends on the natural periods and natural vibration modes of the dam, on the response spectrum ordinates, and on the response quantity of interest. The first three to five modes generally contribute the most, but for dams with numerous closely spaced modes with periods longer than 0.1 sec, the contribution of modes beyond the third may be significant. Some response quantities such as nodal displacements and arch stresses normally require fewer modes than cantilever and shear stresses to achieve more than 90% of their "exact" values.

As a general rule, the response spectrum analysis should include sufficient number of modes until the computed response quantities are at least 90% of their "exact" values. Since the "exact" response values are not known in advance, a trial and error procedure may be adapted, in which successive analyses are repeated with additional modes until the addition of modes does not affect the result more than a few percent. Alternatively, the analysis may be carried out by including a minimum of five modes or by considering all modes having natural periods longer than 0.1 sec (frequencies < 10 Hz), whichever gives more number of modes.

Combination of modal response.

The maximum displacements, element stresses, and reaction forces (arch thrusts) computed for each significant mode of vibration must be combined appropriately to obtain the total response of the dam due to each component of the earthquake ground motion. Since the maximum modal responses do not occur at the same time during the earthquake excitation, the complete quadratic combination (CQC) method or the square-root-of-the-sum-of-the-squares (SRSS) method may be used to obtain an approximate estimate of the total response.

The CQC modal combination method (Wilson, Der Kiureghian and Bayo 1981) is based on the random vibration theory and can be used if the duration of the strong motion portion of the earthquake record is several times longer than the fundamental period of the dam and if the response spectrum ordinates vary slowly over the dominant period range of the dam. Both of these conditions are easily satisfied for most arch dams using smooth response spectra with 5% damping or more. The CQC formula for the maximum total displacements $u^k_{\max}$ due to the k component of the earthquake ground motion is given by

$$u_{\max}^{k} = \sqrt{\sum_{m=1}^{p}\sum_{n=1}^{p} u_{m,\max}^{k}\rho_{mn}u_{n,\max}^{k}} \qquad 11\text{-}6.7$$

where $u_{m,\max}^{k}$ and $u_{n,\max}^{k}$ are the maximum modal displacements for modes m and n, respectively, and p is the number of modes considered; and ρ_{mn} is the cross-modal coefficient which for the constant modal damping ξ is defined by:

$$\rho_{mn} = \frac{8\xi^{2}(1+r)r^{\frac{3}{2}}}{\left(1-r^{2}\right)^{2} + 4\xi^{2}r(1+r)^{2}} \qquad 11\text{-}6.8$$

in which r is the ratio of natural periods T_m/T_n. For well separated modes ($r < 0.75$) and a 5% damping, ρ_{mn} is less than 0.1, indicating negligible cross-correlation between the modes. Whereas for closely spaced modes ($r > 0.75$) and especially for higher damping, cross-modal coefficient increases showing significant interaction between the modes.

For dams with well separated modes, cross-modal coefficient, ρ_{mn}, approaches zero (for $m \neq n$), and the CQC method converts into the standard SRSS method:

$$u_{\max}^{k} = \sqrt{\sum_{n=1}^{p}\left(u_{n,\max}^{k}\right)^{2}} \qquad 11\text{-}6.9$$

While the SRSS method leads to conservative estimates for the well-separated modes, it may provide conservative or unconservative results when the modes are closely spaced.

Combining for multi-earthquake components.

The total maximum response of the dam due to each component of the earthquake ground motion is obtained using one of the modal combination methods described above. The maximum response due to all three components (two horizontal and vertical) of the earthquake ground motion should be obtained using the SRSS method:

$$u_{\max} = \sqrt{\sum_{k=1}^{3}\left(u_{\max}^{k}\right)^{2}} \qquad 11\text{-}6.10$$

11-6.2.3 Presentation and Interpretation of Results

The basic results of a response-spectrum analysis include natural frequencies and mode shapes, maximum nodal displacements, and maximum element stresses. Maximum nodal

displacements and maximum element stresses are due to the earthquake loading only. They must be combined with the effects of static loading in order to obtain the total maximum response values.

Natural frequencies and modes of vibration

In a response spectrum analysis, the modal properties including the natural frequencies and natural modes of vibration for the dam system must be known and thus are computed first. T he natural frequencies and modes of vibration provide important information on the dynamic characteristics of the dam, its level of interaction with the impounded water, and its level of response to earthquake loading characterized by a response spectrum. In order to acquire an advance knowledge of the dynamic behavior of the dam and also to examine the accuracy of the results, the computed natural modes of vibration should be presented in the form of deflected shapes shown in Fig. 11-6.2, or in other appropriate forms.

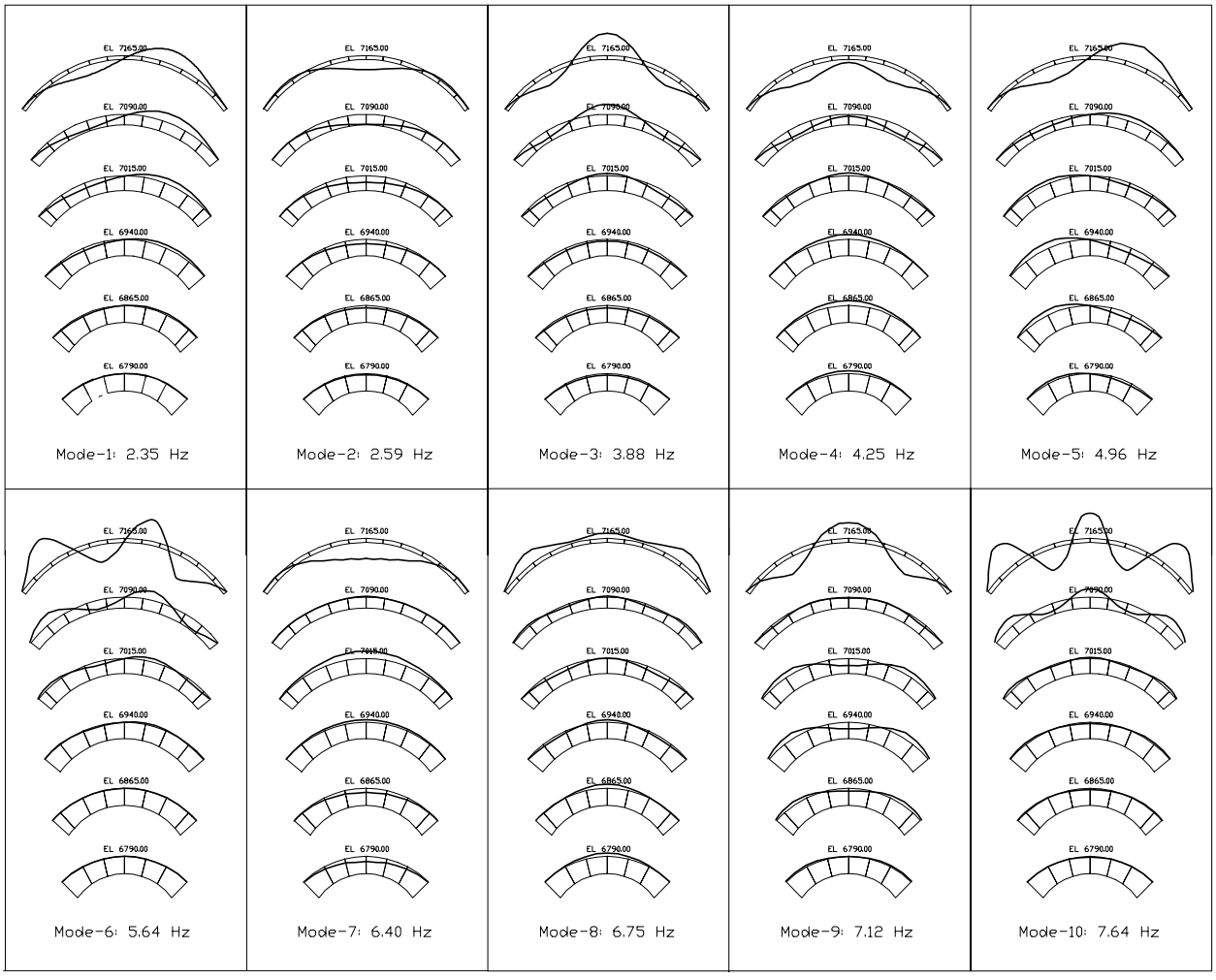

Fig. 11-6.2 Ten lowest vibration modes of Marrow Point Dam with full reservoir and flexible massless foundation.

Dynamic response quantities

The maximum nodal displacements and element stresses are obtained by combining responses from the individual modes and multi-component earthquake input. The resulting dynamic displacements and stresses estimated in this manner are all positive but for evaluation they must be assumed to be positive or negative. The positive dynamic stresses are interpreted as the maximum tensile stresses, whereas the negative dynamic stresses serve as the minimum compressive stresses. The response spectrum stresses generally occur at different of times, thus static equilibrium checks cannot be performed to validate the results.

Total maximum stresses

For evaluation of the earthquake performance of arch dams, the response-spectrum estimates of the dynamic stresses (σ_d) must be combined with the static stresses (σ_s) due to the usual loading combination (Section 11-4.5.3). Since response-spectrum dynamic stresses can be either positive or negative, this combination leads to the maximum total tensile stresses and the minimum total compressive stresses:

$$\sigma_{\max,\min} = \sigma_s \pm \sigma_d \qquad 11\text{-}6.11$$

Only similarly oriented stresses such as the static and dynamic arch stresses, static and dynamic cantilever stresses, and the static and dynamic shear stresses can be combined in this manner. The basic stress results needed for evaluation include arch and cantilever stresses on the upstream and downstream faces of the dam. The resulting total stresses may be displayed in the form of stress contours shown in Figs. 11-6.3 and 11-6.4. These results were computed for Morrow Point Dam due to the static loads discussed previously in Section 11-5.2.3 and the example response spectra described in Section 11-4.4.

The envelope of maximum total tensile stresses in Fig. 11-6.3, show the computed peak tensile arch and cantilever stresses on the upstream and downstream faces of the dam that generally occur at different times during the earthquake excitation. Similarly, the envelope of minimum total compressive stresses in Fig. 11-6.4 exhibits the non-concurrent peak compressive arch and cantilever stresses on the upstream and downstream faces of the dam. The dam performance is considered satisfactory if the evaluation criteria set forth in Section 11-1.4.4 is met. In cases where high tensile stresses indicate significant joint opening and tension cracking will occur, consideration of stress histories, concurrent stresses, and the number and duration of significant tensile stress excursions computed using a time-history analysis provide additional information for evaluation of the earthquake performance of the dam.

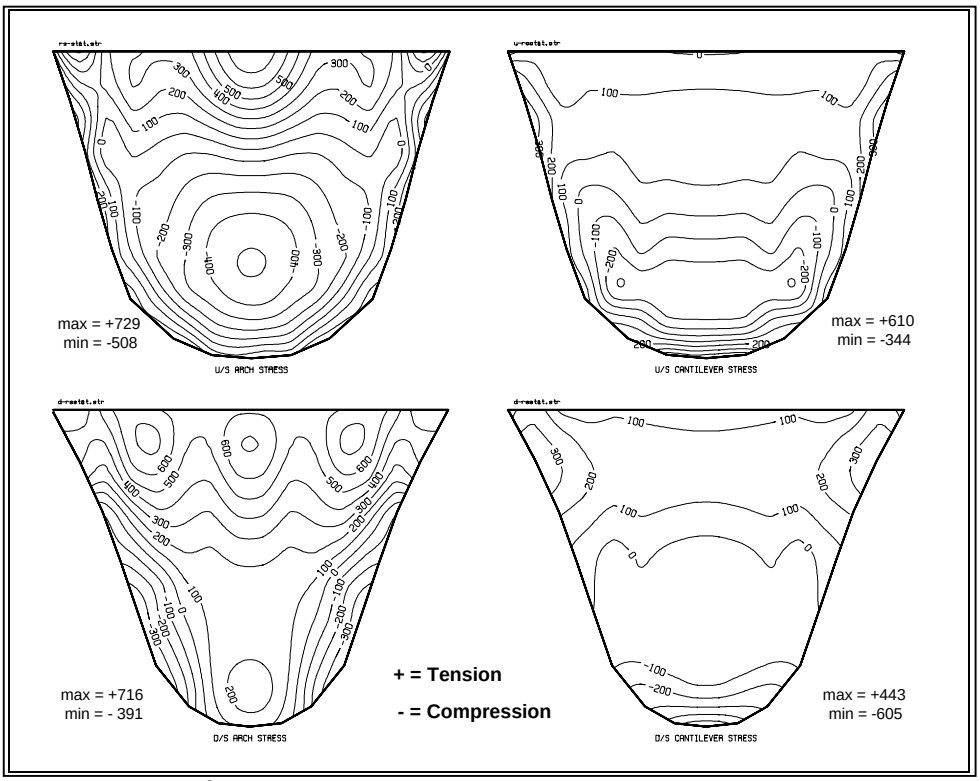

Fig. 11-6.3 Envelope of maximum total (static + SRSS) tensile stresses (in psi) on upstream and downstream faces of Morrow Point Dam on flexible foundation with full reservoir due to upstream, vertical, and cross stream response spectra .

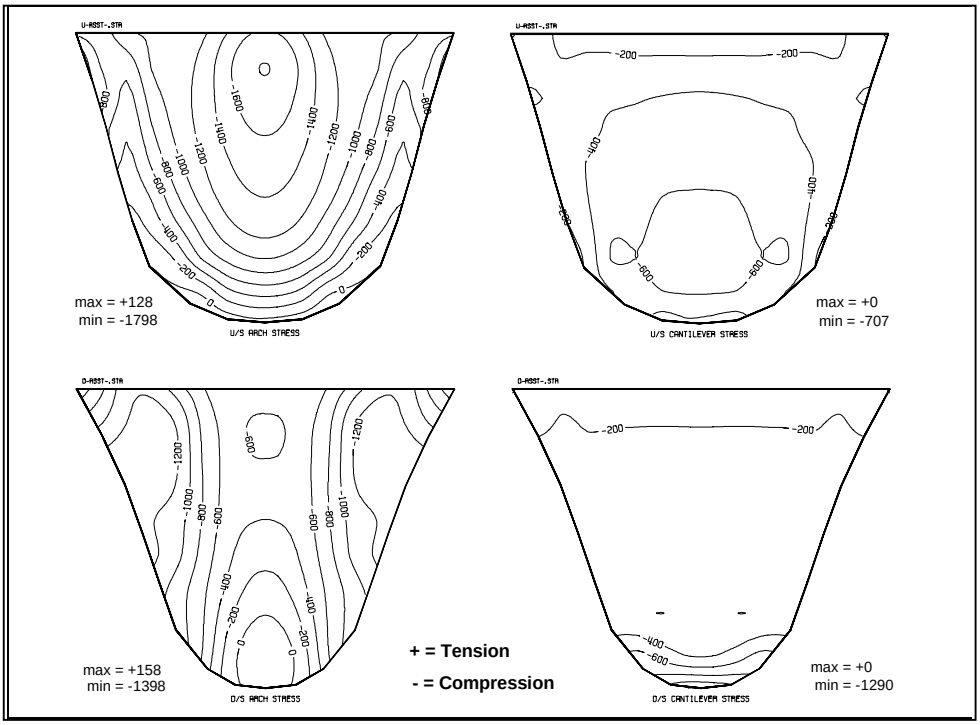

Fig. 11-6.4 Envelope of minimum total (static SRSS) compressive (in psi) on upstream and downstream of Marrow Point Dam on flexible foundation with full reservoir due to vertical, upstream, and cross valley response spectrum.

11-6.3 Finite-Element Time-history Analysis

The response of arch dams to earthquakes can also be evaluated by the time-history method of analysis. Although time-history method is applicable to both linear and non-linear response behavior of dams, the linear time-history analysis is most commonly used for seismic safety evaluations of arch dams. In most cases, linear time history analysis coupled with engineering judgement is sufficient to evaluate the safety of an arch dam under seismic loading. If severe damage is indicated, nonlinear dynamic analysis can be done and will be accepted by the FERC. Currently however, the FERC has no acceptance criteria for the allowable level of damage . No matter how accurate, nonlinear analyses are subject to numerous assumptions that would still require engineering judgement .

The linear time-history response analysis is advantageous because of its ability to analyze time dependent characteristics of the dynamic response. This provides additional information for safety evaluation of the dam such as whether or not high stresses occur simultaneously, have short duration, and repeated many times. The seismic input for linear time-history analysis consists of three components of the earthquake ground motion acceleration time histories developed and applied to the dam in accordance with guidelines of Sections 11-4.4. The finite-element model of the dam-water-foundation system is developed as described in Section 11-6.5.1. Dynamic material properties are used for the concrete and the foundation rock with a constant damping ratio in accordance with Section 11-6.1. If applicable, the reservoir-boundary absorption coefficient is selected as described in 11-6.5.1.3. The maximum and history of nodal displacements and element stresses are computed by the time-history mode-superposition method or by the direct integration of the equations of motion.

11-6.3.1 Structural Models

The three-dimensional finite-element models of the arch dam and the foundation rock for the linear time-history analysis are identical to those described previously for the response spectrum analysis. The dam-water interaction effects may be represented by an added hydrodynamic mass model or by the frequency- dependent hydrodynamic terms discussed in 11-6.5.1.

The added hydrodynamic mass models are applicable to arch dams for which the fundamental frequency of the reservoir water is at least 2 times greater than the fundamental frequency of the dam. The finite-element incompressible added-mass model is the preferred model for the added-mass representation. However, the generalized added-mass model is also acceptable when it gives conservative results.

11-6.3.2 General Principles

Linear time-history analysis uses acceleration time-histories as the seismic input, and computes complete response histories of the dam for the entire duration of the earthquake ground shaking. A time-history response analysis provides not only the maximum stress values, but also the sequencing, spatial extent and number of excursions beyond any specified stress value, all of which together with the rational interpretation are essential parts of a dam safety evaluation.

The complete response history of the dam structure to earthquakes is obtained by the solution of the equations of motion. The equations of motion assembled for an idealized dam-water-foundation system generally contain several hundreds to several thousands of ordinary differential equations. In general, these equations are coupled and can be solved simultaneously by direct integration method, or separately by the mode-superposition method. Both methods are applicable to the linear dynamic response analysis, but only direct method is usually employed in the non-linear dynamic analysis.

11-6.3.2.1 Direct Integration Methods

In direct integration the coupled system equations of motion is solved by a numerical step-by-step integration procedure. The term “direct” simply means that prior to the numerical integration, the equations are not transferred into a different form. A direct integration method is based on two basic principles: 1) the equations of motion are satisfied at discrete time intervals Δt apart, and 2) a variation of displacements, velocities, and accelerations must be assumed within each time interval Δt. It is, in fact, the form of the assumption of variation of displacements, velocities, and acceleration that determines the stability, accuracy, and efficiency of the integration procedure. The direct integration method is not restricted to the linear analysis as is the modal-superposition method discussed in 11-6.3.2.2. Therefore, it can be used when the contraction joint opening and material or geometric non-linearity are considered.

A numerical integration procedure is either called *explicit* or *implicit.* When the solution at time $t+\Delta t$ is based on the equilibrium conditions at the previous time step t, the integration method is called an explicit integration method. Methods that use equilibrium conditions at time $t+\Delta t$ to obtain solution at time $t+\Delta t$ are called implicit integration methods. The implicit method is normally selected for the linear earthquake response analysis of arch dams. The main advantage of the implicit method is that it is *unconditionally* stable: this means there is no mathematical limit on the size of the time in-

terval, and Δt can, in general, be selected much larger than that for the explicit methods. The time interval Δt should be small enough that response in all modes which significantly contribute to the total structural response is calculated accurately. For example, when the lowest p frequencies and mode shapes of the dam are considered significant, the smallest period is T_p , and thus $\Delta t = T_p /10$ should provide sufficient accuracy.

Some of the commonly used implicit integration methods include Houbolt integration scheme, Newmark's integration scheme, and Wilson θ method. Both the Newmark's and Wilson θ methods are an extension of the linear acceleration method, in which a linear variation of acceleration from time t to $t+\Delta t$ is assumed. For certain selection of the integration parameters, the Newmark's method converts to the constant-average-acceleration and the linear acceleration schemes. The linear acceleration scheme can also be obtained using $\theta = 1$ in the Wilson θ method.

11-6.3.2.2 Mode Superposition Method

The time-history mode-superposition method involves similar step-by-step integration described above, except that integration is applied to the uncoupled equations of motion. The coupled equations of motion are first transferred into uncoupled modal equations using the natural frequencies and natural modes of vibration. The equation of motion for each mode, Eq. (11-6.1), is then integrated for the entire duration of the ground shaking. The response history for each mode can be obtained by the Duhamel integral (Clough and Penzien, 1993)

$$Y_n(t) = -\frac{L_n}{M_n}\frac{1}{\omega_{nD}}\int_0^t \ddot{u}_g(\tau)\exp\left[-\xi_n\omega_n(t-\tau)\right]\sin\left[\omega_{nD}(t-\tau)\right]d\tau \qquad (11\text{-}6.12)$$

or other integration schemes described above. In this equation, $\omega_{nD} = \omega_n\sqrt{1-\xi_n^2}$ is the damped vibration frequency, but its difference with the undamped frequency is negligible for damping ratios of less than 20% and is normally ignored. The displacement response history of the dam for the nth mode is given by

$$u_n^k(t) = Y_n(t)\phi_n \qquad (11\text{-}6.13)$$

which when combined algebraically for the lowest p modes and for three components of the earthquake ground motion, the total displacement histories are obtained.

$$u(t) = \sum_{k=1}^{3} \sum_{n=1}^{p} u_n^k(t) \qquad (11\text{-}6.14)$$

These operations are also performed for other response quantities. For example, the displacement history in Eq. (11-6.13) and the displacement-stress relationships are used to obtain the stress history in the *n*th mode, and then are combined according to Eq. (11-6.14) to obtain the total dynamic stress histories.

11-6.3.2.3 Total Static Plus Dynamic Stresses

Total stresses required for the evaluation of the earthquake performance of the dam are obtained by algebraic addition of the initial static stresses due to the usual loading combinations and the dynamic stress histories. In a linear response analysis, static and dynamic responses are usually computed by two separate analyses and combined afterwards to obtain the total response.

11-6.3.3 Presentation and Interpretation of Results

The basic results of a time history analysis include response histories of the nodal displacements and element stresses computed for the entire duration of the earthquake ground shaking.

11-6.3.3.1 Mode Shapes and Nodal Displacement Histories

Mode shapes and frequencies are computed when the time-history mode-superposition method is employed. In this case mode shapes are presented and evaluated as described in 11-6.2.3.

The magnitude and time history of nodal displacements provide a visual means for evaluation and validation of results. As a minimum, displacement time histories at several critical locations along the dam axis such as the mid-crest and quarter-span points should be presented and evaluated. From displacement magnitudes, for example, it is possible to decide whether the displacements are sufficiently small to infer that the stability of the dam is maintained. Comparison between displacement components at some strategic locations (mid-span, quarter-span, etc.) can provide insight to the dynamic response behavior and a means for validation of the results. Fig. 11-6.5 shows displacement response histories for the mid-crest point of Morrow Point Dam due to earthquake input acceleration time histories given in Fig.11-4.6. As expected, Fig. 11-6.5 indicates that the mid-crest displacement of the symmetric Morrow Point Dam is largest in the stream direction. It also shows that the response of Morrow Point Dam (with hydrodynamic

added-mass model) to vertical component of the ground motion is small, as evident by the magnitude of the vertical displacements.

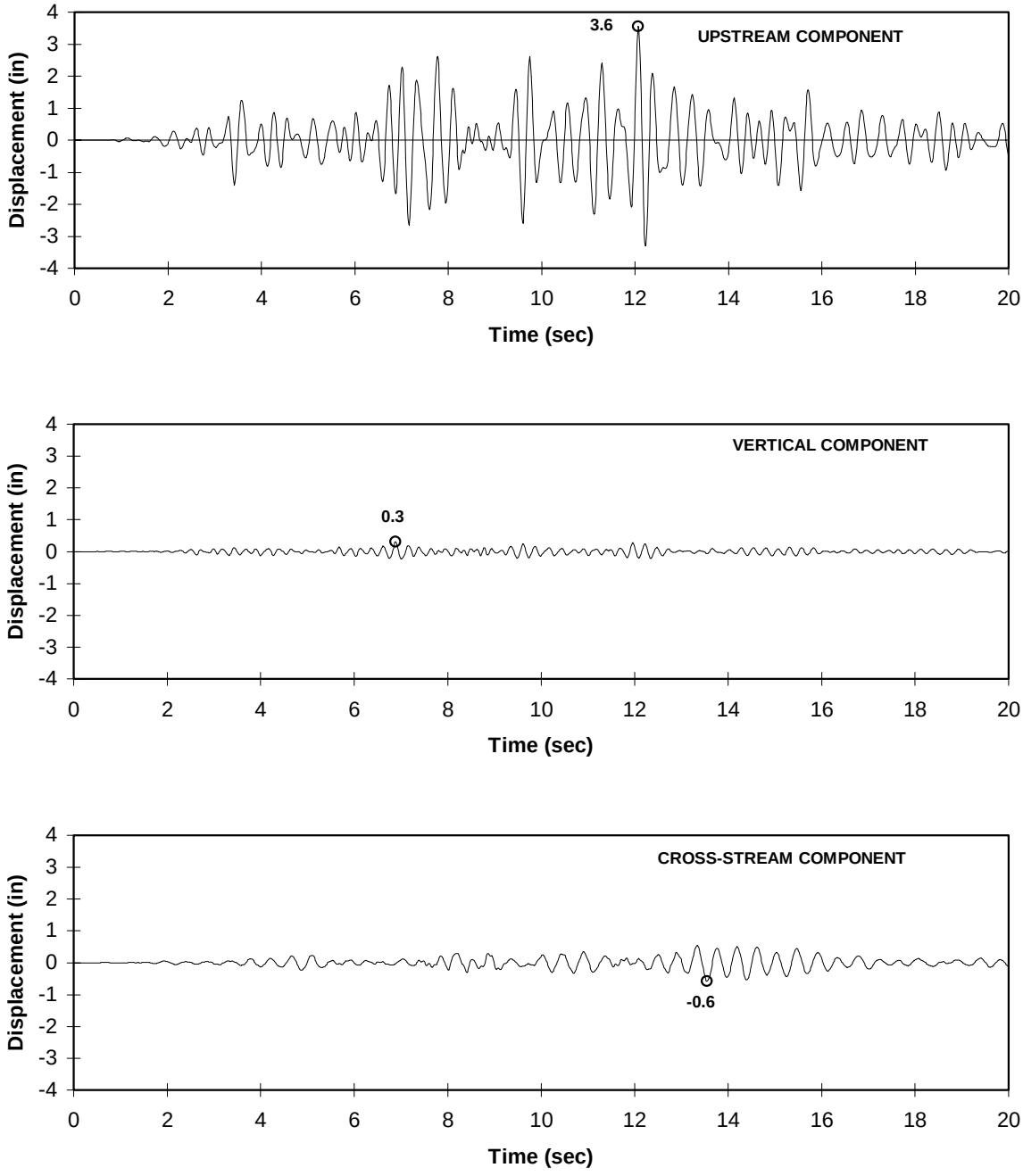

Fig. 11-6.5 Displacement time histories of center of dam crest.

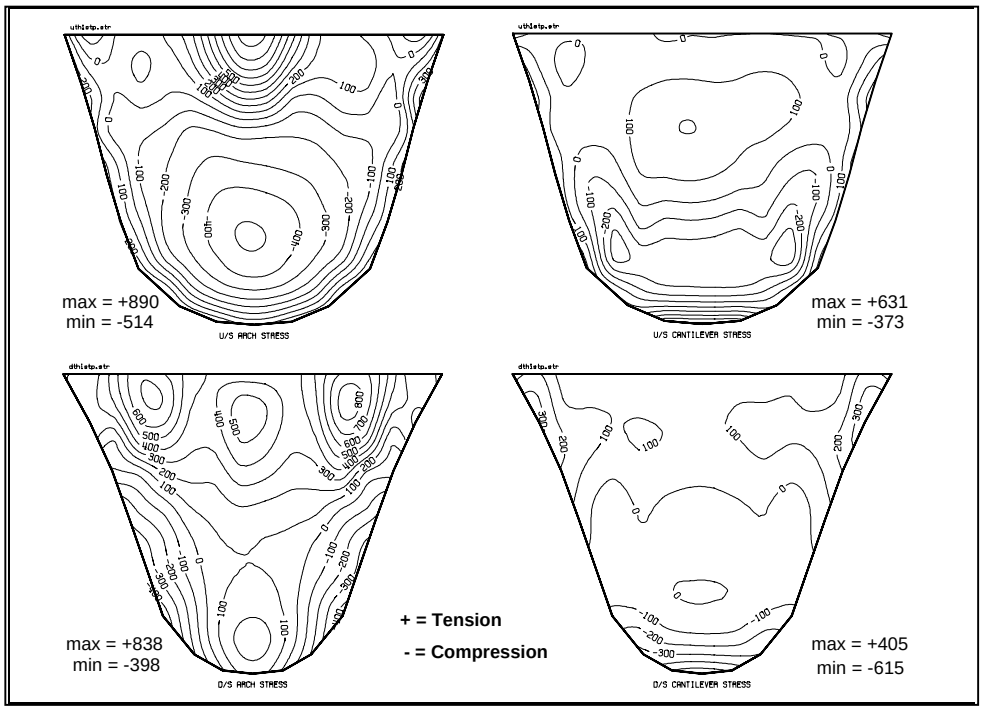

Fig. 11-6.6 Envelope of maximum tensile stresses due to static plus upstream, vertical, and cross-stream earthquake acceleration time histories

Linear continuum models typically under predict deflections because they ignore the effects of cracking and joint opening. For this reason, excessive displacement should be of concern. Engineering judgement is required to decide when deflections should be considered excessive. In one instance, a dynamic analysis of a dam revealed that while dynamic stresses in the service bridge piers were within reason, the predicted deflections indicated that the bridge would fall off the piers. What deflections can be tolerated must be evaluated on a case by case basis.

11-6.3.3.2 Envelopes of Maximum and Minimum Total Stresses

The envelopes of maximum and minimum total stresses are the first stress results to be presented and evaluated. They should be presented as stress contour plots of arch stresses and cantilever stresses on each face of the dam. The magnitudes of maximum and minimum arch and cantilever stresses at each stress point on faces of the dam, are obtained by first adding static stresses to the dynamic stress histories and then searching for the maximum and minimum values through their respective histories. Contours of the resulting maximum and minimum stresses obtained in this manner represent the largest tensile (positive) and the largest compressive (negative) stresses that occur at any location in the dam during the entire earthquake excitation. It is evident that the maximum or minimum stresses at different locations generally occur at different times, thus are non-concurrent. Fig. 11-6.6 is an example of maximum tensile stress contours for Morrow Point Dam. These contours are used to identify the regions where the excessive tensile stresses may suggest contraction joint opening and/or cracking. The extent and severity

of damage is determined by further examination of stresses in these regions and consideration of the time-dependent nature of the dynamic response, as discussed in the following sections.

Similarly, contours of the minimum stresses in Fig. 11-6.7 indicate the largest compressive stresses that could develop in the dam during the earthquake ground shaking. They should be compared with the allowable compressive stress to ensure that they meet the required factors of safety given in Table 11-1.1. Usually compressive stresses are small and within the allowable values, but may become critical if cracking significantly reduces the area of concrete available for transmitting cantilever forces.

If envelop values show that both tensile and compressive stresses satisfy the performance requirements for the Extreme Loading Combination, the dam will be considered safe against overstressing and no further stress evaluation will be required. Otherwise, a more detailed stress evaluation (discussed in the following sections) should be conducted, so that the expected level of damage and the stability conditions of the dam can be determined. After the numerical results have been evaluated for reasonableness, the stress results should be evaluated with respect to the guidance laid out in 11-1.4.4

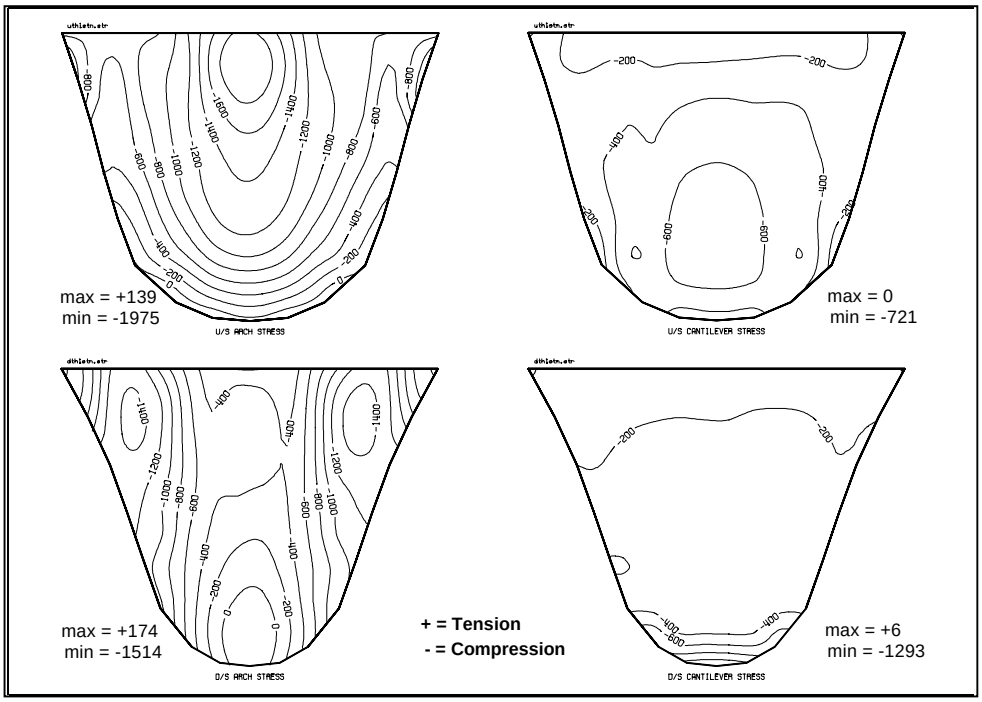

Fig. 11-6.7 Envelope of highest compressive stresses due to static, plus upstream, vertical and cross valley earthquake acceleration time histories.

11-6.3.3.3 Simultaneous or Concurrent Critical Stresses

The envelopes of maximum and minimum stresses discussed in 11-6.3.3.2 indicate the largest tensile and compressive stresses that are developed on faces of the dam at any time during the earthquake excitation. They serve to identify the overstressed regions, the location of largest maximum stress points (called the *critical stress points*), and the time-steps at which critical stresses reach their peaks. This information is used to obtain the concurrent (or simultaneous) stresses corresponding to the time-steps at which the critical arch and critical cantilever stresses reach their peak values. Fig. 11-6.9 shows concurrent stress contours at the time of maximum critical arch stress occurring at location SP-1, and Fig. 11-6.11 presents concurrent stresses at the time of maximum critical cantilever stress associated with location SP-2. In this example, time history of the critical arch (Fig. 11-6.8) and critical cantilever stresses (Fig. 11-6.10) are compared with an assumed tensile strength of the intact concrete as an indicator of the severity of tensile stresses. The earthquake performance of the dam should be carried out in view of the criteria stated in 11-1.4.4.

Concurrent stresses obtained in this manner can be interpreted as snap shots of the critical stress distributions. They serve to identify the location and extent of overstressed regions at critical time steps. In addition, since concurrent stresses are given for both faces of the dam, the severity of possible joint opening and cracking can be estimated from the comparison of stresses on opposite faces of the dam.

11-6.3.3.4 History of Critical Maximum Stresses

When maximum and concurrent stresses show significant tensile stresses, the time histories of the peak tensile stresses should be presented and evaluated. Time histories of the most critical arch and cantilever stresses are examined to estimate the amount of damage that could be expected. If the tensile strength of the concrete is exceeded many times by large amounts, more damage is to be expected than if stress excursions above the concrete strength are few and of short duration.

The critical arch stress history shown in Fig. 11-6-8, shows several significant tensile stress cycles that can momentarily open the contraction joint at the crown with no serious consequences, as discussed in the next section. The critical cantilever stress history shown in Fig. 11-6.10 indicates that only one stress peak exceeds the tensile strength of the intact concrete by 5%. This localized stress peak together with several lower tensile stress cycles is partly fictitious and may be interpreted to have been caused by the assumption of linear-elastic behavior for the foundation rock, a material which is fragmented by joints and fissures and can resist limited tension. This again has no significant effect on the stability of the dam.

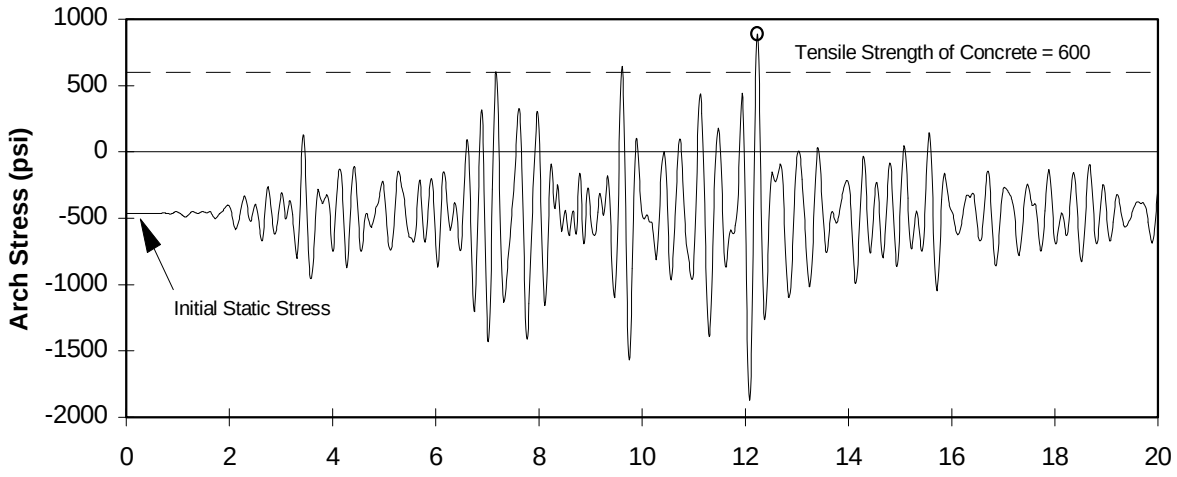

Fig. 11-6.8 Arch stress time history at point SP1 (Shown in Fig. 11-6.9) Point of maximum instantaneous tensile arch stress.

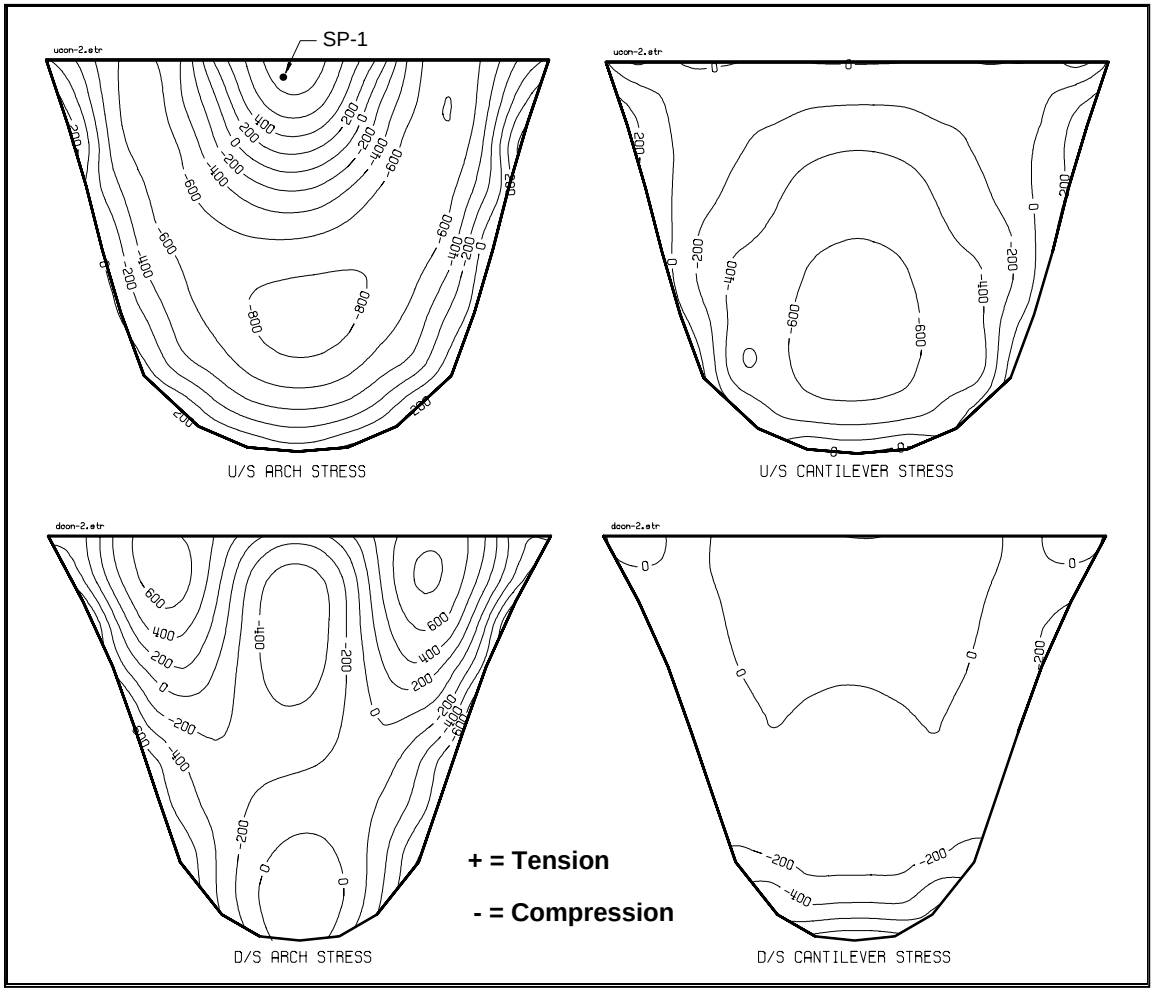

Fig. 11-6.9 Maximum tensile arch stress contours @ t=12.23 sec.

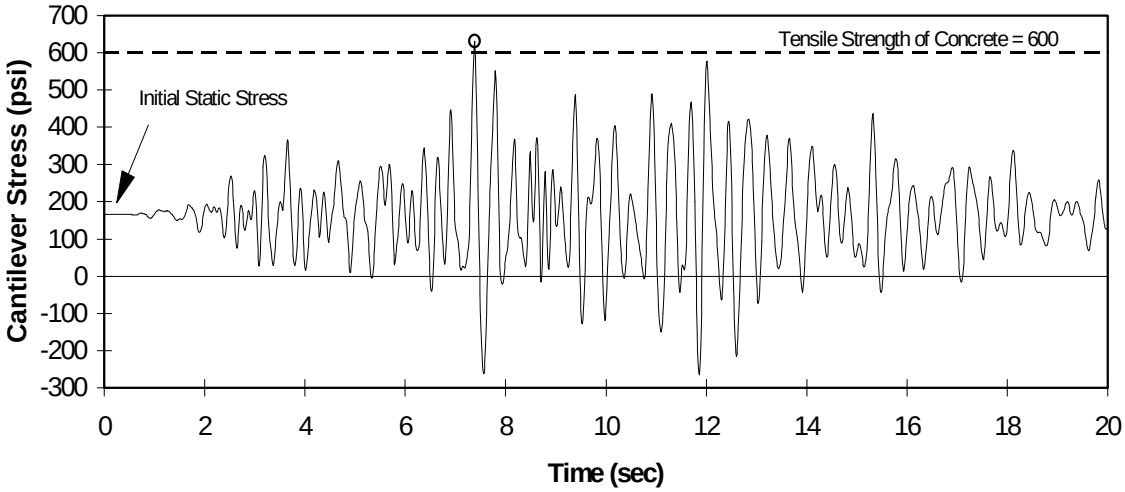

Fig. 11-6.10 Cantilever stress time history at location SP-2 (shown below), where the largest tensile cantilever stress occurs.

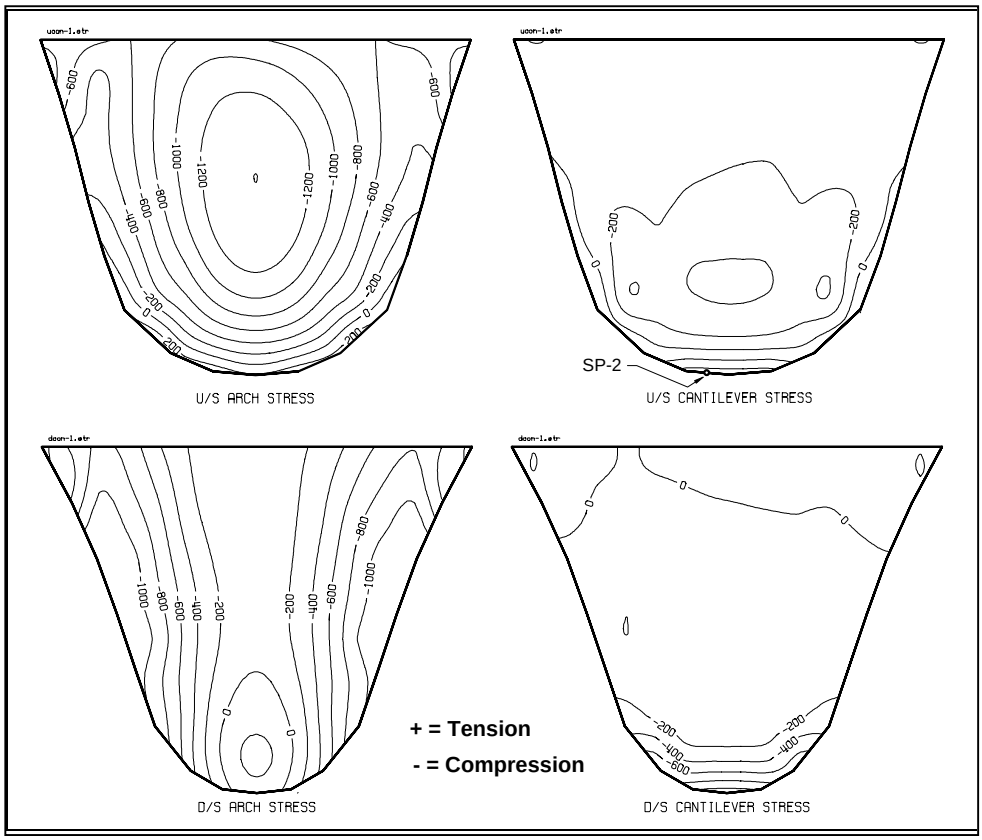

Fig. 11-6.11 Instantaneous stresses at the time of maximum tensile cantilever stress (t = 7.38 sec) due to static plus upstream, vertical, and cross-stream earthquake ground acceleration time histories.

11-6.3.3.5 Final Evaluation of Stress Results

Evaluation of Arch Stresses. Considering that the vertical contraction joints in arch dams can resist little or no tension, the arch tensile stress distribution through the dam thickness

can be interpreted as brief joint opening as the dam vibrates in response to earthquake ground motion. The joints, however, are usually designed to limit upstream-downstream shearing translation.

An accurate characterization of the behavior of the joint opening and closing mechanism and its effects on redistribution of stresses can probably be captured only by a non-linear dynamic analysis (Fenves et. al. 1989). However, severity of joint opening may be roughly estimated from contour plots of the average arch stresses to ensure that the joint openings are small and that the cantilevers bounded by the partial joint openings are not overloaded. Fig. 11-6.12 illustrates an approximate procedure for estimation of the extent of joint opening. Assuming that the vertical joints cannot resist tension, even a momentary net tensile force across the joints might indicate a joint opening. The vertical extent of joint opening may be approximated by the extent of the region showing net tensile arch stresses across the joint. A joint opening presumably releases arch stresses across the joint and transfers overturning forces to the cantilevers. The cantilever blocks must have sufficient tensile strength to resist the additional overturning to remain stable. The basic concept, therefore, is first to identify possible cantilever monoliths bounded by partial joint openings, and then to assess their stability, considering that they must resist additional forces resulting from momentary loss of arch action.

After the critical tensile arch stresses have been established, time histories of the upstream and downstream arch stresses at location of the largest tensile arch stress are averaged to obtain the time history of the average arch stresses at that location. Each positive stress pulse in the resulting averaged time history is indicative of net tensile arch stresses across the dam thickness. For example, the middle graph in Fig. 11-6.12 suggests that the contraction joints at location of the largest arch tensile stress are subjected to 16 cycles of net tensile arch stresses, each of which might momentarily open the joint for hundredth of a second. The largest joint opening is expected to occur at t = 12.23 sec, when the net tensile stresses reach their maximum value. Next the concurrent stresses corresponding to the time of maximum net tensile stress (t = 12.23 sec) are retrieved and averaged separately for the arch and cantilever stresses. Tension region in the resulting average arch stress contours (bottom graph in Fig. 11-6.12) indicates the location and approximate depth of joint opening. The corresponding average cantilever stress contours show the magnitudes of cantilever stresses and hence the reserve capacity available to resist additional cantilever stresses should the contraction joints open. For small and moderate joint openings, the partially free cantilevers bounded by opened joints may remain stable through interlocking (wedging) with adjacent blocks. The extent of interlocking depends on the depth and type of shear keys, and on the amount of opening to be expected. If the results indicate excessive joint separation with little or no wedging ac-

tion, then the most critical "free" cantilever bounded by two opened joints should be identified and analyzed for overturning stability.

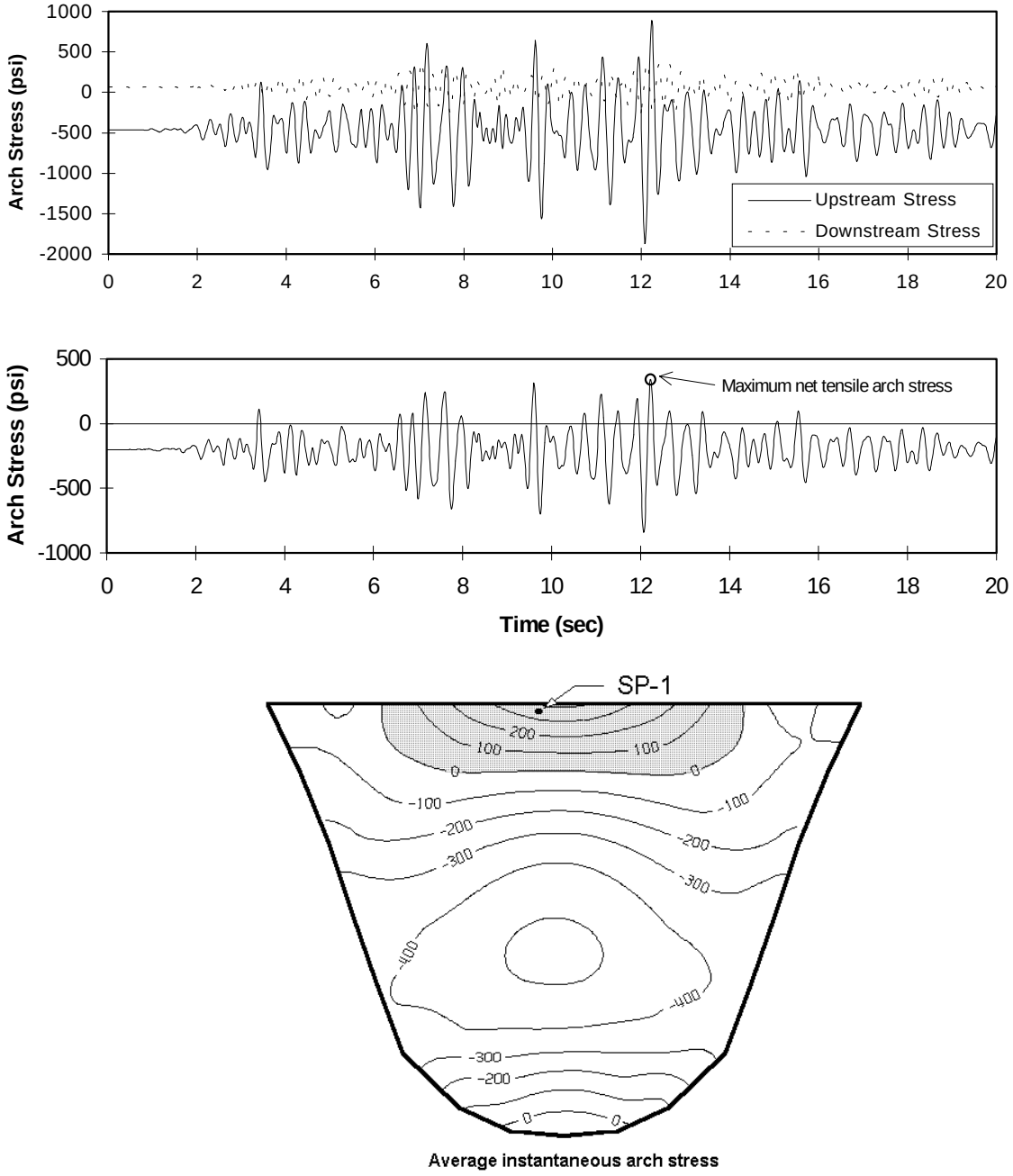

Figure 11-6.12 Procedure for identification of potential free cantilevers.

Stability Analysis of Free Cantilevers. When contraction joint opening occurs, what should be shown is that a free cantilever bounded by the temporarily opened joints will not fail. In order to insure the free cantilever remains stable, the total vertical force re-

sultant across the lift joint in question must be compressive and fall within the structure. Even if the resultant force across the lift joint falls temporarily outside the base, it is usually the case that the overturning forces are of in-sufficient duration to topple the free cantilever.

Fig. 11-6.13 shows the possible failure mode for a free cantilever block defined by two fully opened contraction joints and a horizontal lift joint. For the amount of time that vertical contraction joints are open, the free cantilever ‘s behavior is governed by differential equation 11-6.15

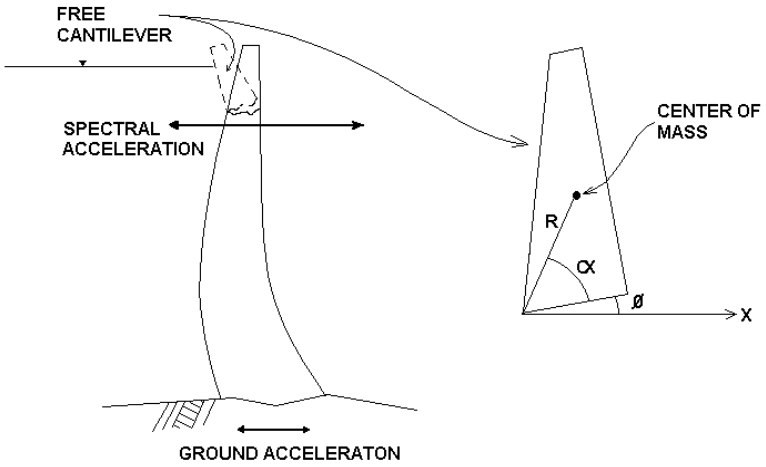

Fig. 11-6.13 Free body diagram of a cantilever with associated forces.

$$-M_{HD} + A_S WR \sin(\alpha+\phi) - WR\cos(\alpha+\phi) - M_{HS} = \left(\frac{\delta^2\phi}{\delta t^2}\right)\rho I_P \qquad (11\text{-}6.15)$$

Where:

M_{HD} = Moment due to hydrodynamic pressure (function of time)
A_S = Acceleration of the structure at the location of the block (function of time)
M_{HS} = Moment due to hydrostatic pressure
W = Weight of free cantilever block
R = Distance from pivot point to block center of mass
ρ = Mass Density of block
I_P = Polar moment of inertia about pivot point

Equation 11-6.15 can be solved numerically. A_S and M_{HS} can be obtained directly from a linear elastic time history analysis, or approximated by combining significant modes of vibration from a spectral analysis. Equation 11-6.15 assumes that the horizontal lift joint upon which the block sits is de-bonded, and therefore it is a very conservative treatment of the problem. In most cases, the results of this type of conservative block rocking analysis show that even if a free cantilever can form, it does not displace very much.

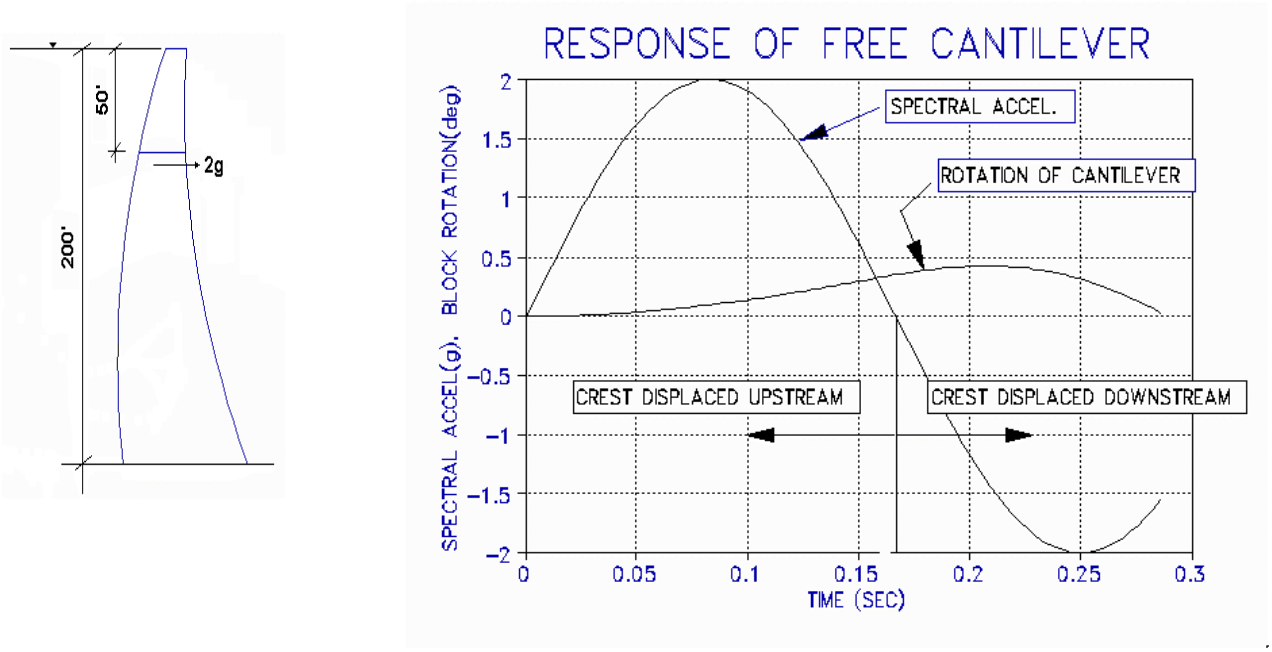

Fig. 11-6.14 Example of response of free cantilever block to sinusoidal acceleration of 2g @ 3Hz.

In the example depicted in Fig 11-6.14, equation 11-6.15 results in a peak rotation of 0.4°. It also indicates that the cantilever block should fall back into place as acceleration switches sign. In this example, even if free cantilevers do form they can not topple. It should also be noted that shear keys often prohibit cantilevers from being fully dis-engaged unless joint opening exceed the key depth or the keys have failed.

The toppling of blocks under seismic excitation is further treated by George Housner in his1963 article in the Bulletin of the Seismological Society of America.

Evaluation of Cantilever Stresses. At the dam-rock interface, the excessive tensile cantilever stresses can be interpreted as openings of the rock-concrete joints or of the joints within the rock below. The magnitudes of these stresses usually decrease when the probable weakness of the fragmented foundation rock in resisting tension is accounted for in the analysis. When subjected to tensile loading, the foundation region adjacent to the base of the dam "softens" as rock joints open and additional micro-cracks develop, but the magnitudes of stresses should not be such that this region would develop major cracking or would expand beyond the base of the dam. In severe cases, the influence of the fragmented rock on the stress results and crack propagation can be accounted for by assuming a reduced modulus (smeared crack) for the foundation-rock elements attached to the dam which would limit tension-resistance capability of the dam-rock interface.

For locations within the body of the dam away from the foundation boundary, tensile cantilever stresses exceeding the tensile strength of lift joints can be expected to cause cracking. Cracking should be assumed to occur along the lift joints or in the direction normal to the major principal stresses, if the directions of cantilever and major principal stresses differ significantly. The tensile cracking should be assumed to propagate through the dam thickness, if tensile cantilever stresses are also developed on the opposite face of the dam. In general, tensile cantilever stresses result from bending of the cantilevers which exhibit compression on the opposite face. In these cases, cracking usually occur only on a portion of the dam section experiencing tensile stresses in excess of the tensile strength of the concrete. However, so long as the excessive tensile stresses occur over a very limited area (less than 5% of the dam surface area) and do not exceed the tensile strength more than 5 cycles, it can reasonably be concluded that the cracking does not necessarily indicate unacceptable performance for the MCE event. Nevertheless, the extent of such cracking should be estimated and the computed stress distributions should indicate that the adequate compressive capacity exits to accommodate subsequent load redistributions. In addition, the vector plots of principal stresses at critical instance of time should be evaluated to confirm that the indicated regions of tensile cracking are not likely to join together to form surfaces along which partial sliding failures might occur.

11-6.3.4 Time-History Stability Analysis

The safety against sliding along the dam-foundation interface or along the potential foundation failure planes or wedges is determined on the basis of shear-friction factors of safety. The shear-friction factor of safety is defined as the ratio of the resisting to "*driving*" forces along a potential failure surface. The resisting forces are obtained from shear strength of the dam-foundation interface (11-2.3.1) or that of the potential foundation

failure planes or wedges (11-2.3.2). The driving forces acting on the dam-foundation interface are obtained from integration of the interface stresses or interface nodal forces computed as part of the finite-element analysis described previously. The driving forces for stability analysis of a rock wedge consist of the dam thrust and the static and seismic inertia forces acting on the wedge.

In the time-history earthquake analysis, factors of safety are obtained by combining the "driving" force histories due to the ground motion with "driving" forces due to the usual static loads including the uplift. At each time step, the seismic and static driving forces are combined and then transformed into a resultant force having components normal and tangential to the failure surface. Similar to the static analysis, the resisting forces are represented by shear strength of the foundation-dam interface or the potential foundation failure planes or wedges, and the driving forces are taken as the resultant of shear forces acting on the failure surface. The time history or instantaneous factor of safety is then computed from the ratio of the resisting to driving forces at each time step.

The time-history factor of safety starts with a value equal to the static factor of safety and then oscillates as the dam or the rock wedge responds to the ground shaking. Under earthquake excitation, the stability is maintained and sliding does not occur if the factor of safety is greater than one (Table 11-1.1). A factor of safety of less than one indicates that sliding may occur. In this situation, the sliding may be permitted, if it can be shown that the permanent displacement is small and that the safety of the dam will not be jeopardized. Even small movement of an abutment rock wedge or gravity thrust block could have drastic effects on the stress distribution with the dam. In such a case, it must be shown that the dam can continue to retain the reservoir even with support from the abutment wedge or thrust block reduced or eliminated. A rough estimate of the permanent sliding displacement can be obtained using the Newmark's rigid block model (Newmark, 1965). According to Newmark's concept, the sliding takes place during a short period of time when the ground acceleration cycles exceed a value known as critical acceleration, and diminishes when the ground acceleration falls below this value and the velocity reaches zero. The critical acceleration is the acceleration at which the sliding initiates and is obtained by equating resisting with driving forces.

11-6.4 Alternative Analysis Techniques

The procedures discussed in this section are not intended to rule out the use of alternative techniques. As the state of the art advances, new techniques which more accurately treat all aspects of the dynamic behavior of the arch dam/foundation/reservoir system will be-

come more common. The FERC will always favor the simplest way to evaluate dam safety.

11-6.5 Reservoir and Foundation Effects

Dynamic response of arch dams to earthquake ground motion is affected by interaction between the dam and impounded water, interaction between the dam and foundation rock, damping, and the characteristics of earthquake ground motion. A realistic appraisal of the seismic safety of the dam is achieved, if the effects of these factors are understood and properly represented in the analysis.

11-6.5.1 Dam-Water Interaction

Interaction of an arch dam with the impounded water leads to an increase in the dam vibration periods. This is because the dam cannot move without displacing the water in contact with it. The fact that water moves with the dam increases the total mass that is in motion. This added mass increases the natural periods of the dam, which in turn affects the response spectrum ordinates and hence the effective earthquake inertia forces. It can also cause an increase in damping due to partial absorption of pressure waves at the reservoir boundary and radiation towards the upstream. These effects tend to change the earthquake response of the dam with respect to that for the dam with empty reservoir, with the net result depending on the characteristics and component of earthquake ground motion and on the dam-water interaction model used.

11-6.5.1.1 Generalized Westergaard Added-Mass

The added-mass representation of dam-water interaction during earthquake ground shaking was first introduced by Westergaard (1933). In his analysis of a rigid, 2D, gravity dam with a vertical upstream face, Westergaard showed that the hydrodynamic pressures exerted on the face of the dam due to the earthquake ground motion is equivalent to the inertia forces of a body of water attached to the dam and moving back and forth with the dam while the rest of reservoir water remains inactive. He suggested a parabolic shape for this body of water with a base width equal to 7/8 of the height, as shown in Fig. 11-6.15.

A general form of the Westergaard added-mass concept which accounts for the 3D geometry (Clough 1977; Kuo 1982) can be applied to the earthquake analysis of arch dams. The general formulation is based on the same parabolic pressure distribution with depth used by Westergaard (Fig. 11-6.15), except that it makes use of the fact that the normal

hydrodynamic pressure P_n at any point on the curved surface of the dam is proportional to the total normal acceleration, $\ddot{u}_n^t$:

$$P_n = \alpha \ddot{u}_n^t \tag{11-6.16}$$

$$\alpha = \frac{7}{8} \rho_w \sqrt{H(H-Z)} \tag{11-6.17}$$

where ρ_w is mass density of water, α is Westergaard pressure coefficient, and H and Z are defined in Fig. 11-6.15. The normal pressure P_n at each point is then converted to an equivalent normal hydrodynamic force by multiplying by the tributary area associated with that point. Finally, the normal hydrodynamic force is resolved to its Cartesian components, from which a full 3x3 added-mass matrix at each nodal point on the upstream face of the dam is obtained (Kuo 1982):

$$m_a = \alpha A \lambda^T \lambda \tag{11-6.18}$$

where A is the tributary surface area and λ^T is a vector of normal direction cosines for each point. Note that while the added-mass terms are coupled with respect to the nodal degrees-of-freedom, they are uncoupled with respect to individual nodes. Such a 3x3 full nodal added-mass matrix can easily be incorporated in a computer program using consistent mass matrix (non-diagonal), but it should be diagonalized for those programs that employ diagonal mass matrix.

The basic assumptions of the generalized Westergaard method are: 1) pressure at any point on the face of the dam is expressed by the Westergaard parabolic shape, and 2) the same parabolic shape is used for all three components of the earthquake ground motion. It should be noted that there is no rational basis for these assumptions, because they do not meet the conditions imposed in the original Westergaard analysis which included a rigid dam with vertical upstream face being subjected to the upstream component of ground motion only.

The Westergaard method usually gives the largest added-mass values, as evident by its increasing the vibration periods the most. However, this does not automatically give the largest stresses, because response of the dam also depends on the characteristics of the earthquake ground motion. If vibration periods of the dam fall in descending region of the response spectrum, the larger Westergaard added-mass will shift the periods further into region of smaller effective earthquake forces and thus smaller stresses. The Westergaard added-mass model may be used in the preliminary analysis and also in the final

evaluation provided that the results show that the dam is safe with an adequate margin of safety with little or no damage.

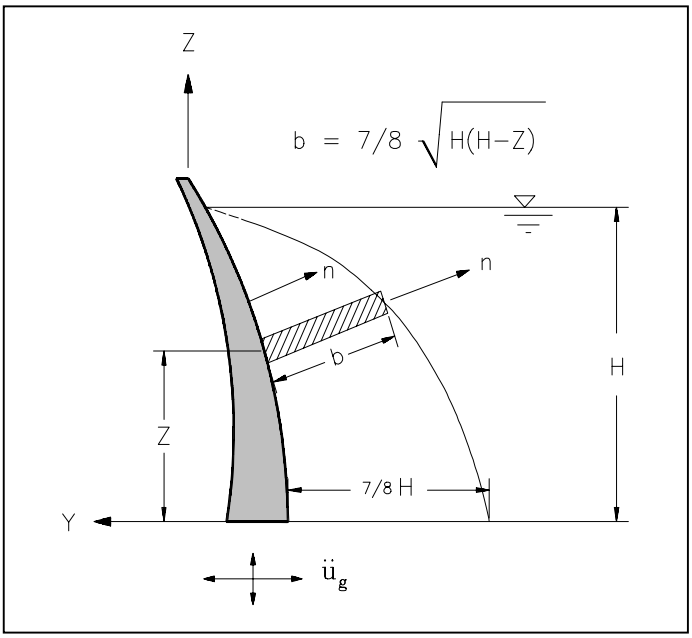

Fig. 11-6.15 Generalized Westergaard added hydrodynamic mass model for arch dams.

11-6.5.1.2 Incompressible Finite-Element Added-Mass

The added-mass representation of the impounded water can be obtained more accurately by a finite-element solution of the pressure wave equation, which fully accounts for the complex geometry of the dam and the reservoir (Kuo, 1982; Ghanaat, 1993b). The impounded water represented by the wave equation 11-6.19 is discretized using a finite-element mesh of incompressible liquid elements, with nodal pressures as the unknowns (Fig. 11-6.16a). The solution is obtained by numerical procedures with the following boundary conditions:

$$\frac{\delta^2 P}{\delta x^2} + \frac{\delta^2 P}{\delta y^2} + \frac{\delta^2 P}{\delta z^2} = 0 \qquad \text{11-6.19}$$

1. The hydrodynamic pressures at the water - free surface are assumed to be zero, that is the effects of surface waves are neglected.
2. The reservoir bottom and sides, as well as a vertical plane at the upstream end of the reservoir model, are assumed to be rigid (Fig. 11-6.16a). For rigid boundaries the normal pressure gradients or the total normal accelerations are zero.

3. The normal pressure gradients at the dam-water interface are proportional to the total normal accelerations of the fluid.

The finite-element mesh of the incompressible water can be developed to match the reservoir topography, but in most cases a prismatic model constructed by projecting the dam nodal points in the upstream direction would suffice. It should at least extend three times the water depth in the upstream direction and include three or more layers of elements in that direction, with distances between successive sections increasing with distance from the dam. The computed pressures for the nodal points on the upstream face of the dam are then converted into equivalent nodal forces, from which an added-mass matrix representing the inertial effects of the incompressible water is obtained. The resulting added-mass matrix is a symmetric full matrix coupling all nodal degrees-of-freedom on the upstream face of the dam. This matrix can be directly used in computer programs with the consistent mass (non-diagonal) capabilities, otherwise it should be appropriately diagonalized. The diagonalization of the mass matrix should be performed such that the procedure gives the correct total hydrodynamic forces for rigid body acceleration of the dam.

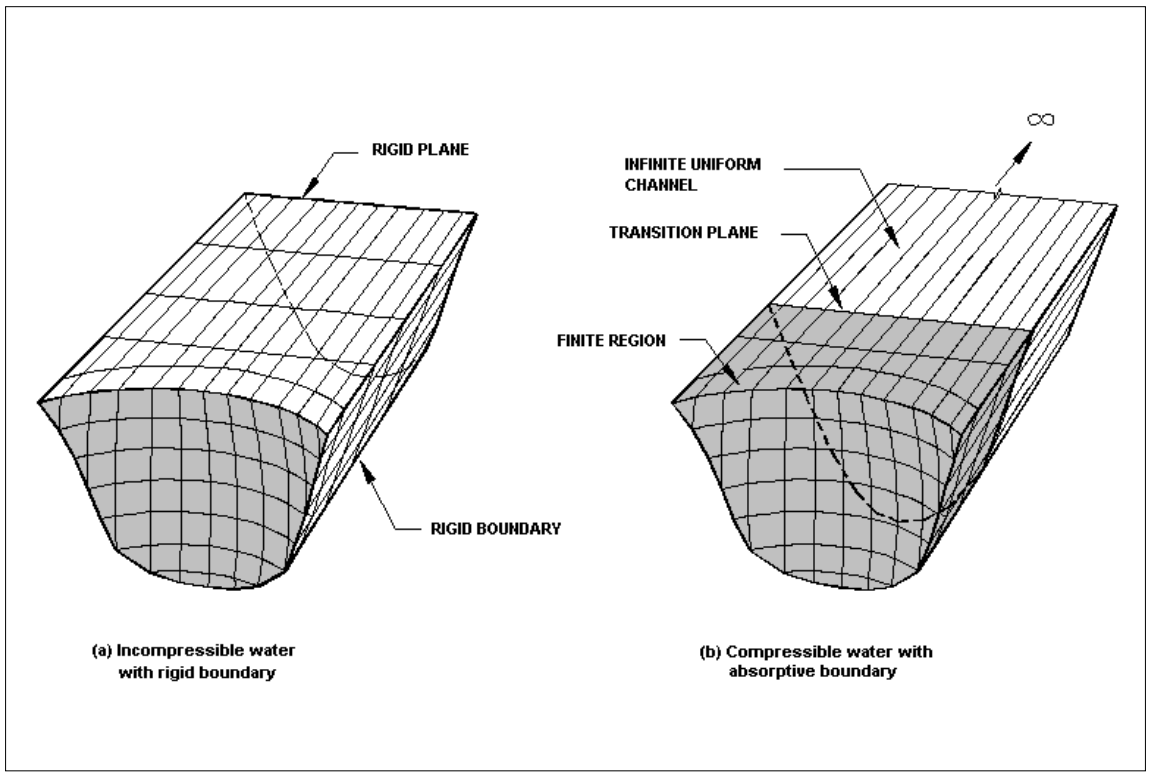

Fig. 11-6.16 Finite element models of fluid domain with and without water compressibility.

11-6.5.1.3 Compressible Water with Absorptive Reservoir Boundary

The added-mass representation of the impounded water described above ignores the effects of water compressibility and reservoir boundary absorption. A refined dam-water interaction analysis including these factors (Fok and Chopra, 1985) indicates that water compressibility and reservoir boundary absorption can significantly affect the hydrodynamic pressures and hence response of arch dams to earthquakes. Rigorous formulation of dam-water interaction in analyzing arch dams, introduces frequency-dependent hydrodynamic terms in the equations of motion that can be interpreted as an added mass, an added force, and an added damping (Chopra, 1988). The added-mass component of the dam-water interaction reduces vibration frequencies of the dam, especially for the vibration frequencies corresponding to the fundamental mode. The reductions in vibration frequencies in turn affect the response spectrum ordinates and hence the effective earthquake inertia forces. The added force component of the dam-water interaction increases the dam response due to the upstream and vertical ground motions, but decreases that due to the cross-stream ground motion, because the added force for the cross-stream excitation is out-of-phase with the effective earthquake inertia force. The added damping component of the dam-water interaction arising from the energy absorption at the reservoir boundary reduces the fundamental resonant response due to the upstream and vertical components of ground motion, but slightly increases the response due to the cross-stream component. The net effect, however, is an overall reduction of the dam response. At higher excitation frequencies, the added-damping which is dominated by the radiation energy of hydrodynamic pressure waves propagating in the upstream direction, reduces the dam response below that for the dam with empty reservoir, for all components of ground motion.

Finite-element model

Procedures for earthquake response analysis of arch dams including dam-water interaction, water compressibility, and reservoir boundary effects, have been developed (Fok, Hall, and Chopra, 1986). The finite-element models of the dam and the foundation rock for such analyses are identical to those described previously. The finite-element model of the impounded water, however, consists of a finite-region adjacent to the dam and a uniform channel of infinite length (Fig. 11-6.16b). The finite-region is idealized as an assemblage of fluid elements and can be developed to match the reservoir topography. As a minimum, it should include three element layers and extend upstream a distance equal to the water depth. The infinite region is discretized using infinitely long subchannels coupled to the finite region at a transmitting boundary.

Reservoir boundary absorption

A hydrodynamic pressure wave impinging on the reservoir boundary is partly reflected into the water, and partly refracted (absorbed) into the boundary materials. The partial absorption at the reservoir boundary is approximately represented by a reflection coefficient known as "α", which is the ratio of reflected to incident wave amplitudes. The reflection coefficient α varies between 1 and -1, where $\alpha = 1$ represents a nonabsorptive (rigid) boundary with 100% reflection, $\alpha = 0$ corresponds to a complete absorption with no reflection, and $\alpha = -1$ characterizes 100% reflection from a surface with an attendant phase reversal.

Parametric studies (Fok and Chopra, 1985) of the dam-water interaction indicate that the earthquake response of arch dams, particularly due to vertical and cross-stream components of ground motion are sensitive to the values of α. If the reservoir boundary materials are relatively soft (small α's), an important fraction of the reservoir water energy can be absorbed, leading to a major reduction in the dynamic response of the dam. Therefore, the values of α for the design and safety evaluation of dams subjected to earthquake loading should be measured or selected conservatively. Experimental procedures for measuring α in-place (Ghanaat and Redpath, 1995), have resulted in values of α ranging from -0.55 to 0.66 at seven dam sites (Table 11-6-1). The results indicate that the reflection coefficient of the bottom materials could vary significantly for different sites. Another important finding of the study was that α values for the alluvium, silt, and other sedimentary material at the reservoir bottom could markedly differ from those for the reservoir side walls consisting of rock. In this situation, two values of α should be used, one for the sediment materials at the bottom and another for the rock on the side walls.

Because the value of α can effect the dam's response, a parameter sensitivity study will be required when α is assumed to be lower than 0.8. Conservative values of α shall be assumed.

Table 11-6.1 Measured reflection coefficient for bottom sediments and rock at seven concrete dam sites (Ghanaat, Redpath 1995)

Dam Name	**Bottom Material**	**α**
Folsom	Bottom sediments with trapped gas, such as that from organic matter	-0.55
Pine Flat	Bottom sediments with trapped gas, such as that from organic matter	-0.45
Hoover	Bottom sediments with trapped gas, such as that from organic matter	-0.05
Glen Canyon	Sediments	0.15
Monticello	Sediments	0.44
Glen Canyon	Rock - Jurassic Navajo sandstone	0.49
Crystal	Rock - Precambrian metamorphic rocks	0.53
Morrow Point	Rock - biotite schist, mica schist, micaceous quartzite, and quartzite	0.55
Monticello	Rock - sandstones interbedded with sandy shale and pebbly conglomerate	0.66
Hoover	Rock - Canyon walls	0.77

11-6.5.2 Dam-Foundation Interaction

Interaction of the dam with the foundation rock leads to an increase in vibration periods, primarily due to flexibility of the foundation rock. Dam-foundation interaction also decreases the dam response if damping arising from material damping in the foundation rock and the radiation damping associated with wave propagation away from the dam are considered in the analysis. These effects of dam-foundation interaction depend on the foundation flexibility (Chopra and Tan 1996). As the foundation rock becomes more flexible, radiation damping increases and vibration periods elongate further.

In practice, dam-foundation interaction effects are typically represented by a "*standard*" massless foundation model, in which only flexibility of the foundation rock is considered but its inertia and damping are ignored. A rigorous treatment of dam-foundation interaction is represented by the foundation impedance matrix (i.e. frequency-dependent stiff-

ness matrix), which is computed for an unbounded homogeneous foundation rock region assuming to contain an infinitely long canyon of uniform cross-section. A parameter study of Morrow Point Dam with the standard and refined dam-foundation interaction models (Chopra and Tan 1996), indicates a substantial reduction in dynamic stresses if inertia and damping effects of the foundation rock are included. The results of this study, when combined for all three components of the earthquake ground motion, show that the standard foundation model overestimates maximum dynamic stresses by 6%-to-10% for E_f/E_c = 2, by 12%-to-22% for E_f/E_c = 1, by 29%-to-46% for E_f/E_c = 1/2, and by 45%-to-78% for E_f/E_c = 1/4. It should be noted that E_f/E_c = 1/2 and 1/4 represent extreme cases of highly fractured rock, which even if existed at a site, do not normally extend beyond shallow depths. The refined dam-foundation interaction model ignores this condition and assumes the same low modulus ratio for the entire unbounded foundation rock region. Another factor is that the results may depend on characteristics of the earthquake ground motion and on the assumption of uniform earthquake input. These are some of the important issues that require further studies, before this unconservative dam-foundation interaction can be used in practice. The FERC will welcome any attempt to account for dam foundation interaction more accurately, however it must be realized that whenever more parameters are required for an analysis, more uncertainty is introduced. This uncertainty must be covered by higher safety factors or parameter sensitivity studies. The uncertainties discussed above tend to make the continued use of standard massless foundation model attractive.

11-6.5.2.1 Size of Standard Foundation Rock Model

The standard foundation rock model for dynamic analysis is identical to that for the static analysis (Section 11-5.2.1.2). It is developed on semi-circular or rectangular planes cut into the canyon walls at the dam-foundation contact surface, with each plane oriented in the upstream-downstream direction as moving from the base to the dam crest. In static analysis, size of the foundation model is selected on the basis of static deflections and stresses, whereas in dynamic analysis it is selected such that the vibration frequencies and mode shapes of the dam are computed more accurately. Vibration frequencies of the dam decrease as the size of flexible foundation model increases (Clough et al. 1985; Fok and Chopra 1985), but the reduction diminishes beyond a certain size depending on the modulus ratio of the foundation to the concrete (E_f/E_c). Similar to the static analysis, a foundation model extending one dam height in the upstream, downstream, and downward directions (R_f = dam height, for semi-circular foundation model) is also adequate for dynamic analysis when E_f/E_c is equal or greater than 1. For more flexible foundation rock

with E_f/E_c ratios equal to 1/2 and 1/4, the foundation model should extend 1.5 and 2 times the dam height in all directions, respectively.

11-6.5.2.2 Effects of Foundation Modulus

Dam-foundation interaction reduces natural frequencies of the dam and affects mode shapes primarily due to foundation flexibility. The effects of foundation flexibility on the natural frequencies and mode shapes increases as the modulus ratio E_f/E_c decreases. The variation of the natural frequencies for the five lowest modes with the modulus ratio is shown in Fig. 11-6.17. The natural frequencies are normalized with respect to their values for a rigid foundation. This figure shows that the natural frequencies are more sensitive to modulus ratios of less than 1, and that they reduce significantly below their values for a rigid foundation as E_f/E_c becomes less than 1/2; this trend is also true for the higher natural frequencies.

Foundation modulus affects higher mode shapes more than the fundamental symmetric and anti-symmetric mode shapes. The change in mode shapes increases as the modulus ratio E_f/E_c decreases; modulus ratios of 1/2 and smaller may even produce mode shapes that are considerably different from those for a rigid foundation. Thus, for a more flexible foundation rock with the modulus ratio less than 1, it is important that the foundation modulus be determined more accurately by conducting field investigations or performing sensitivity studies that considers the lowest possible modulus values.

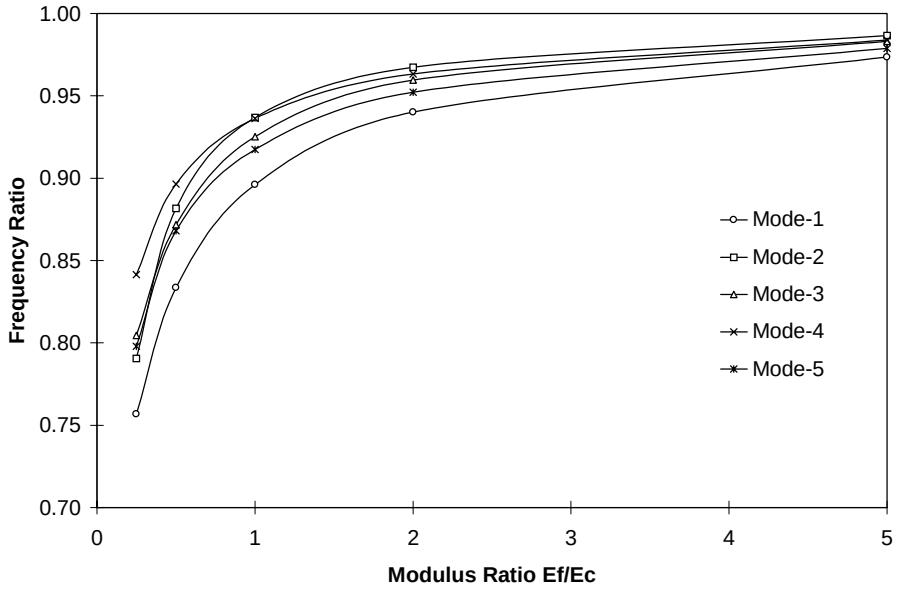

Fig. 11-6.17 Variation of five lowest frequencies of dam-foundation rock system with modulus ratio of foundation to concrete.

Variation of foundation modulus with abutment also affects natural frequencies and especially mode shapes of the dam. These effects are most significant when the modulus ratio of the weaker abutment to concrete is less than 1/2, but can be ignored, as modulus ratio of the weaker abutment approaches unity, or when modulus ratios for both abutment are greater than unity. In these cases, variation of foundation modulus with abutment can be ignored. Only the modulus of the weaker abutment may be used and applied to the entire foundation rock model.

Variation of foundation modulus with elevation affects the natural frequencies and mode shapes in the same manner discussed for static deflections and stresses in Section 11-5.5.1. More flexible upper abutments tend to reduce natural frequencies and affect mode shapes, especially for the higher modes. These effects, however, are much less than for those cases where one abutment or the entire foundation region comprises of low modulus materials as discussed previously. The effects of variation of foundation modulus on frequencies and mode shapes and thus on dynamic response of the dam should be considered when the region of weaker zones are substantial and their moduli are less than the modulus of the concrete. When the modulus of the foundation rock including weak zones are higher than the modulus of the concrete, the effects of variation of modulus with elevation can be ignored and the smallest modulus may be used for the entire foundation.

11-6.5.2.3 Foundation Boundary Condition

The standard massless foundation model contains a volume of foundation rock region that extents a distance equal to one or two dam heights in the upstream, downstream, and downward directions. Since wave propagation is ignored in such a model, all nodes on exterior surfaces of the foundation mesh are fixed in space, as shown in Figs. 11-5.2a and 11-5.3a.

11-6.5.3 Direction of Ground Motions

The seismic input for time-history analysis of arch dams consists of three acceleration time histories that are applied simultaneously at the fixed boundaries of the foundation model; in the stream, vertical, and cross-stream directions. Although the vertical ground motion is always applied in the up-down direction, the direction for the two horizontal components is not obvious and should be selected carefully. Even if the peak ground accelerations for the two horizontal components are the same, their sustained duration of

maximum shaking which can affect the number of critical peak stresses may be different. Fig. 11-6.18 demonstrates that, an example arch dam subjected to three components of ground motion develops higher number of stress peaks when the more energetic horizontal component of ground motion is applied in the stream direction. Since this is generally true in most cases, the more energetic component of ground motion should be applied in the stream direction.

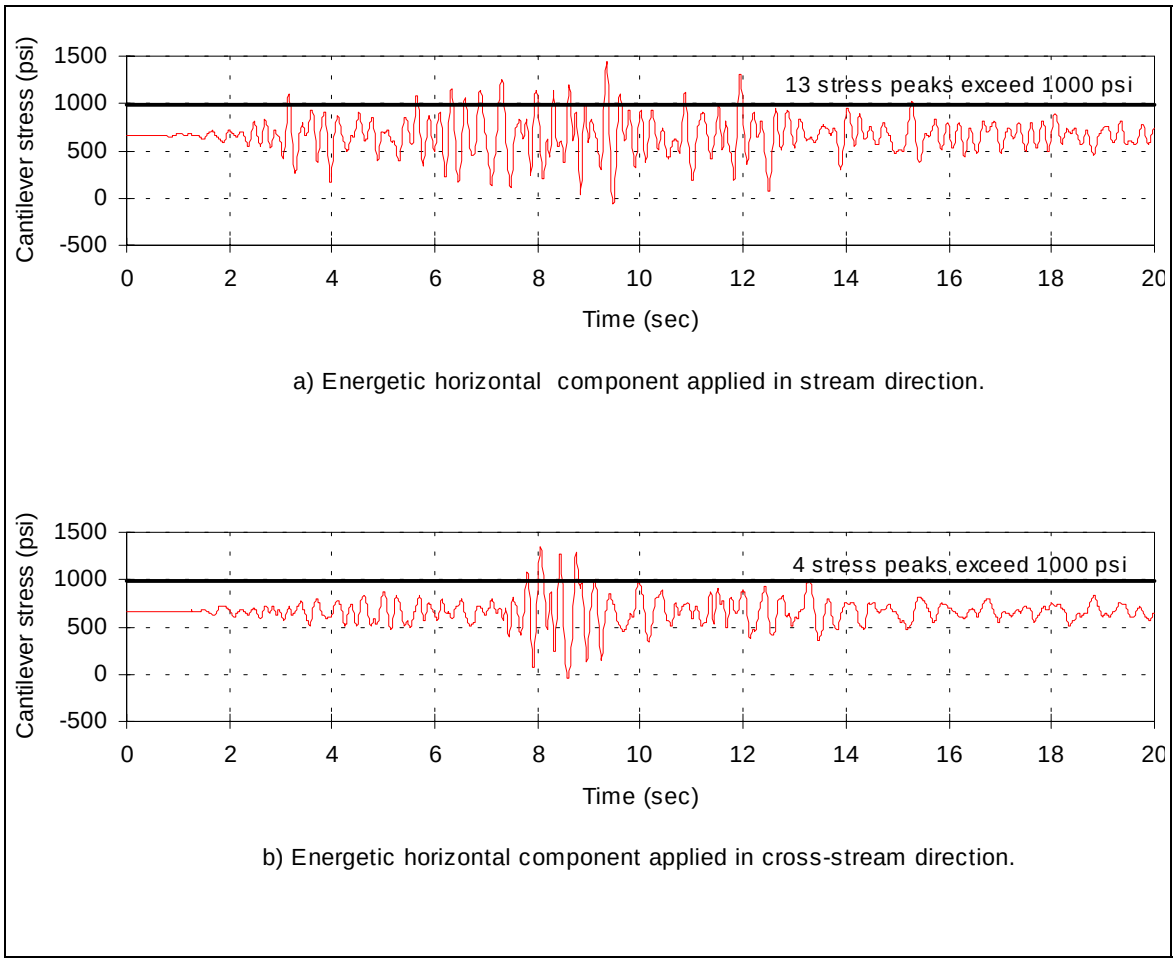

Fig. 11-6.18 Time histories of cantilever stress on upstream face of dam

11-6.6 Post-Earthquake Safety Evaluation

A post-earthquake safety evaluation is required to assure the safety of the dam if: 1) a maximum credible earthquake should occur near the dam site, and 2) the predicted performance of the dam due to a postulated MCE event should indicate substantial damage.

Should an intense earthquake occur near any dam, a very detailed examination should be made as soon as possible to evaluate the extent of damages that may have resulted. Dur-

ing the post-earthquake inspection, the galleries and downstream face of the dam should be examined for evidence of new cracks and of working of existing cracks and monolith joints. Other visible damages to look for include vertical offsets or settlement, horizontal movement of the crest, and joint separation within the body of the dam and at the interface with thrust block(s). The abutments should be carefully examined for evidence of cracking, rockfalls, and rock mass sliding. Also, detailed inspections should be made for damage to appurtenances such as gates and their lift mechanisms, intake and elevator towers, and transmission towers and substation equipment at the site. In addition to the detailed inspections of the dam system and its abutments, measurements from the position indicating system (if installed) should be carefully studied for possible evidence of permanent displacements caused by earthquake, because such permanent changes may be the best indicators of any significant internal damage done to a dam or its foundation. The change in leakage past the gates, or into the galleries and shafts, and a change in the seepage through the abutments should be noted and examined.

In the case of safety evaluation of an existing dam, even though substantial damage is permitted under the MCE excitation, the inflicted damage should not weaken the dam to a point where its capacity to resists static loads and aftershocks is threatened. The procedures for post-earthquake evaluation for static loads and aftershock events are discussed below.

11-6.6.1 Evaluation for Static Loads

If post-earthquake inspection or seismic safety evaluation due to a postulated maximum earthquake event indicates that the dam has or might suffer substantial damage, the performance of the dam in its damaged condition should be evaluated to assure that the safety of the dam to resist static loads has not been threatened. This is because the damage inflicted upon the dam might have weakened its capacity to resist sustained static loads, which require a more demanding performance criteria than the transient seismic loads.

In these cases, a post-earthquake static analysis considering the effects of cracks is required. A possible simple approach to account for the effects of cracking is to perform a FE linear elastic static analysis, as described in Section 11-5.2, with reduced modulus for the elements affected by cracks. In such analysis, the effects of opened contraction joints indicating loss of arch action may be simulated by introducing double nodes at the location of joint openings. The location and extent of cracks and joint openings should be determined from the earthquake safety analysis of the dam, or from the post-earthquake inspections should an actual earthquake excite the dam.

11-6.6.2 Evaluation for Aftershock Events

Aftershock earthquakes invariably occur after any major quake, but the rate of aftershock activity decreases rapidly with time after the main shock. Although the aftershocks are not as intense as the main shock, in some cases they could be severe enough to produce additional damage and possibly limit the use of the dam. After a major earthquake, safety assessments of the damaged dams should be a major priority for the dam owners and the government agencies. Such assessments are critical to determination of the level of hazard from an aftershock event. Depending on the severity of damage, the conditions of the dam may be described by a classification system comprising of three categories: Safe, Limited Usage, and Unsafe. These categories are defined as follows:

- *Safe*: No apparent hazard found, although repairs may be required. Cracking is primarily surficial and confined to small regions of the dam and abutments. Contraction joints may open and close during the earthquake excitation, but they are close with minimal offsets after the shaking stops. Original load-resisting capacity of the dam is not significantly reduced; thus no restriction of water level is required.

- *Limited Usage*: Hazardous condition believed to be present due to damage resulting from relatively significant cracking and permanent joint separation of the dam, or possible minor sliding of the thrust blocks or abutment rock masses resisting the dam thrusts. If necessary, reservoir water level should be lowered to reduce the possible major aftershock hazard. The continuous usage should be confined to low water levels until the necessary repairs and strengthening measures have been accomplished.

- *Unsafe*: Extreme hazard condition with imminent danger of collapse from an aftershock. Such a condition has not occurred in the past, mainly because no dam with full reservoir has ever been subjected to a maximum credible earthquake. Should such an extreme case occur, the damage is expected to be widespread with major cracking, joint opening with offsets, and possible sliding originating along the cracked sections within the dam, at the dam-foundation interface, or along the planes of weakness within the abutments. The reservoir water should be lowered and warning issued for immediate evacuation of the population living downstream.

When a seismic safety evaluation of an existing dam predicts substantial damage due to a postulated maximum credible earthquake, the performance of the dam to withstand the major aftershocks should also be evaluated. Any seismic response analysis of a dam for aftershocks should consider the effects of cracking and other structural damage that might have weakened the dam during the application of the main shock. When subjected to a

strong aftershock, the dam may suffer additional damage but its capacity to retain the reservoir water should not be jeopardized. The magnitude of the aftershock selected for the safety evaluation should be consistent with those observed in the past earthquakes. Table 11-6.2 shows the main shock and the largest aftershock sequence of some recent earthquakes.

Table 11-6.2 Main shock and largest aftershock of some recent earthquakes.

Earthquake	**Main Shock**	**Largest Aftershock**	**Time of Aftershock**
1983 Idaho	M_L= 7.3	M_L= 5.8	6 hours later
1984 Morgan Hill, CA	M_L= 6.2	M_L= 4.5	9 days later
1985 Chile	M_s = 7.8 M_b = 6.9	m_b = 6.5	52 min. later
1987 Wittier Narrows, CA	M_L= 5.9	5.3	3 days later
1988 Armenia	M_b= 6.3	5.9	5 min. later
1989 Loma Prieta, CA	M_w = 6.9	5.0	33 hours later
1994 Northridge, CA	M_w = 6.7	5.9	1 min. later

M_L= Local Magnitude

M_s = Surface-wave Magnitude

m_b = Body-wave Magnitude

11-7 INSTRUMENTATION

11-7.1 Purpose and Need for Instrumentation

The observed historical behavior of a dam provides the best indication of the dam's future performance. As such it is essential that existing arch dams be provided with adequate instrumentation for evaluation of dam safety and for the verification of the analytical models used to predict their performance under unusual and extreme loading conditions.

The most common instrumentation for arch dams includes measurements of movements, reservoir and tailwater levels, seepage, uplift pressures, and ambient and internal temperatures. In regions of high seismicity, it is also important to install earthquake instrumentation system to record both the earthquake ground motions that excite the dam and the dynamic motions of the structure that result from this excitation. A complete discussion of the types of instruments typically used at arch dams is contained in Chapter 9. The following paragraphs are intended to help staff understand the special requirements in evaluating the instrumentation layout, frequency of measurements, and evaluation of the collected data at arch dams.

11-7.2 Special Instrumentation Considerations for Arch Dams

The layout for monitoring seepage and uplift at arch dams is the same as other concrete dams. In general, seepage should be monitored at various elevations along abutment contacts in order to determine if areas of seepage are influenced by reservoir elevation, loading on the foundation, ground water, or a combination of these. While uplift may not be an important factor in the stresses in the body of the dam, it can be extremely important in the stability of the abutments, and instrumentation should be considered for any areas where potential failure wedges may form.

Temperature can play a significant role in the behavior of an arch dam. As discussed in Section 11-4.5, the evaluation of arch dams includes either "winter" or "summer" mean concrete temperatures in each load combination. These concrete temperatures can be measured directly by embedding instruments in the concrete or can be approximated by using reservoir and air temperatures. Thermometers, thermocouples, or thermistors embedded at various depths in the concrete provide the best means of determining the magnitude and timing of the temperature loads. Embedded instruments should be installed at various elevations near the center of the dam cross-section and near each face to obtain a reliable approximation of the maximum and minimum concrete temperatures. The primary advantage to direct measurement of concrete temperatures is that it eliminates the uncertainty in estimating concrete temperatures based on

reservoir and air temperature data. The primary disadvantage to embedded instruments is the cost of installing the instruments and taking regular measurements.

When using reservoir and air temperatures to estimate the concrete temperature, the procedures discussed in section 11-4.3 should be followed. It should be clearly understood that the timing of the peak average concrete temperatures would not coincide with the timing of the peak ambient conditions. It will usually take the mass concrete one or two months to respond to the ambient conditions depending upon, among other factors, the thickness of the dam and the thermal properties of the concrete. For example, if minimum air temperatures typically occur in mid-January, the minimum mean concrete temperature could occur sometime between the first of February to the end of March. In other words, the "winter" temperature loading could be the concrete temperatures that occur in early spring. This fact can be extremely important when establishing the timing of measurements or when determining reservoir levels occurring at usual minimum and maximum concrete temperatures.

In measuring deflections in arch dams, the instrumentation points should be established at the crown cantilever and near the quarter points as seen in Figure 11-7.1. If the dam is slightly non-symmetrical, then the points should be set at the crown cantilever and at points mid-way between the crown cantilever and the abutment contacts. For highly non-symmetrical dams, additional points should be added at equal intervals along the longest side of the crest.

11-7.3 Frequency of Measurements

The frequency of measurements should generally agree with the monitoring schedules in Chapter 9. As noted in Section 9-6, even though existing dams have generally reached equilibrium with imposed loads, baseline data must be obtained to compare with subsequent measurements. In any instrumentation program it is especially important that the range of extremes be captured. As such, it is preferable to take monthly measurements until the adequacy of the equipment, personnel, and procedures are known and all patterns can be clearly identified. This may take 2 to 3 years of monthly measurements before the frequency can be reduced to quarterly.

Once the timing of the measured extremes has been clearly defined, quarterly measurements can be scheduled which will capture those extremes each year. The quarterly measurements of deflections will usually correspond to the times of minimum and maximum **concrete temperatures** and/or minimum and maximum **normal reservoir elevations**. If the reservoir variation does not sufficiently affect the deflections of the dam, then the frequency of the measurement could be extended to semiannual at the times of minimum and maximum seasonal extremes, with additional measurements taken whenever an unusual reservoir level occurs (for example, very low water levels during droughts).

11-7.4 Presentation of Data and Interpretation of Readings

Deflection data for arch dams should always be converted to radial and tangential deflections as shown in Figure 11-7.1. Terms such as “North and South”, “Upstream and Downstream", etc. are not appropriate for a curved structure such as an arch dam and should not be used.

Instrumentation data should be plotted with respect to time. Reservoir elevation should be included on the plot so that linkage between reservoir elevation and instrument output can be observed. Examples are shown in Figure 11-7.2 and 11-7.3. Since temperature plays a major role in dam behavior, it may also be appropriate to include temperature data on the plot. The radial deflections should be seasonal with maximum upstream deflection occurring at the time of maximum mean concrete temperatures and the maximum downstream deflection occurring at the time of minimum mean concrete temperatures. Deflection data that doesn't match these trends could indicate that the accuracy or precision of the instrumentation program is not adequate.

When plotting instrumentation data the scale used in the plots is extremely important. Trends and relationships can be lost if the scale not appropriate for the data shown.

11-7.5 Comparison of Predicted and Measured Deflections

Once staff has confidence that the deflection measurements are of sufficient accuracy and precision and are representative of the actual behavior of the dam, the next step is to compare the measured deflections with those predicted by the analytical methods discussed earlier in this chapter. The purpose of these comparisons is to gain confidence that the mathematical model is an accurate predictor of structural behavior. If there is a credible comparison of predicted and measured deflections under normal loading conditions then there is additional confidence that the mathematical model may be able to predict the behavior of the dam under flood and seismic load conditions.

However, caution should be exercised in attempting to require an exact comparison between the mathematical model and the measured data. An exact comparison is not always realistic. Among other problems, there are usually limits to the accuracy and precision of the measurement techniques. There can also be problems associated with gaps in data or changes in equipment or personnel. In addition, while the structure response is nonlinear the mathematical models usually assume linear elastic behavior. Unless there are numerous thermometers throughout the dam and unless temperature and deflection measurements are made daily, it is doubtful that the exact loading conditions will apply to both the measured and predicted deflections.

These limitations do not preclude making a comparison that can be reasonable and useful to the dam safety engineer. For example, an arch dam that has survey points at the crest of the dam but has no embedded thermometers to measure concrete temperature. Assume that the historical data collected indicates that the instrumentation procedures are of sufficient accuracy and precision and all trends are consistent with expected behavior. Also assume these points are measured in the late winter (February) and late summer (August) and the range of annual deflection is typically in the order of 0.9 inches. If a finite element model of this dam predicts a winter-to-summer deflection of 1.2 inches it could be concluded that the model is a reasonable predictor of the dam's behavior. However, if the finite model predicts deflections of 2.0-inches, then the material or loading assumptions used in the model may need to be re-evaluated.

11-7.6 Long Term Instrumentation Performance

The life span of embedded electronic instruments is finite. It is to be expected that the output from imbedded temperature sensors, strain gauges, and piezometers will become unreliable over time, and instruments will eventually have to be abandoned. For this reason, instrumentation plans should include redundancy to attempt to offset the attrition that will occur. It is also important to obtain sufficient information early, while the majority of instruments are still functioning.

7.7 Interpretation of Data

The gathering and recording of instrumentation data is of little value if it is not reviewed and interpreted by personnel who understand the implications of the data. This review should be timely, so that instrument readings that are unexpected can be quickly double checked. Of prime importance is the discernment of trends in the data over time. The absolute values of the readings are of lesser value. For this reason, it is important to avoid changes is reading and recording procedures. If readings from an instrument change from what is expected, this should be noted.

The readings from various instruments should be correlated. For example, does an increase in a piezometer reading correspond to a movement? Does temperature effect gallery drain flow? It is only through the careful interpretation of the readings from all instruments that the behavior of an arch dam is properly understood.

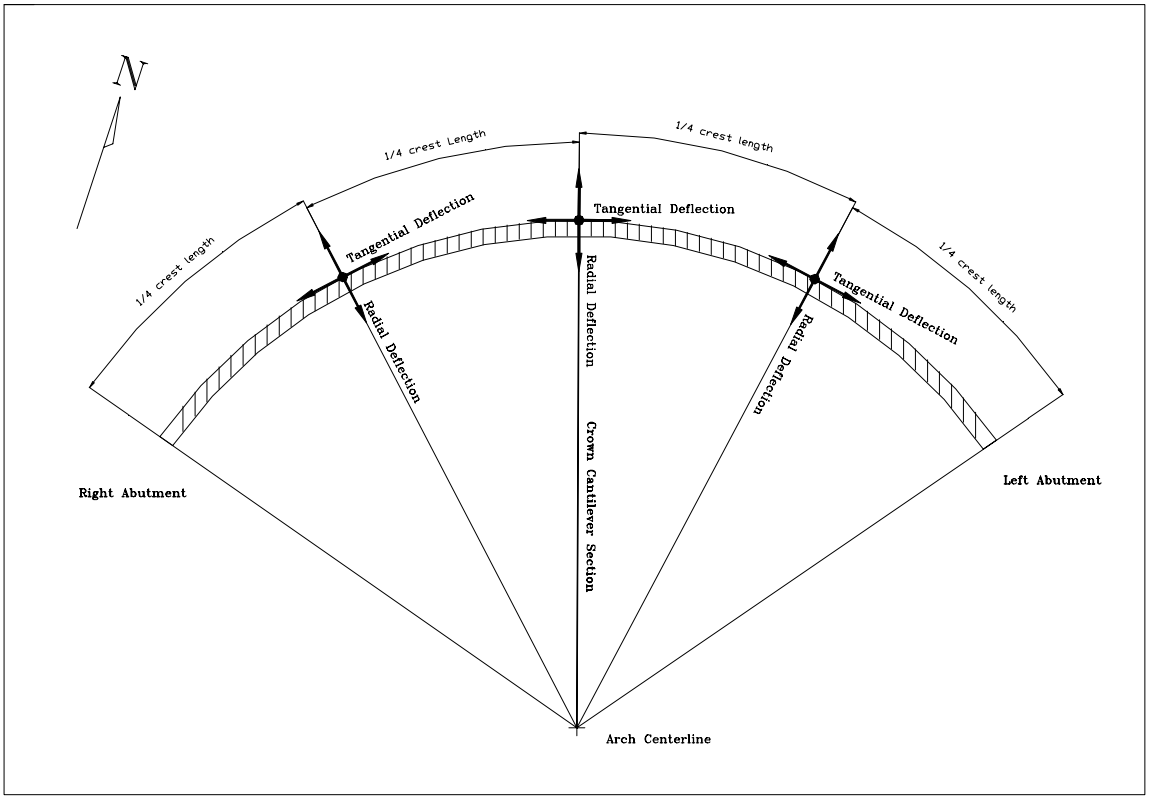

Fig. 11-7.1 Typical layout for a symmetric arch dam

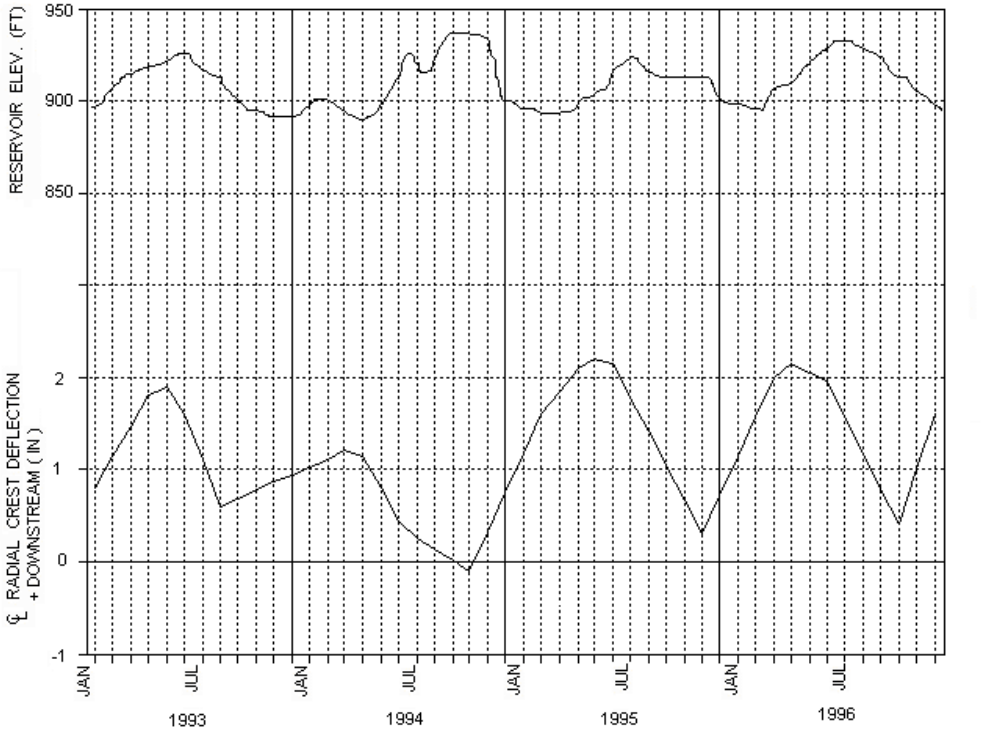

Fig 11-7.2 Deflection plot with reservoir elevation included.

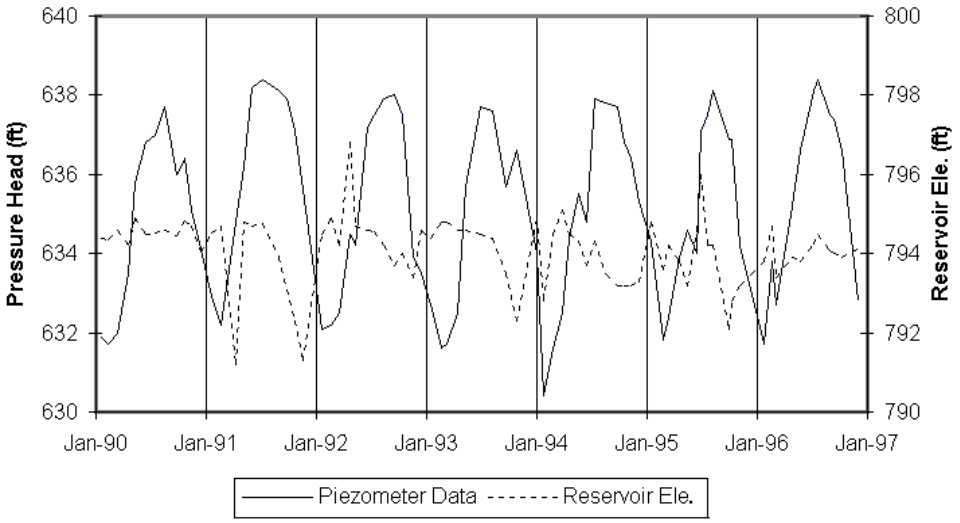

Fig. 11-7.3 Piezometer data

11-8 HISTORIC DAM INCIDENTS

11-8.1 Overview

There is no comprehensive listing of arch-dam failures. However, available listings are contained in more than one publication. Babb and Mermel (1968) listed 600 dam incidents (including failures) of which only seven involved arch dams, 2 involved multiple arch dams, and 2 involved gravity-arch dams. The dams they list are as follows: Arequipa (Peru, 1965); Matilija (U.S.A., 1965); Vajont (Italy, 1963); Malpasset (France, 1959); Moyie River (U.S.A., 1938); Alla Sella Zerbino; Allessandria (Italy, 1935); Lake Lanier (U.S.A., 1926); Gleno (Italy, 1923); Lake Hodges (U.S.A., 1918); Manitou (U.S.A., 1917); and Tolla (France, 1892).

The International Commission on Large Dams (ICOLD) Bulletin 99 (1995) lists seven arch dam failures, three of which are also listed by Babb and Mermel (Malpasset, Gleno, and Moyie River). The other four arch dam failures listed by ICOLD are: Leguaseca (Spain, 1987), Meihua also called Plum (China, 1981), Idbar (Yugoslavia, 1960); and Vaughn Creek (U.S.A., 1926).

In addition, in a paper entitled "Lesson from Serious Incidents at Seven Arch Dams" presented at the 1997 annual conference of the Association of State Dam Safety Officials, G.S. Sarkaria described incidents at Le Gage, El Fryle, Koelenbrein, and Zeuzier dams.

Following is a summary of the historical incidents and failures involving arch dams:

Arequipa, Peru. This thin-arch concrete dam failed in 1965 as a result of fractures caused by a vibrating penstock which passed through the dam. Inflow was normal at the time.

Matilija, California. The concrete dam was completed in 1949 and was a combination of gravity and arch structure. It was 163 feet high with a crest length of 620 feet. In 1965 the dam was judged to be unsafe as a result of deterioration of the concrete due to expansive aggregate. Foundation conditions were also judged to be poor. The reservoir was drained, the dam was eventually demolished, and the site was submerged by a new dam downstream.

Vajont, Switzerland. This thin-arch concrete dam, which is 905 feet high, was overtopped by a huge landslide-generated wave. Inflow to the reservoir was normal at the time. The resulting overtopping was estimated to be as much as 300 feet. The dam

itself suffered little damage, but the reservoir was a total loss. The resulting flood caused great loss of life in the downstream areas. A detailed description of failure of Vajont Dam is provided in Section 11-8.2.1.

Malpasset, France This thin-arch concrete dam, which was 218 feet tall, failed due to a movement of the left abutment in December 1959. The movement was thought to be due to sliding on a rock wedge formed by intersection of a fault with gneissic foliation in the rock of the left abutment. The principle cause of the failure was not directly due to the passage of a flood in that the dam was never overtopped. However, a very large flood was being passed when the failure occurred. The official death toll was 396 people killed in the ensuing flood, which suddenly struck the village of Frejus. The dam was a complete loss and is further discussed in Section 11-8.3.

Le Gage, France This Very thin 150' high arch dam developed extensive cracking on both faces of the dam after first filling of the reservoir in 1955. Cracking continued to worsen for the next 6 years. After the failure of Malpasset dam, Le Gage was abandon and a new thicker arch dam was constructed upstream.

El Fryle Dam, Peru This 200' high arch dam experienced a major slide on one of the abutments during filling. The dam did not collapse. A concrete thrust block abutment was constructed and the dam was saved.

Moyie River, Idaho This 53-foot high concrete arch dam, located on the Moyie River, was approximately 64 feet thick at the base and 24 feet wide at the crest. During passage of a major flood in 1926, the spillway, which was located on one abutment, was undermined. The erosion completely washed out one of the abutments. The abutment was replaced and the dam is still in use.

Alla Sella Zerbino, Allessandria, Italy This concrete arch-gravity structure was only 39 feet high with a crest length of 262 feet and a reservoir capacity of 14,000 AF. It failed on August 13, 1935, as a result of overtopping and sliding on its foundation. One hundred lives were lost.

Lake Lanier, North Carolina This constant-radius concrete arch dam was constructed in 1925. It had a thickness of 12-1/2 feet at the base and 1 foot at the top. It was 62' high with a crest length of 236 feet. One of the abutments (cyclopean masonry) washed out as a result of the failure of soft rock in the abutment on January 21, 1926. The remainder of the dam was unharmed.

Gleno, Italy This multiple-arch concrete dam contained 25 arches for a total length of 250 feet. Concrete gravity sections made up the ends of the dam. Total crest length was 863 feet. The dam was 143 feet high. It was completed in 1923 and failed on December 1, 1923 only 30 days after filling. Nine arches fell due to a poor masonry base. Some 600 persons lost their lives.

Lake Hodges, California This multiple-arch concrete dam was completed in 1918 by the City of San Diego. It was 136 feet high with a crest length of 616 feet and a reservoir capacity of 33,550 AF. The dam was damaged by cracked piers in 1918 but did not completely fail.

Manitou, Colorado This concrete arch dam was 50 feet tall with a crest length of 300 feet. A portion of the dam failed in 1924 due to deterioration of the concrete.

Tolla, France This very thin arch dam was 295' high with a crest length of 435 feet. Owned by Electricite DeFrance, the dam experienced severe cracking. It was buttressed in response. Cracking may have been the result of large temperature stresses.

Koelnbrein, Austria Cracks and substantial leakage appeared in the lowest foundation gallery when the reservoir was 80% full two years after first filling. Full uplift pressure was observed over the entire base in the central portion of the dam. Major repair was undertaken between 1989 and 1994.

Zeuzier, Switzerland The dam behaved satisfactorily for 20 years, then began to deflect upstream due to riverward movement of the left abutment.

Lequaseca, Spain This concrete multiple-arch dam, which was 66 feet high with a crest length of 230 feet and held a reservoir volume of only 16 AF, was constructed in 1958 and failed in 1987. The dam body failed structurally, apparently due to deterioration due to both aging and the effects of freezing and thawing. No details of the failure are given in the literature.

Meihua (Plum), China This experimental masonry arch dam was 72 feet high and had a crest length of 211 feet. It was completed in 1981 held a reservoir of only 93 AF. It failed shortly after filling in 1981. The dam failed as a result of structural failure due to excessive uplift movement along a peripheral joint as described in Section 11-8.3.2. The scheme was abandoned after failure.

Idbar, Yugoslavia This concrete arch dam was 125' high with a crest length of 354 feet. It was completed in 1959 and failed in 1960. Failure was during first filling and resulted from piping and erosion of the foundation.

Vaughn Creek, USA This concrete arch dam was 62' high with a crest length of 312 feet. The dam was completed in 1926 and failed during first filling. Seepage and poor materials in the dam caused failure.

The above incidents indicate that safety of an arch dam can be threatened by overtopping due to major floods and landslides, abutment sliding, erosion of foundation-abutment rock, and the deterioration or poor construction materials. They also show that small, thin arch dams could be susceptible to vibrating appurtenant structures such as a penstock passing through the dam, and that thermal cracks caused by nonuniform temperature distribution could result in failure of thin arch dams. Significant landslide and abutment failure cases are described in Section 11-8.2 and 11-8.3, respectively. A notable case of severe overtopping and damage to stilling basin caused by the passage of extreme floods is provided in Section 11-8.4. Although no arch dam has ever reported to fail from earthquake ground shaking, performance of several arch dams, and in particular Pacoima Dam, under significant earthquake excitation are described in Section 11-8.5. The effects of alkali-aggregate reactions (AAR) and a summary of case histories of concrete arch dams with AAR problems are given in Section 11-8.6.

11-8.2 Landslide Case

11-8.2.1 Vajont Dam

The Vajont Dam, constructed between 1957 and 1960 is located on the Vajont River in northern Italy near the towns of Longarone, Pirago, Casso and Erto. The dam is a 276 meter (905 ft.) high, double curvature, thin arch dam. On 9 October 1963 during reservoir filling a catastrophic landslide movement occurred suddenly over a 2 km (1.2 mile) reach of the southern or left bank of the reservoir. According to Muller (1987) the slide mass consisted of a volume of 275 million cubic meters (360 million cubic yards), which generated a wave 260 meters (853 feet) high. Hendron and Patton (1985) describe a wave which crested 100 meters (328 feet) above the top of the dam and had a height of 70 meters (230 feet) downstream at the confluence of the Vajont and Piave Rivers. More than 2,000 people lost their lives in this catastrophe. Longarone and Pirago were the towns most severely affected. The dam structure itself survived the overtopping by the wave of water and the impact of the load of earth placed against it by the landslide, thus

providing an excellent example of the structural strength of an arch dam.

11-8.2.1.1 Geologic Conditions Contributing to Failure

The dam is located in the Dolomite Region of the Italian Alps in a narrow valley with steep side slopes. Jurassic and Cretaceous age limestone are the predominant rock types represented in the valley walls and in the landslide mass. Many have studied the geology. Hendron and Patton (1985) include as Appendix G "Synthesis of Geological Studies of the Vajont Landslide" by Edoardo Semenza (1966-67) which gives a clear discussion of the details of the geology.

The dip of the formations generally controls the configuration of the landslide surface, which forms a somewhat chair-like structure described by Muller (1987) with the upper portion dipping rather steeply toward the valley while the lower or seat portion flattens into a more nearly horizontal configuration. Semenza (1966-67) offers evidence that the landslide mass had moved previously in geologic time and that it had previously blocked the valley. During an investigation in 1959 he and F. Giudici discovered an uncemented mylonitic zone extending 1.5 km (0.93 miles) along the left side of the valley. They also concluded that a rock mass on the right side of the valley was a remnant of a prehistoric landslide. Semenza thinks that the gorge that existed when the dam was constructed had been eroded through the old landslide mass by the Vajont River. Hendron and Patton (1985) also concluded that the 1963 slide was a result of the reactivation of an old slide.

Semenza (1966-67) described the rock mass as being intensely fractured and faulted and containing solution cavities and sinkholes. These features would likely provide easy access for water to infiltrate the rock mass. Hendron and Patton (1985) found during their investigation that interbeds of clay existed in the formations adjacent to the slide planes. These clay beds could be the source of the low resistance to shear that was needed to explain the initiation of the landslide.

11-8.2.1.2 Stability Analysis

Several attempts were made to explain the landslide by using back analysis as a means of developing data on the many factors involved in the landslide development. Hendron and Patton (1985) provide a very plausible analysis and description. Their work on the clay beds that were discovered adjacent to the failure surface provides strong evidence that the low shearing resistance of the clay may have provided a path for development of the landslide shear planes. They concluded that the peak strength of the failure plane

materials was lost during prehistoric slide movements and that the residual strength of the materials was appropriate for use in back analysis.

Hendron and Patton (1985) also compared the rate of measured movement that occurred in the slide mass during the years immediately preceding the failure with precipitation, reservoir level, and water in piezometers. This analysis lead them to the conclusion that rainfall rate was a major factor in the activity of the slide. Where others had concluded that reservoir filling levels governed the rate of movement, they demonstrated that rate of precipitation was more closely associated with the rate of movement measured in the slide. The sinkholes mentioned above, as well as the intensely fractured condition of the rock, both could provide ready access for rain water to enter the rock mass.

11-8.2.1.3 Response of the Arch Dam Structure

According to Muller (1987) the thin arch dam resisted the forces imposed by the landslide failure and suffered only minor damage. The crest of the dam was the only portion damaged and that was not severe. In summarizing the August 1985 Purdue University Workshop on Dam Failures, Dr. G.A. Leonards (1987) stated that it had been reported that the Vajont Dam withstood a load eight times greater than it designed to withstand. In this same workshop Dr. J. Laginha Serafim (1987) noted that the dam survived the impact and overtopping of an asymmetrical wave of water and stones that subjected the structure to more than double the design load. This provides an excellent demonstration of the strength of a well-designed arch dam.

11-8.2.1.4 Lessons Learned

This catastrophic landslide failure demonstrated to the dam building profession the importance of performing detailed geologic investigations of the rim of narrow steep walled valleys which are planned as the reservoir for large dams. These studies should focus on locating and analyzing existing or potential landslides that could slide with sufficient volume and velocity to displace a wave of water that could endanger lives or property.

The failure mechanism of a large landslide mass such as this is very complex and difficult to evaluate as the failure is progressing. Even the leading experts may fail to reach precisely correct conclusions if they do not fully understand all of the factors affecting the landslide. In this case, the failure to realize that rainfall was more a factor than reservoir level in the rate of movement of the slide mass led the decision makers to think that the landslide could be controlled by adjusting the level of the reservoir and the

rate of filling. When dealing with a slow moving landslide it is imperative that all significant factors affecting its movement be identified and considered in all decisions regarding stabilization or control.

11-8.3 Abutment Failure Cases

11-8.3.1 Malpasset Dam

The Malpasset Dam located on the Reyran River in France, was a double curvature, thin arch dam with a maximum height of about 197 ft. (60 m) and a crest length of about 732 ft. (223 m) according to Londe (1987). Its thickness varied from 22.25 ft. (6.78 m) at the base to 4.92 ft. (1.5 m) at the crest. The dam failed in 1959 after a slow initial filling period which Londe says took about 5 years and was within about one ft. (30 cm) of the spillway crest at the time of failure.

The failure occurred due to movement within the left abutment foundation which caused the dam to rotate about the right abutment and ultimately collapse. According to Londe (1987) the failure occurred as a sudden movement. He says that 30 minutes before the failure a workman was painting the crest and observed nothing unusual to warn of the impending failure.

According to Serafim (1987) and Londe (1987), Malpasset was the first failure of a thin arch dam. Its failure resulted in the destruction of the city of Frejus, France, with much loss of life and property. The design of the dam was under the supervision of Andre Coyne, who was considered one of the most eminent dam designers in the world.

11-8.3.1.1 Geologic Conditions Contributing to Failure

The following description of geologic conditions is a synopsis based upon the description presented by Londe (1987).

The dam site is located in a banded gneiss formation in the Tanneron Massif. The dip of the foliation is between 30 and 50 degrees in a downstream direction and toward the right abutment. The left abutment, which failed, tends to be schistose, as does the lower part of the right abutment. The foliation/schistocity is due to layers of micaceous minerals and fine networks of microscopic openings near the layers of mica. The joint system is composed of three different patterns or sets. The spacing is very close, varying from 2-3 cm to as much as 20-50 cm. They are very tight and irregular in shape There are numerous shears and faults and they tend to be oriented parallel to the three joint sets.

They are characterized by breccia and mylonite.

The left abutment failure wedge was formed on its downstream side by a fault dipping 45 degrees upstream and striking east-west. The strike of the fault is parallel to the chord of the arch and is symmetrical with regard to each abutment. The upstream portion of the wedge was formed by a stepped pattern of sheared planes that followed the foliation planes in the gneiss. The foliation planes dip toward the river on the left abutment and are not symmetrical on each abutment. The existence of the fault was not known at the time of design. It was located from 49 ft. (15 m) to 131 ft. (40 m) below the foundation and exited at the surface beneath overburden some 65 ft. (20 m) downstream.

The rock was very impervious and when pressure tested with water the average take was less than one Lugeon unit. It was consequently not thought to require pressure grouting except in the interface zone between the concrete and the foundation. After the dam failed, detailed laboratory tests performed on the rock revealed that its permeability decreased markedly under compressive stress. This became a major factor in the theory developed to explain the failure.

In-situ tests of the rock mass modulus of deformation revealed a foundation with a low elastic modulus which averaged 180,000 psi (1260 MPa). Intact samples tested in the laboratory had much higher values, ranging from 1,214,300 psi (8500 MPa) to 8,571,000 (60,000 MPa). This demonstrates the importance of either determining the modulus of deformation by in-situ tests or reducing the laboratory values from testing intact samples by an appropriately determined reduction factor.

Unconfined compression tests performed on intact laboratory samples gave average values of 8285 psi (58 MPa) for dry specimens and 6070 psi (42.5 MPa) for saturated specimens. The test results, however, were very widely scattered.

After the failure occurred, a laboratory testing program was performed to evaluate the extent of stress concentration at depth in the foundation taking into consideration the discontinuities in the rock mass. Photoelastic modeling techniques were used. This confirmed that the load applied by the dam could induce high stress at considerable depth in the foundation concentrated along discontinuities in the rock mass. This was significant in providing one of the factors necessary to the development of the theory of failure.

11-8.3.1.2 Theory of Cause of Failure

Londe (1987) provides a theory of failure that satisfies all of the facts revealed during the extensive investigations that followed the event. Following is a synopsis of the explanation of failure provided in the referenced paper.

A large wedge of rock was removed in the left abutment by the failure. As stated above, this wedge was bounded on the downstream side by a fault striking parallel to the chord of the arch and dipping upstream at about 45 degrees. The upstream side of the wedge was bounded by shears parallel to the gneissic foliation of the rock. There seems to be little doubt that the failure occurred due to sliding of the rock in this wedge. The difficult question to answer was how the forces involved could be resolved to explain the movement that had occurred within this wedge.

The thrust from the arch on the left abutment was almost parallel to the foliation in the rock. Because of this parallel alignment, the stress distribution and dissipation with increased depth normally expected in design was unable to develop in the left abutment. This left it concentrated in a segment of the rock mass and essentially undiminished with depth which allowed it to concentrate at the downstream fault. Because this parallel alignment with the foliation did not exist on the right abutment, stress in that rock mass was able to dissipate with depth as is normally expected.

As the reservoir filled, the stress in the rock mass in the left abutment increased abnormally and the unusual sensitivity of the gneiss to decreased permeability with increased stress came into play. This resulted in very high uplift pressures that may have approached full reservoir head. This uplift pressure provided an upward force which contributed significantly to movement of the rock wedge that ultimately failed. As the rock wedge began to move under the combined forces of the arch and the uplift, the upstream foundation crack frequently associated with arch dams began to enlarge and increase the uplift pressure downstream. At some point the rock in the wedge was no longer able to resist the forces and was lifted out of the foundation. As this block of rock began to move, the thrust of the dam was translated up the abutment and had to be carried by the abutment thrust block and wing wall. The loads were so great that they could not restrain them. The left abutment failed and the dam rotated around the right abutment which had not failed. This resulted in sudden collapse of the dam and release of the water in the lake.

Wittke and Leonards (1987) report on a finite element analysis of the interaction of the dam and its foundation which supports the mechanism of failure reported by Londe

(1987) and described above, but provides some additional insight into the rock mechanics logic involved in the explanation. Their analysis indicates that a large stress reduction takes place perpendicular to the foliation on the upstream side of the wedge due to water forces on the upstream face of the arch dam and to the water seepage forces under and around the structure. This results in increased permeability parallel to the schistocity and high seepage pressures in the very adverse upward direction along the upstream side of the failure wedge. Ejection of the rock wedge would occur as explained by Londe (1987) but this additional analysis indicates that the friction angle resisting movement on the fault may have been as low as 15 to 20 degrees where Londe thought it to be about 30 degrees.

11-8.3.1.3 Lessons Learned

Abutment analysis must include 3 dimensional analysis of any rock wedges that may be capable of failure under the loads applied by the dam thrust and under uplift forces created by seepage from the reservoir.

Detailed geological investigations must be conducted in the abutments to identify all adversely oriented rock discontinuities.

Very complex and unique conditions may exist in the rock that forms the abutments that may not be readily evident. For example the unexpected reduction in rock mass permeability under increasing load that resulted in the development of an underground dam in the left abutment at Malpasset and resulting high uplift downstream of the dam.

Foundations of arch dams should be drained to reduce uplift forces.

Instruments should be provided in the abutments to monitor uplift pressure and deflections in the foundation.

The existence of an upstream crack near the heel of an arch dam is now generally accepted.

11-8.3.2 Experimental Plum Dam

Plum Dam, located in Fujian Province in south-east China, was an experimental cylindrical arch dam with a height of 72 ft (22 m) and a crest length of about 238 ft (72.6 m). The dam failed in September 1981 shortly after it was completed in May of the same year. Since the dam was an experimental structure built at a coastline site, its failure caused negligible property damage and no loss of life.

Field investigations indicated that the failure occurred possibly due to the upward and downstream sliding of the dam along a peripheral joint. This mode of failure and the dam geometry is further described in Section 11-5.6.1 and Figs. 11-5-23 and 11-5.24. The dam was built as a masonry structure composed of granite blocks in the main body of the dam and included a peripheral joint between the dam and its artificial concrete abutment. The joint surfaces were coated with bitumen and polyvinyl chloride was used to seal the joint.

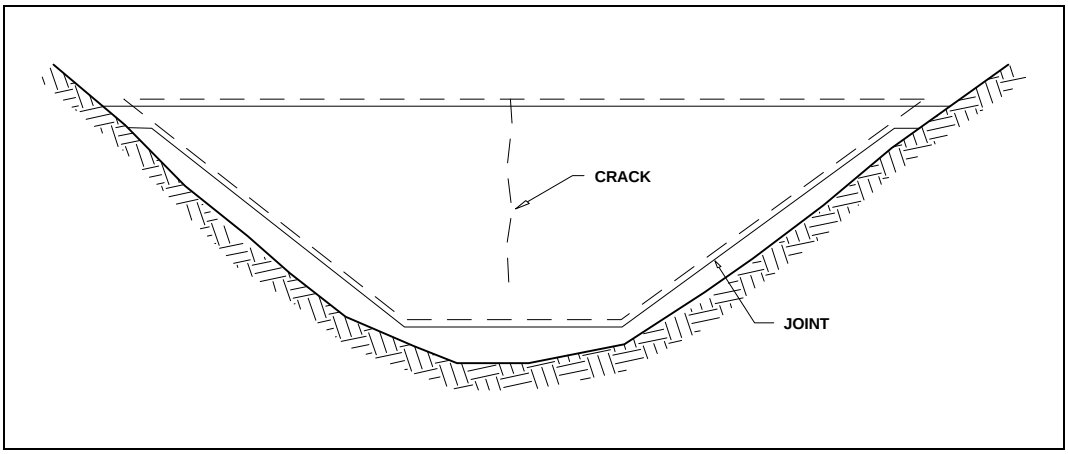

Fig. 11-8.1 Upward sliding of Plum Arch Dam along its artificial flat abutment.

Completed in May 1981, full storage of the reservoir was reached in June 1981, and the dam was overtopped by 1 foot over the crest on July 20. The dam was overtopped again on September11 and 12, but no damage or unusual behavior was observed. On the morning of September 18, the dam was inspected and nothing unusual was noticed. At 1:25 pm on the same day a local person had walked across the dam, but 10 minutes later the dam ruptured spectacularly without any warning.

Field investigations of the failure resulted in the following observations:

- The artificial concrete abutment was found to be intact with no sign of cracking or movements.
- The dam body was totally destroyed with smaller debris from the right and central portions of the dam found long distances downstream. Large trapezoid blocks were found near the left abutment.

- The top 5.6 ft (1.7 m) of the dam, which had no peripheral joint, was sheared off at both abutments along the masonry placement joints. At the right abutment, debris showed signs of upward movement of 2 to 3 inches (5 to 8 cm). At the left abutment some debris were found upstream, confirming that the rotation of the dam must have occurred with respect to this abutment.
- Peripheral joint surface showed two sets of frictional traces, one parallel to the dam axis and another inclined toward the downstream at 30°. The traces parallel to the dam axis were light and those toward the downstream were deep scratches at the upper elevations and shallow traces at lower levels.

Based on the above observations and detailed inspection of the failed dam, the following scenario was offered as the most probable mode of failure

- The body of the dam moved up along the peripheral joint, producing the first set of frictional traces parallel to the axis of the dam.
- The upward movement in turn caused widening of the horizontal arch spans, stressing the crown to the point of rupture.
- The asymmetric topography and the site geology caused the rupture of the dam to be offset toward the right side.
- The sudden failure of the structure was triggered by shearing of the top portion which did not include any joint.
- The sudden release of pressure caused the water to rush through the rupture and allowing the material to fall back onto the peripheral joint, thus producing the second set of traces on the joint surface.
- The material from the right side was washed downstream, but the left side rotated about the left abutment causing some debris to be pushed upstream.

11-8.4 High-Discharge Induced Incidents

11-8.4.1 Failure of Arch Dams

One of the chief causes of dam failure, considering all types of dams, is overtopping or inadequate spillway capacity. However, the number of arch dams that have been damaged or have failed while passing extreme floods is quite small. The International Commission on Large Dams (ICOLD) Bulletin 99 (1995) lists only one arch dam that failed due to overtopping (Alla Sella Zerbino Dam, see 11-8.1). One possible

explanation for the fact that overtopping is not as significant in arch dams as in other types of dams could be that arch dams are typically built on sound rock foundations. The chief danger from overtopping an arch dam would be erosion of the abutments or the foundation. Thus, a minor amount of overtopping of an arch dam may not be dangerous as long as the abutments and foundation are sound and the depth of overtopping is not great and does not occur with a long duration. A description of the experience with Gibson dam is notable and is presented here because the dam, although severely overtopped, did not fail.

Gibson Dam. Gibson dam is an concrete arch-gravity dam on the Sun River in Montana which was completed in 1929. It is protected by a "morning-glory spillway" near the left abutment which is controlled by six 34-ft by 12 ft radial gates which were added in 1938 to increase the reservoir capacity. Although the dam did not fail, it was overtopped for 20 hours at a depth of approximately 6.5 feet during passage of a record flood in June of 1964. Although some rock was plucked from the abutments, neither the dam nor the abutments suffered significant damage and stability of the dam was never threatened. It is of interest to note that the spillway gates were only partially open at the time the overtopping began. Since the caretaker's house was on the opposite side of the dam, the controls for the gate were not accessible after overtopping began.

11-8.4.2 Damage to Stilling Basins and Plunge Pools

Plunge Pools. As the previous section states, only a few arch dams have failed or been damaged by the passage of extreme floods. However, serious threats to arch dams could arise as a result of erosion of the downstream plunge pool if the erosion were to occur near enough to the dam. Kariba dam in Zimbabwe provides an example of such a threat. Kariba, completed in 1962, is a 426-foot high arch dam which impounds the world's largest man-made lake. The spillway consists of six orifices (28 x 30 feet) which discharge through the dam and impact in the downstream plunge pool. The rock is generally regarded to be sound gneiss. When the dam was designed in 1955, two power plants were envisioned and it was estimated that the spillway would discharge only about once in five years. However, the second power plant was never built; as a result the spillway has operated more frequently than planned with spill durations of several months. By 1967 the maximum scour depth in the plunge pool had reached 160 feet and a total volume of more than 500,000 cubic yards of rock was removed and carried downstream by the flow. By 1981 the scour depth had reached almost 200 feet and there was considerable concern about the potential instability of the dam foundation. As a result, some repairs have been made to the plunge pool and erosion seems to have been abated. However, a prolonged drought in the drainage basin above Kariba has greatly reduced the frequency of spills for the past several years. Currently, the plunge pool is

being monitored annually and necessary repairs are being made including rock bolting and placement of concrete in critical areas.

A side issue at Kariba is erosion of the abutments by runoff produced by spray. As much as four inches of water per day falls on some parts of the abutments when the spillway is operating. Gravel has been placed on the abutments in critical areas to prevent serious erosion.

11-8.5 Earthquake Induced Damage

Concrete arch dams have an excellent record of performance with respect to earthquake motion. No failure has ever resulted from earthquake damage to an arch dam. It must be realized however, that very few major earthquakes have occurred close to an arch dam. Major earthquakes on the order of the maximum credible earthquake are very rare events, and in most cases the MCE for a given dam site represents an unprecedented loading condition.

Among some 43 arch dams in 14 countries that are known to have been subjected to significant earthquake excitation (Serafim, 1987), only four have experienced a maximum or a near-maximum earthquake shaking with epicenter close to the dam site. The four arch dams are Pacoima, Lower Crystal Springs, and Gibraltar dams in the United States, and Ambiesta Dam in Italy. Except for Pacoima Dam, which suffered damage during two recent earthquakes, all other 42 dams experienced very little or no damage. Following is a description of the performance of Pacoima Dam and other three dams for their historical or design significance:

11-8.5.1 Pacoima Dam

The Pacoima Dam constructed in 1929 is located across Pacoima Creek in the San Gabriel Mountains about 5 miles north of San Fernando in southern California. The dam is a 372 ft high, moderately thick concrete arch dam, with a crest length of 640 ft. The dam is made of ten 50-foot-wide cantilevers separated by vertical contraction joints. The left-most joint (looking downstream) is the interface between the dam and a low-gravity thrust block that is built into the left abutment. Pacoima Dam was designed for static loads only, with no consideration for earthquake loading. The design was checked in 1928 by stress analysis using the crown cantilever trial-load method (Section 11-5.3.1). The principal functions of Pacoima Dam are flood control and water conservation.

There are seven significant faults within a 3.8-mile radius of the dam, with the San Andreas fault located 20 miles northeast of the dam. The two largest earthquakes in the

dam site region so far this century are the 1971 San Fernando (moment magnitude M_w 6.7) and the 1994 Northridge (M_w 6.7) earthquakes. The 1971 and 1994 earthquakes occurred on different fault systems and differ primarily in the dip of the faults, with a north-northeast-dipping fault plane in 1971 and a south-southeast-dipping fault plane in 1994 (EERI, 1995). The 1994 sequence started deeper and was more damaging because it produced stronger ground motions. Although severely shaken, Pacoima Dam survived both earthquakes with no noticeable cracking of the dam in 1971 and with some visible cracks and block offsets in 1994, which attests to strength reserve inherent in arch dams.

11-8-5.1.1 Performance during the San Fernando Earthquake

On February 9, 1971, Pacoima Dam was subjected to a M_w 6.7 earthquake originating on the part of Sierra Madre fault system which passes beneath the dam at a depth of 3 miles. The focus of the main shock was 4 miles north of the dam, at a depth of about 8 miles where the faulting initiated. The fracture then propagated up and to the south, past under the Pacoima Dam, and intercepted the surface after reaching a length of about 10 miles. Pacoima Dam survived the severe ground motion of this major event without any observed cracking in the arch.

An accelerograph located on the left abutment 52 ft above the dam crest recorded, a then unprecedented value of 1.25g on both horizontal components and maximum value of 0.70g on the vertical direction. Post-earthquake studies indicated that base-rock peak acceleration might have been in the range of 0.6 to 0.8g, thus relating the high peak accelerations to the canyon topography effects and possible shattered condition of the bedrock. In addition, the dam included a Wilmot Seismoscope at the crest which was seriously damaged during the first few seconds of the crest motion, so that no record of the dam response was obtained.

The Pacoima Dam was designed with no consideration for earthquake loading, but it did not develop structural cracks or experience relative movements between adjacent blocks as a result of the 1971 earthquake. The main damage was a separation of the arch dam from the left thrust block of 3/8 in. at the crest and extending downward about 50 ft. The left abutment, however, experienced extensive cracking of the gneissic granite-diorite rock. Many cracks penetrated through the gunite coating into the rock below, and slight movement of large blocks of rock mass occurred. Following the earthquake, stability of the dam was evaluated using the three-dimensional finite-element analysis and the left abutment supporting the thrust block was subsequently strengthened with 35 post-tensioned tendons to increase stability against future earthquakes. The crack in the thrust block and the open joint between the dam and the thrust block were also repaired.

According to Hansen and Roehm (1979), the exceptional performance of Pacoima Dam during the 1971 event can be related in part to the following :

- the tensile strength of the concrete is significantly increased when subjected to rapid strains;
- the rock foundation absorbs a portion of the earthquake's energy;
- inelastic behavior of the concrete contributes to an ultimate capacity for the dam considerably greater than that predicted by elastic analysis; and
- the grouted vertical contraction joints with low tensile capacity provide planes across which large horizontal tensile stresses are relieved.

In addition, it should be noted that at the time of the earthquake, the water level for the flood control Pacoima Dam was 147 ft below the crest. A higher water level can be expected to cause more damage than that observed during the 1971 event. The duration of strong ground motion was also approximately 7.5 seconds. A magnitude 8+ earthquake of longer duration on the San Andreas Fault would probably be a more severe test of the dam.

11-8-5.1.2 Performance During the Northridge Earthquake

On January 17, 1994, Pacoima Dam once again was subjected to a damaging earthquake of M_w 6.7. The epicenter was approximately 11 miles southwest of the dam. The earthquake occurred on a deep concealed thrust fault beneath the San Fernando Valley. The rupture began at 12 miles, and terminated at a depth of about 4 miles, leaving no obvious surficial expression. Although the Northridge earthquake was the same size as the 1971 San Fernando earthquake, it produced stronger ground shaking. The dam withstood the larger shaking, but experienced more damage in the abutments and in the body of the dam than occurred during the 1971 event.

Strong Motion Records.

Following the 1971 San Fernando earthquake, Pacoima Dam was extensively instrumented with additional sensors, so that strong motion response of the dam and its abutments during future earthquakes can be recorded. The accelerometer on the upper left abutment recorded accelerations of 1.47g and 1.70g on the horizontal components and 1.36g on the vertical component, as opposed to the peak accelerations of 1.25g horizontal and 0.7g vertical measured previously at the same location in the 1971 event. The downstream records obtained approximately 430 feet downstream from the base of the

dam, showed peak accelerations of 0.44g and 0.20g on the horizontal and vertical components, respectively. These records clearly illustrate the effect of canyon topography on ground motion, as evident from differences in acceleration amplitudes and waveforms of the upper abutment and the downstream motions. At the base of the dam, peak acceleration was 0.54g in the radial direction and 0.43g in the vertical direction. The radial peak accelerations at the left quarter-point of the crest and at 80% of the dam height reached 2.3g. Peak accelerations exceeding 2g were recorded at the center of the crest, but the corresponding strong motion records could not be digitized because the traces exceeded the range of instruments and became intertwined. The dam strong motion records showed higher frequency components than the downstream and base records, possibly a result of higher mode contributions and/or impact caused by closing of the contraction joints.

Observed Damage

During the Northridge earthquake, the severely shaken Pacoima Dam suffered damage both in the left abutment and within the dam body. The damage observed at the site was consistent with the strong shaking indicated by the accelerograms, and was more severe than occurred during the 1971 San Fernando earthquake. Again, the water surface at Pacoima Dam was low and stood at 131 feet below the crest.

Damage visible at the site (County of Los Angeles, 1994) included rock slides, extensive cracking of the shotcrete cover of the left abutment, opened contraction joint between the dam and thrust block on the left abutment, and several cracks on the downstream face of the dam. The contraction joint between the dam and thrust block opened and remained open 2 inches at the crest, decreasing to 1/4 of an inch at the bottom of the joint (60 feet below the crest), at which point a large diagonal crack extended down the thrust block to meet the foundation rock (Fig. 11-8.2). Apparently, the diagonal crack and contraction joint opening were caused by movements of two rock masses on the left abutment: Rock Mass A, and Rock Mass B. Rock Mass A and its adjacent Rock Mass B which is supporting the thrust block, are underlain by a slip plane (Plane 1 in Fig. 11-8.2) and are known to have marginal factors of safety against sliding. Survey measurements made after the earthquake indicated that Rock Mass B slipped about 2-3 inches horizontally and 2 inches down, thereby accounting for opening in the contraction joint between the dam and thrust block, while Rock Mass A moved 16-19 inches horizontally and up to 14 inches down. During the 1971 event, Rock Mass A moved 50% less and the movement of Rock Mass B was slight but enough to open up the same joint by 3/8 of an inch. The 35 tendons installed to secure the thrust block after the 1971 earthquake may have played a significant role in limiting the movement of Rock Mass B during the Northridge earthquake.

Over-stressing of the dam was indicated by permanent block offsets and by several cracks visible on the downstream face of the left-most block between elevations 1,925 feet and 1,967 feet. Two lift joints at elevations 1,967 feet and 1,978 feet showed evidence of broken bond and remained open slightly. Several cracks were found on the crest, each ran diagonally from the recessed corner of a shear key to either the upstream or downstream face, thus indicating working of monolith joints during the closing. Opening of the contraction joints was evident by their clean appearance after the earthquake. Permanent vertical offsets were observed along most joints, with the right block always remaining lower than the left block. The post-earthquake measurements with laser plumb line showed a permanent upstream displacement of the dam crest of 2 inches.

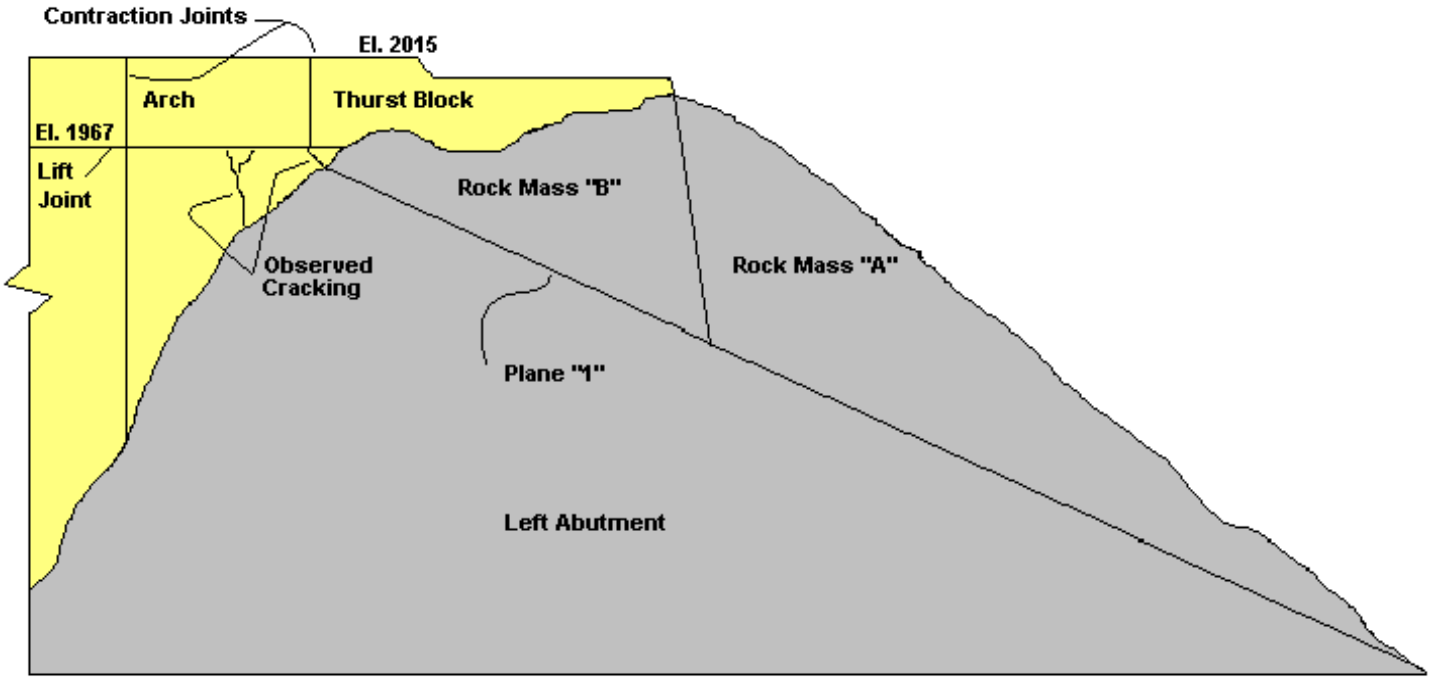

Fig. 11-8.2 Downstream elevation of the left side of the Pacoima Dam arch and the thrust block showing cracking.

Possible failure modes

From the damage observed during the Northridge earthquake, earthquake induced failure would probably involve the upper 65 feet of the dam. Such failure could originate from loss of the thrust block caused by a sliding failure of rock masses A and B, or through cracking and opened contraction joints in the dam itself, which could lead to unstable

concrete blocks. In either case, a failure of the upper part of the dam more likely would not release the reservoir water, because the intake to the tunnel spillway is 65 feet below the crest. Only concurrent flood and a damaging earthquake might possibly result in a sudden release of water or leakage through opened joints, but more likely the lower part of the dam would remain intact.

11-8.5.2 Other Significant Cases

11-8.5.2.1 Lower Crystal Springs Dam

One of the earliest cases of a concrete dam excited by a major earthquake was Lower Crystal Springs Dam located in San Mateo, California, about 20 miles south of San Francisco. Completed in 1890, the 154-ft-high, 600-ft long, curved gravity dam withstood the 1906 San Francisco earthquake (estimated magnitude of 8.3) without a single crack, even though it was located within 1,100 ft of the San Andreas fault rupture and earthquake loading had not been considered in its design. The dam was shaken again during the Loma Prieta earthquake of October 17, 1989, a magnitude 7.1 earthquake that occurred 40 miles south of the dam. The ground motion at the dam site was more moderate this time, and again, the dam was not affected.

A recent seismic safety evaluation of the dam showed that Lower Crystal Springs Dam could be expected to resist the forces of a magnitude 8.5 earthquake with no serious structural damage.

The excellent performance of the dam was attributed to a high reserve capacity arising from:

- The truncated cross section was designed as a gravity dam, but was curved in plan for additional load resistance by the arch action.
- The meticulous design included the use of interlocking blocks staggered so that there were no continuos horizontal or vertical joints through the dam.
- The foundation rock was highly fractured with visible fracture surfaces which absorbed much of the earthquake's strain energy.

11-8.5.2.2 Gibraltar Dam

Gibraltar Dam, a 169-foot-high arch dam built in 1920 near Santa Barbara, California, suffered no damage during the 1925 Santa Barbara earthquake of magnitude 6.3 which occurred beneath the dam. I has been reported "*the dam was so severely shaken that a watchman who was on the dam at the time had difficulty in standing up*." This and earlier

experience at Lower Crystal Springs dams provided the early evidence that properly built arch dams could be expected to perform satisfactory under earthquakes, even though the earthquake forces were not considered in the design of the dam.

11-8.5.2.3 Ambiesta Dam

Ambiesta Dam, built in an area of high seismicity near Gemona in northern Italy, is an arch structure specifically designed to withstand earthquakes. The 194-foot-high dam with a crest length of 475 ft was designed as a symmetric arch with striking downstream overhang, which the designers believed would resist the exceptional overloads that the dam might ever experience (Hansen and Roehm, 1979).

An actual test of the design occurred during the 1976 Gemona-Friuli earthquake of magnitude 6.5, which generated a maximum acceleration of 0.33g at the right abutment of the dam located about 14 miles away from the epicenter of the quake. The dam was also subjected to a foreshock of magnitude 4.5 about one minute before the main event, and to 4 major aftershocks of magnitude 5.1, 5.5, 5.9, and 6.0 that struck the region in a period of more than 4 months.

Hansen and Roehm (1979) reported that neither the Ambiesta dam nor 13 other concrete arch dams in the region suffered any damage from these events. In particular, the experience at Ambiesta Dam confirmed the results of model studies that indicated much larger acceleration of 0.95g in the transverse direction, or an acceleration of 0.76g in the vertical direction would be required to induce damage in the dam.

11-8.6 Detrimental Chemical Reactions

Detrimental chemical reactions such as alkali-aggregate reactions (AAR), also known as alkali-silica reaction (ASR) or alkali-carbonate reaction (ACR), have been found in a large number of concrete dams and hydroelectric plants around the world. The reactions occur between certain aggregates and alkalis in the cement, leading to the formation of gels which then absorb water and expand, causing increased stress, micro-cracking of the concrete and structural deformations. Three basic requirements for expansive AAR to occur are: 1) presence of deleteriously reactive aggregates, 2) sufficient concentration of alkali, and 3) adequate levels of moisture in the concrete. Hobbs (1990) notes that where alkalis come primarily from the cement, AAR expansion has been observed to be largely complete in 8 to 15 years. However, there are some increasing cases which suggest that the supplementary alkalis provided by the coarse aggregates might be significant, thus creating "*auto-generation*" conditions with an indefinite period of expansion..

Charlwood and Solymar (1995) have reported 104 worldwide known cases of AAR in hydraulic structures, of these 32 cases are concrete arch dams listed in Table 11-8.1. For each dam, the table includes name, height, location, date of construction, a brief description of damage, and the repair performed on the structure. Most arch dams with AAR were built prior to discovery of AAR in California (Stanton 1940), or shortly after when clues on the AAR processes were still emerging. However, a few cases of AAR reported in South Africa and Mozambique occurred in the 1960's and even as recent as 1974. A large number of arch dams subjected to AAR have continued to function adequately for many years. Well-known cases include Gene Wash and Copper Basin and Parker dams, where substantial strains occurred within the first 20 years after the construction but expansion appear to have ceased. In cases such as Stewart Mountain, Churchil, and Gmued dams, strengthening measures were required; in Matilija, the upper 40 ft of the dam was replaced due to severe deterioration of the concrete; and in Drum Afterbay the reaction was continuing at such a high rate that the dam was taken out of service and replaced by a new arch structure immediately downstream.

The primary adverse effects of expansive AAR in arch dams include micro-cracking and structural deformations. The micro-cracking typically extends to shallow depths and can lead to loss of tensile and shear strength of the concrete, although the compressive strength may be retained. The deformations typically cause upstream and upward movements, which can lead to additional cracking and reduced strength in the dam concrete. They can also result in overstressing and cracking of lift joints, thus reducing shear strength along the lift lines. In fact, loss of joint shear strength has been of concern in static and particularly in seismic safety assessments when combined arch-cantilever action is necessary (e.g. Stewart Mountain where anchors were installed). Other adverse effects may include leakage, leaching, loss of gate clearances, and problems at the abutments or spillway openings where significant structural discontinuities exist.

The case histories described in the subsequent sections illustrate that the effects of expansive AAR can range from minor cracking to major abnormal movements; the reaction may have ceased or the expansion rates are slow and ongoing. Nevertheless, as the condition of the dam worsens the potential for the subsequent failure due to the imposed loads increases. Therefore, it is prudent that appropriate performance parameters for safety evaluation of arch dams affected by AAR are developed. One such performance parameter based on the visual and instrumentation monitoring of the dam has been developed and implemented by USBR as part of their dam safety program development (Veesaert and LaBoon 1995).

Table 11-8.1 Summary of case histories of concrete arch dams with AAR problems (adopted from Charlwood and Solymar, 1995)

Dam	Height (m)	Country	Year Built	Damage	Repair or Replacement
Alto Ceira	37	Portugal	1949	movements, cracking	Under study
Bartlett (multiple arch)	87	Arizona, USA	1936	some strength loss	lithium hydroxide tests
Bimont	87	France	1952	expansion, cracking	grouting, epoxy coating on affected parts
Cahora Bassa	170	Mozambique	1974	swilling but no cracking	Under study
Churchill	39	South Africa	1943	horizontal cracking	Strengthening/extension of buttress with reinforced concrete
Coolidge	77	Arizona, USA	1929	deterioration	concrete, spillway gate reinforcement
Copper Basin	64	Calif., USA	1938		Reaction completed
Dinas	14	Wales, UK	1957	serious cracking	epoxy sealing, cut exp. joint, grouting
Drum Afterbay	25	Calif., USA	1924		Replaced in the 1960's
Gene Wash	48	Calif., USA	1937	strength loss	Reaction completed
Gmuend	30	Austria	1945		Strengthened by adding gravity section
Gibraltar	50	Calif., USA	1920		
Horse Mesa	93	Arizona, USA	1927	surface deterioration, some joint separation	Surface repair
Kariba	126	Zambia/Zimbabwe	1955	cracks in spillway	
Keerom	36	South Africa	1954	cracking	Grouting
Matilija	58	Calif., USA	1947	spillway gate jams, cracking, joint opening	Cutting a 85 m long and 9 m deep notch in 1965, replacem. of upper 12 m
Maury	72	France	1947	cracks	
N'Zilo/ Delcommune	75	Zaire	1952	Extensive cracking	
Owyhee	127	Oregon, USA	1932	cracking after 5 yrs and deterioration after 11 yrs	
Parker	96	Calif., USA	1938	surface cracking and strength loss	Expansion assumed ceased by 1965
Pathfinder	65	Wyoming, USA	1909	deterioration of parapets and power house walls	Surface repair
Paul Sauer /Kougha	82	South Africa	1969	cracking lift joints, movement	
Peti	46	Brazil	1946		
Pietersfontain	29	South Africa	1966	none but low tensile strength	
Poortjlieskloof	36	South Africa	1955	horizontal cracking	Minor
Roode Elsburg	72	South Africa	1968	none	
San Esteban	115	Spain	1955	U/S deterioration, seepage	U/S water proffing, grouting of joints
Santa Luzia	76	Portugal	1943	movements	Possible seal of u/s
Santeetlah	61	N. Carolina, USA	1928	cracking	Slot cut, epoxy grouting, extra concrete
Stewart Mountain	63	Arizona, USA	1930	expansion. movement, deterioration	Grouting, structural modification, expansion ceased
Stolsvatn (multiple arch)	18	Norway	1970?	surface cracking, freeze thaw damage	Epoxy coat, Foundation anchors
Stompdrift (multiple arch)	49	South Africa	1965	cracking, opening joints	Grouting of construction joints

11-8.6.1 Kouga Dam, South Africa

Kouga Dam (formerly Paul Sauer Dam), is a 78m (256 ft) high, 317 m (1040 ft) long, double curvature arch dam completed in 1969. In 1981, an evaluation of the monitoring program revealed that the dam crest was rising slowly with the center of the crest also moving slowly upstream (Elges et al. 1995). The movements, which amounted to 8 mm vertical movement at the time, were suspected to be the results of AAR. A further investigation, which included laboratory testing of concrete cores, concluded the expansion measured in the dam is caused by the alkali-aggregate reaction. The cement used for the construction of the dam is now is regarded as high-alkali cement.

The geodetic measurements taken twice a year from 1972 to date, indicate a continuous expansion trend since 1976. The expansion now amounts to a total upward displacement of 22 mm. A crack on the upstream side indicates that the spillway has suffered more severe AAR, and that the bulging of the spillway sill has raised its level between 25 and 45 mm. Since 1984 expansion appears to be decreasing, but it is not clear whether AAR is decreasing or the successive and prolonged periods of low water levels are responsible for the reduction.

11-8.6.2 Santa Luzia, Portugal

This thin cylindrical arch dam with a maximum height of 76 m (250 ft) and a crest length of 115 m (377 ft) was completed in 1943. The expansion due to AAR was detected from the continuous upstream and upward movements of the crest (Ramos et al., 1995). Since the first filling of the reservoir, geodetic and alignment measurements have been used to monitor such movements. The maximum upward displacement of the crest accumulated over a period of 40 years is reported to be about 50 mm. During the same period the maximum upstream movement has reached 30 mm. The mineralogical and petrographic analyses conducted on the dam concrete samples showed that AAR has occurred from the reaction between the reactive silica provided by cataclastic quartz, and the alkalis supplied by feldspars aggregates ("auto-reaction"). Apart from providing the necessary alkaline environment, the low-alkali-content cement has little value to the reaction. Ongoing deformation monitoring, periodic ultrasound pulse velocity tests, and structural analysis are being considered for better characterization of AAR and its effects on the long-term performance of the dam.

11-8.6.3 Alto-Ceira Dam, Portugal

Completed in 1949, Alto-Ceira is a thin arch dam with a maximum height of 37 m (121-ft) and a crest length of 120 m (394-ft). Shortly after the first filling of the reservoir, the dam began experiencing increasing movements in the upstream and upward directions,

accompanied with extensive cracking both in the upstream and downstream faces of the dam (Ramos et al., 1995). Numerous studies including visual inspections, mapping of cracks, core testing, and petrographic analysis of concrete samples were conducted to identify the source and effects of such expansion on the operation and safety of the dam. The studies concluded that alkali-silica reactions are responsible for the expansion. It was determined that the reactions occur among quartz and metapelite aggregates containing reactive silica, feldspar aggregates as a supplementary source of alkalis, with the cement providing the alkaline environment necessary for the reaction. In such cases, the presence of alkalis in feldspar aggregates creates "*auto-reaction*" conditions (Ramos et al. 1995), in which the expansion may continue indefinitely. The measured deformations and 3D finite-element analysis of the dam indicate that expansion has now advanced to the entire dam. Recent ultrasound pulse velocity tests showed significant deterioration of the concrete; and a survey of cracks indicated major cracks have reached a depth of about 60 cm (2-ft). Ongoing expansion continues at approximately constant rates, which if not reduced, inevitably might adversely affect the operation and possibly the safety of the dam.

11-8.6.4 Cahora-Basa Dam, Mozambique

The 170m-high Chora-Basa Dam with a crest length of 300 m, is a double curvature arch dam constructed between November 1971 and December 1974. Since the first filling of the reservoir in January 1975, the dam has been showing continuous movements in the upstream and upward directions. The expansion of the concrete was first detected by continuous rising of the strains measured by a group of 50 extensometers embedded in the concrete, and later was confirmed by the alignment measurements and petrographic analysis of concrete samples. The reaction is also suspected to have developed by "*auto-reaction*" caused by the presence of alkalis in the aggregates. Expansion at the moment is rather moderate, showing a maximum upstream bulging of about 11 mm accumulated between 1977 and 1994. The expansion has not induced any visible cracking, but a more elaborate testing and analysis program is underway to better characterize its development and effects on the safety of the dam.

11-8.6.5 Gene Wash and Copper Basin, California

Located close together in San Bernardino County, California, Gene Wash and Copper Basin were constructed in 1937 and 1938 using the same materials. Gene Wash is a 131-foot-high arch structure with a gravity thrust block on the right abutment, and Copper Basin is a taller arch with a maximum height of 187 feet.

Within the first 20 years after their construction, both dams experienced active expansions and extensive pattern cracking. During this period the total deformation of the dam reached 11 to 12 cm in the upstream and about 9 cm in the upward direction, and then decreased essentially to zero for the past 40 to 50 years. A comprehensive concrete testing program indicated that the expansion was caused by autogenuous growth due to AAR. While the effects of this distress are still evident, it appears that the dams have stopped deteriorating, and that the AAR is in a dormant state.

11-8.6.6 Horse Mesa, Arizona

The 93 m (305 ft) high Horse Mesa Dam with a crest length, including the abutment spillways, of 201 m (660 ft), is a thin arch dam completed in 1927. Located about 65 miles northeast of Phoenix, the dam impounds Apache Lake on the Salt River in central Arizona.

After the discovery in 1946 of AAR problems at Stewart Mountain Dam, cores were taken from the Horse Mesa Dam. Tests showed AAR has occurred, but to an insignificant degree. Additional cores taken in 1968 indicated no deterioration of the concrete and produced satisfactory compressive strength. The reaction has caused typical surface cracking and minor expansions in the dam concrete with permanent deformations of the arch without affecting the integrity of the dam. Also, there appears to be disbonded lift joints as evident by seepage passing along the downstream face of the dam. At the present time, the dam crest is deforming approximately 0.25 mm/year (0.01 inch/year) upward, and between 0.25 and 0.75 mm/year (0.01 and 0.03 inch/year) upstream (Veesaert and LaBoon 1995).

11-8.6.7 Owyhee, Oregon

Constructed between 1928 and 1932, Owyhee Dam is a concrete thick-arch structure with a maximum height of 127 m (417 ft) and a crest length of 183 m (600 ft). Deterioration and cracking of concrete, which first appeared in 1948, is continuing and is thought to be caused by AAR (Veesaert and LaBoon 1995). An investigation conducted in 1988 concluded that AAR is occurring at varying degrees in the dam. It is strong in the upper and outer portions of the dam, and only mild to nonexistent in the lower and deep interior portions.

According to Veesaert and LaBoon (1995), a monitoring program began in 1985 shows an upstream movement at an average rate of 9 mm/year (0.37 inch/year) near the center of the dam, with much slower upward movements averaging less than 2 mm/year. Ongoing visual and instrumentation monitoring indicate dramatic increases in seepage when the reservoir water level is near or above elevation 2650 ft (crest El. 2675 ft),

probably because of significant cracking in the upper 50 to 75 feet of the dam which has occurred as a result of AAR. Although AAR cracks and seepage through the concrete reduce sliding resistance, the computed large factors of safety indicate that the relatively thick gravity-type sections of Owyhee Dam tend to preclude this type of failure.

11-8.6.8 N'Zilo, Zaire

Completed in 1952, N'Zilo (formerly Delcommune) Dam in Zaire is a thin double curvature arch dam about 246 feet high, which suffered an expansion of approximately 1000 micro-strain in 30 years, resulting in extensive cracking.

REFERENCES

American Society of Testing Materials (1984a), “Standard Test Method for Determining the In Situ Modulus of Deformation of Rock Mass Using the Rigid Plate Loading Method,” ASTM-D4394-84, Annual Book of ASTM Standards, Vol. 04.08, Philadelphia, PA.

American Society of Testing Materials (1984b), “Standard Test Method for Determining the In Situ Modulus of Deformation of Rock Mass Using the Flexible Plate Loading Method,” ASTM-D4395-84, Annual Book of ASTM Standards, Vol. 04.08, Philadelphia, PA.

Annandale, G. W. (1995), “Erodibility,” Journal of Hydraulic Research, Vol. 33, No. 4, International Association for Hydraulic Research, Delft, The Netherlands.

Babb, A.O. And T.W. Mermel (1968), Catalog of Dam Disasters - Failures and Accidents, PB 179 243, U.S. Bureau of Reclamation, Washington, D.C.

Barnes, H.H. (1977), Roughness Characteristics of Natural Channels, U.S. Geological Survey Water-Supply Paper 1849, Arlington, Virginia.

Barton, N., Lien,R., and Lunde, J. (1974), “Engineering Classification of Rock Masses for Design of Tunnel Support,” Rock Mechanics Vol. 6, No. 4.

Barton, N., “The Shear Strength of Rock and Rock Joints (1976),” Int. J. Rock Mech. Min. Sci. & Geomech. Abstr. Vol. 13 pp. 255-279, Pergamon Press, Great Britain.

Barton, N. And Choubey, V. (1977), “The Shear Strength of Rock Joints in Theory and Practice” Rock Mechanics, Vol. 10 pp. 1-54, Springer-Verlag, Wien, Austria.

Barton, N. (1988), “Rock Mass Classification and Tunnel Reinforcement Selection Using the Q-System,” in Rock Classification Systems for Engineering Purposes: ASTM STP-984, Kirkaldie, L. (Ed.), American Society of Testing and Materials, Philadelphia, PA.

Bathe, K.J. and Wilson, E.L., (1974). "*Thick Shell Structures*," Proceedings International Symposium on Structural Mechanics Software, University of Maryland, College Park, Maryland.

Bathe, K.J., and Wilson, E.L. (1976). "*Numerical Methods in Finite Element Analysis*," Prentice-Hall, Englewood Cliffs, NJ.

Bieniawski, Z.T. (1979), “The Geomechanics Classification in Rock Engineering Application”, Proceedings of 4th International Congress on Rock Mechanics, ISRM, Montreux, Balkema, Rotterdam, Vol. 2.

Bieniawski, Z.T. (1990), “Tunnel Design by Rock Mass Classifications,” Technical Report GL-79-19, U.S. Army Corps of Engineers, Waterways Experiment Station, Vicksburg, MS.

Billings, M.P. (1954), “Structural Geology,” Prentice Hall, Inc., Englewood Cliffs, NJ.

Bradley, J.N. (1952), “Discharge Coefficients for Irregular Overfall Spillways,” Engineering Monograph No. 9, U.S. Bureau of Reclamation, Denver Federal Center, Denver, Colorado.

Burgi, P.H. (1988), “Cavitation Damage and Repair of Glen Canyon Spillway Tunnels,” Advance Dam Engineering, for Design and Construction, (R.B. Jansen, Editor), Van Nostrand Reinhold, New York, New York.

Cameron, C.P., Patrick, D.M., May, J.H., Palmerton, J.B., McAneny, C.C. (1986, 1988a, 1988b, 1989), “Geotechnical Aspects of Rock Erosion in Emergency Spillway Channels,” Tech. Report REMR-GT-3, U.S. Army Corps of Engineers, Waterways Experiment Station, Vicksburg, MS.

Cassidy, J.J. (1970), “Designing Spillway Crests for Negative Pressures,” ASCE, Journal of the Hydraulics Division, Vol. 96, HY3. March.

Charlwood, R. G., and Solymar Z. V. (1995)."*Long-term management of AAR-affected structures - an international perspective*," USCOLD 2nd International Conference on Alkali-Aggregate Reactions in Hydraulic Plants and Dams, Chattanooga, Tennessee, October 22-27.

Chopra, A. K. (1988), "*Earthquake analysis of concrete dams*," Chapter 15 in Advanced Dam Engineering for Design, Construction, and Rehabilitation, edited by Robert B. Jansen, Van Nostrand.

Chopra, A.K., and Tan H. (1996), "*Foundation modeling in earthquake analysis of arch dams*," 16th annual USCOLD lecture series, Los Angeles, California, July 22-26, 1996.

Chow, V.T. (1959), Open Channel Hydraulics, McGraw-Hill Book Company, New York, New York.

Clough, R. W. 1977 (Feb.). *Lecture Notes*, unpublished.

Clough, R.W., Chang, K.T., Chen, H.Q., and Ghanaat, Y. (1985). "*Dynamic Interaction Effects in Arch Dams*," Report No. UCB/EERC-85/11, University of California, Earthquake Engineering Research Center, Berkeley, CA.

County of Los Angeles, (1994), *Report on Initial assessment of the effects of the January 17, 1994, Northridge/San Fernando earthquake on Pacoima Dam, Phase 1*. Prepared by Morrison Knudsen Corporation, April.

CSMIP (1994), "*Strong Motion Records from the Northridge, California Earthquake of January 17, 1994*," Report No. OSMS 94-07, California Department of Conservation, Strong Motion Instrumentation Program.

Davis, C.V. (1969), Handbook of Applied Hydraulics, McGraw-Hill Book Company, New York, New York.

Deere, D.U. and D.W. Deere (1988), "The Rock Quality Designation (RQD) Index in Practice," Rock Classification Systems for Engineering Purposes, ASTM STP-984, (L. Kirkaldie, Editor), American Society for Testing and Materials, Philadelphia, Pennsylvania.

EERI (1995), "*Northridge Earthquake of January 17, 1994 Reconnaissance Report*," Supplement C to Volume 11 Earthquake Spectra, April.

Elges H., Geertsema A., Lecocq P., and Oosthuizen C. (1995), "*Detection, monitoring and modeling of Alkali-Agregate Reaction in Kouga Dam (South Africa)*," USCOLD 2nd International Conference on Alkali-Aggregate Reactions in Hydraulic Plants and Dams, Chattanooga, Tennessee, October 22-27.

Fenves, G. L., Mojtahedi, S., and Reimer, R. B., (1989),"*ADAP-88: A Computer Program For Nonlinear Earthquake Analysis of Concrete Arch Dams*," Report No. UCB/EERC-89/12, University of California, Earthquake Engineering Research Center, Berkeley, CA.

Fok, K. L., and Chopra, A. K. (1985), "*Earthquake Analysis of and Response of Concrete Dams*," Report No. UCB/EERC-85/07, University of California, Earthquake Engineering Research Center, Berkeley, CA.

Fok, K.-L., Hall J. F., and Chopra, A. K. (1986), "*EACD-3D: A Computer Program for Three-dimensional Earthquake Analysis of Concrete Dams*," Report No. UCB/EERC-86/09, Earthquake Engineering Research Center, University of California, Berkeley.

Ghanaat, Y., (1993a), "*Theoretical Manual for Analysis of Arch Dams*," Technical Report ITL-93-1, US Army Corps of Engineers Waterways Experiment Station, July 1993.

Ghanaat, Y., (1993b), "*User's Manual - GDAP: Graphics-Based Dam Analysis Program*," Technical Report ITL-93-3, US Army Corps of Engineers Waterways Experiment Station, Vicksburg, MS.

Ghanaat, Y. and Redpath, B.B. (1995). *"Measurements of reservoir-bottom reflection coefficient at seven concrete dam sites,"* QUEST Report No. QS95-01 issued to the US Army Corps of Engineers, Waterways Experiment Station and Bureau of Reclamation.

Hall, J.F. (1988), "*The Dynamic and earthquake behavior of concrete dams: review of experimental behavior and observational evidence*," Journal of Soil Dynamics and Earthquake Engineering, Vol. 7, No. 2, pp. 58-121.

Hall, J. F. (1988), "*The dynamic and earthquake behavior of concrete dams: review of experimental behavior and observational evidence*," Soil Dynamic and Earthquake Engineering, Vol. 7, No. 2.

Hansen, K.D., and Roehm, R.H. (1979), "*The response of concrete dams to earthquakes*," Water Power & Dam Construction, Vol. 31, No. 4, pp. 28-31.

Henderson, F.M. (1966), Open Channel Flow, The McMillan Company, New York, New York.

Hendron, A.J. (1968), "Mechanical Properties of Rock," Pp 21 to 41, Rock Mechanics in Engineering Practice, Stagg, K.G., and Zienkiewicz, O.C., (Ed.), John Wiley & Sons, N.Y.

Hendron, A.J., Cording, E.J., and Aiyer, A.K. (1971), "Analytical and Graphical Methods for the Analysis of Slopes in Rock Masses," NCG Technical Report No. 36, U.S. Army Corps of Engineers, Waterways Experiment Station, Vicksburg, MS.

Hendron, A.J., and Patton, F.D. (1985), "The Vajont Slide, a Geotechnical Analysis Based on New Geologic Observations of the Failure Surface," U.S. Army Corps of Engineers, Waterways Experiment Station, Vicksburg, MS.

Hill, C. J. (1995), "*Gene Wash and Copper Basin Dams are surviving alkali-aggregate reaction*," USCOLD 2nd International Conference on Alkali-Aggregate Reactions in Hydraulic Plants and Dams, Chattanooga, Tennessee, October 22-27.

Hobbs, D. W. (1990), "Cracking and expansion due to alkali-silica reaction: it's effects on concrete," Structural Engineering Review, pp. 65-79.

Hoek, E. And Bray, J.W. (1981), "Rock Slope Engineering," Institute of Mining and Metallurgy, Elsevier Applied Science, London & N.Y.

Hoek, E., Carvalho, J. & Kochen, R. (1995), "SWEDGE, Analysis of the Geometery and Stability of Surface Wedges", Rock Engineering Group, Univ. of Toronto.

International Commission on Large Dams (1989), "Monitoring of Dams and Their Foundations," Bulletin 68, Paris.

International Commission on Large Dams (1992), "Improvement of Existing Dam Monitoring," Bulletin 87, Paris.

ICOLD (1987), Spillways for Dams, Bulletin 58, International Commission on Large Dams, Paris, France.

ICOLD (1995), Dam Failures, Statistical Analysis, Bulletin 99, International Commission on Large Dams, Paris, France.

ICOLD (1996), Vibrarions of Hydraulic Equipment for Dams, Bulletin 102, International Commission on Large Dams, Paris, France.

Kirsten, H.A.D. (1982), "A Classification System for Excavation in Natural Materials," The Civil Engineer in South Africa, July.

Kuo, J. 1982. "*Fluid-structure Interactions: Added Mass Computations for Incompressible Fluid*," *Report No. UCB/EERC-82/09*, University of California Earthquake Engineering Research Center, Berkeley.

Leonards, G.A. (1987), "Overview and Personal Commentary," Dam Failures, Proceedings of the International Workshop on Dam Failures, Leonards G. A. (Ed.), Purdue University, West Lafayette, Indiana, Aug. 6-8, 1985, Elsevier, N.Y.

Leslie, J.R., and Cheesman, W. J. (1949), "An Ultrasonic Method of Studying Deterioration and Cracking of Concrete Structures," ACI Journal, Proceedings V. 46, No. 1, September 1949, pp. 17-36.

Londe, P. (1973), "Rock Mechanics and Dam Foundations," Bulletin of the International Commission on Large Dams, Paris.

Londe, P. (1987), "The Malpasset Dam Failure" Dam Failures, Proceedings of the International Workshop on Dam Failures, Leonards, G.A. (Ed.) Purdue University, West Lafayette, Indiana, Aug. 6-8, 1985, Elsevier, N.Y.

Londe, P. (1993), "Rock Foundations for Dams," Bulletin 88 of the International Commission on Large Dams, Paris.

Monfore, G.E., and Taylor, F. W. (1954),"*The problem of an expanding ice sheet*," Bureau of Reclamation Memorandum, March 18, 1954 (unpublished).

Mason, P.J. (1984), "Erosion of Plunge Pools Downstream of Dams Due to the Action of Free-Trajectory Jets, Paper 8734, Proceedings of Inst. Civ. Engrs, Part 1, Pp 523-537, London.

Mason, P.J. (1985),"Free Jet Scour Below Dams and Flip Buckets," ASCE Journal of Hydraulic Engineering, Vol. 111, No. 2, February, New York, New York.

Muller-Salzburg, L. (1987), "The Vajont Catastrophe - A Personal Review," Dam Failures, Proceedings of the International Workshop on Dam Failures, Leonards, G.A. (Ed.), Perdue University, West Lafayette, Indiana, Aug. 6-8, 1985, Elsevier, N.Y.

National Research Concil, (1990). "*Earthquake Engineering for Concrete Dams: Design, Performance, and Research Needs*."

Newmark, N.M. and Hall, W.J. (1982) "*Earthquake Spectra and Design; Engineering monographs on earthquake criteria, structural design, and strong motion records,"* Vol. 3: Earthquake Engineering Research Institute, University of California, Berkeley, CA

Patton, F.D. (1966), "Multiple Modes of Shear Failure in Rock," Proceedings of 1st Int. Cong. Rock Mechanics, Vol. 1, No.3.47, Pp. 509-514.

Patton, F.D. (1966), "Multiple Modes of Shear Failure in Rock and Related Materials," Ph.D. Thesis, Univ. of Ill.

Patton, F.D. (1968), "The Determination of Shear Strength of Rock Masses," Terrametrics Short Course on Measurement Systems for Control of Construction and Mining, Denver.

"Portugues Dam Foundation Investigation," Design Memorandum No. 22, an unpublished internal document, U.S. Army Corps of Engineers, Jacksonville District, Jacksonville, FL., (1988).

Raphael, J.M. *"Tensile Strength of Concrete"* , ACI Journal, March-April 1984

Ramos J.M., Btista A.L., Oliveira S.B., de Castro A.T., Silva H.S., and de Pinho J.S. (1995), "*Reliability of arch dams subjetc to concrete swelling*," USCOLD 2nd International Conference on Alkali-Aggregate Reactions in Hydraulic Plants and Dams, Chattanooga, Tennessee, October 22-27.

Roberson, J.A., J.J. Cassidy, and M.H. Chaudry (1998), Hydraulic Engineering, John Wiley and Sons, Inc. New York, New York.

Roberts, D.F. (1977), "Energy Dissipation by Dam Crest Splitters," Transactions of the South African Institute of Civil Engineers, Johannesburg, South Africa, November.

"Rock Testing Handbook," U.S. Army Corps of Engineers, Waterways Experiment Station, Vicksburg, MS., (1990).

Sarkaria, G.S. (1997) "Lessons from Serious Incidents at Seven Arch Dams" Proceedings of the 1997 Annual Conference of the Association of State Dam Safety Officials.

Scott, G.A. and Von Thun, J.L. (1993), "Interim Guidelines Geotechnical Studies for Concrete Dams (Draft)," U.S. Bureau of Reclamation, Denver.

Semenza, C., DiBrai, L., and Capra, U. (1977), "*Ambiesta Dam*", Sixth International Congress of Large Dams, Question 22.

Semenza, E. (1985), “Synthesis of Geological Studies of the Vajont Landslide from 1959 to 1964,” App. G, Technical Report GL-85-5, The Vaiont Slide, A Geotechnical Analysis Based on New Geologic Observations of the Failure Surface, by Hendron, A.J. and Patton, F.D., U.S. Army Corps of Engineers, Waterways Experiment Station, Vicksburg, MS.

Serafim, J.L., and Pereira, J.P. (1983), “Considerations of the Geomechanics Classification of Bieniawski,” Proceedings of the International Symposium on Engineering Geology in Underground Construction, Laboratorio Nacional Engenharia Civil, Lisbon.

Serafim, J.L. (1987), “Malpasset Dam Discussion - Remembrance of Failures of Dams,” Dam Failures, Proceedings of the International Workshop on Dam Failures, Leonards, G.A. (Ed.), Perdue University, West Lafayeete, Indiana, Aug. 6-8, 1985, Elsevier, N.Y.

Serafim, J. L. (1987), "*A Note on the Earthquake Performance of Arch Dams*," Proceedings of China-US Workshop on Earthquake Behavior of Arch Dams, Beijing, China.

Stanton, T. E. (1940),"*Expansion of Concrete Through Reaction Between Cement and Aggregate*," Proceedings, American Society of Civil Engineers, December.

Tan, H. and Chopra, A. K. (1995a). "*Earthquake Analysis of Arch Dams Including Dam-Water-Foundation Rock Interaction*," Earthquake Engineering and Structural Dynamics, vol. 24 (11), pp. 1453-1474.

Townsend, (1965,. "*Control of Cracking in Mass Concrete Structures*," Engineering Monograph No. 34, U.S. Department of the Interior, US Bureau of Reclamation, Denver, CO.

U.S. Army Corps of Engineers (1990), “Hydraulic Design of Spillways”, Engineer Manual EM 111-2-1603, US Army Corps of Engineers, Washington DC

U.S. Army Corps of Engineers (1996) , Ice Engineering, EM-1110-2-1612, Headquarters, Department of the Army, Office of the Chief of Engineers, Washington D.C.

U.S. Army Corps of Engineers (1964), Structural Design of Spillways and Outlet Works, Engineer Manual EM 1110-2-2400, Headquarters, Department of the Army, Office of the Chief of Engineers, Washington D.C.

U.S. Army Corps of Engineers (1990), HEC-2, Water Surface Profiles, Hydrologic Engineering Center, Davis, California.

U.S. Army Corps of Engineers (1984), *"Geotechnical Investigations*," Engineer Manual EM 1110-1-1804, US Army Corps of Engineers, Washington, D.C.

U.S. Army Corps of Engineers (1994), " *Arch Dam Design*," Engineer Manual EM 1110-2-2201, US Army Corps of Engineers, Washington, D.C.

U.S. Army Corps of Engineers (1994), *"Rock Foundations,"* Engineer Manual EM 1110-2-2908, US Army Corps of Engineers, Washington, D.C.

U.S. Army Corps of Engineers , "*Instrumentation for Concrete Structures,"* Engineer Manual EM 1110-2-4300, US Army Corps of Engineers, Washington, D.C

U.S. Bureau of Reclamation (1938), Model Studies of Spillways, Boulder Canyon Project Final Design Reports, United States Department of the Interior, Denver, Colorado.

U.S. Bureau of Reclamation (1977). " *Design of Arch Dams*," Design Manual for Concrete Arch Dams, US Department of the Interior, Denver, CO.

U.S. Bureau of Reclamation (1987). "*Concrete Dam Instrumentation*," US Department of Interior, Denver, CO.

U.S. Bureau of Reclamation (1993), Dam Foundation Erosion, Survey of the Literature, Hydraulics Branch, Research & Laboratory Services Division, Denver Research Center, Denver, Colorado.

Veesaert C.J., and LaBoon J.H. (1995), "*The use of performance parameters in monitoring the safety of dams experiencing alkali-aggregate reaction*," USCOLD 2nd International Conference on Alkali-Aggregate Reactions in Hydraulic Plants and Dams, Chattanooga, Tennessee, October 22-27.

Veronese, A. (1937), "Erosioni de Fondo a Valle de uno Scarico," Annali dei Lavori Publicci, Vol. 75, N0. 9, September, Italy.

Warnock, J.E. (1950), "Hydraulic Similitude," Chapter II of Engineering Hydraulics, (H. Rouse, Editor), John Wiley and Sons, Inc., New York, New York.

Westergaard, H. M. (1933), "*Water pressures on Dams During Earthquakes*," Transactions, American Society of Civil Engineers, Vol 98.

Wilson, E.L. Der Kiureghian, A. Bayo, E.R. *"A Replacement for SRSS in Seismic Analysis"*, Earthquake Engineering, and Structural Dynamics, Vol. 9, pp 187-192 (1981)

Xuehai Luo, Z. Wei, H. Wanchun, and D. Jinglin, (1987), "*Field Vibration on Banxia Arch Dam by Rocket Exciter*," Proceedings of China-US Workshop on Earthquake Behavior of Arch Dams, Beijing.

Zhang, L.-P. and Chopra, A.K. (1991), "*Impedance Function for Three-dimensional Foundations Supported on an Infinite Long Canyon of Uniform Cross-Section in a*

Homogeneous Half-Space," Earthquake Engineering and Structural Dynamics, vol. 20 (11), pp. 1011-1027.

Zienkiewicz, O.C., (1971), "*The Finite Element Method in Engineering Science*," 2nd ed., McGraw-Hill, New York.